Unraveling the environmental record encoded in mollusk shell microstructures

Dissertation
zur Erlangung des akademischen Grades
"Doktor der Naturwissenschaften"
im Promotionsfach Geologie/Paläontologie

Am Fachbereich 09 für Chemie, Pharmazie und Geowissenschaften
der Johannes Gutenberg-Universität Mainz

von
Stefania Milano
geb. in Cuneo, Italien

Mainz 2016

Dekan: Not displayed for reasons of data protection
1. Berichterstatter: Not displayed for reasons of data protection
2. Berichterstatter: Not displayed for reasons of data protection

Datum der mündlichen Prüfung: 13 Dezember 2016

Hiermit erkläre ich, dass ich die vorliegende Arbeit selbstständig verfasst und keine anderen als die angegebenen Quellen und Hilfsmittel benutzt habe.

(Stefania Milano)
Mainz, 24. Oktober 2016

Abstract

Mollusks serve as unique ultra-high-resolution archives of past environmental change. Their shells grow at periodic rates and form distinct growth patterns that can be used as a calendar. Environmental signals are recorded in the shells in the form of geochemical and structural properties that can be dated to the nearest day, month or year with growth lines and increments. However, it is still very challenging to obtain quantitative environmental data from shells, in particular water temperature. For example, shell growth rate is affected by both water temperature and food supply, and shell Sr/Ca and Mg/Ca ratios by water temperature and physiological effects. Likewise, $\delta^{18}O_{shell}$ is a dual proxy that simultaneously records temperature and the isotopic composition of the water. Unrecognized fluctuations in $\delta^{18}O_{water}$, which often occur in coastal settings due to evaporation and freshwater influx or precipitation, can thus result in erroneous temperature estimates. This study investigates the possibility of using shell microstructures as novel, independent proxy of environmental variables, in particular water temperature. The results are included in four manuscripts of which three are published in peer-review journals and one is currently under review in a peer-review journal.

Manuscript I studies the response of shell microstructures of *Cerastoderma edule* to the variation of water temperature during the growing season (May - September). Results indicate that the prism size and shape of the outer prismatic layer reflect changes in temperature. Structural units become larger and more elongated at higher temperatures. Based on this relationship, a model is developed and applied to other shells to test the usefulness of the proxy. Water temperature can be reconstructed with an error of ± 1.7 °C suggesting that microstructures may represent a promising tool for paleotemperature reconstructions.

Manuscript II investigates the effects of acidified conditions on *C. edule* shell formation and structure. Results show a decrease in shell production rate under hypercapnic conditions. Furthermore, ontogenetically young shell portions are affected by shell dissolution. However, the newly formed material is not altered by acidification. Prismatic microstructures do not show significant changes in shell hardness or the size and shape of individual biomineral units. According to this finding, microstructures are not sensitive to changes of pCO_2 and can therefore not be used as proxies for hypercapnia. However, a relationship between microstructure and hardness is observed, indicating that mechanical properties of the shells depend on the architecture at the µm-scale and the relative proportion of calcium carbonate and organic phases.

Manuscript III tests the effect of cooking on the shell microstructure of the gastropod *Phorcus turbinatus*. Aside from the overall appearance of the shell, microstructural organization, stable isotopes and mineralogy are investigated. As indicated by the data, boiling does not affect the shell integrity. However, roasting at temperatures between 300 and 700 °C induces shifts in shell coloration, enlargement of microstructural units, alteration of the chemical composition and transformation

of aragonite into calcite. These features provide a toolkit to identify paleocooking methods and to ensure a suitable selection of shell material for paleoenvironmental reconstructions.

Manuscript IV explores the sensitivity of shell microstructures of *Arctica islandica* to environmental conditions. Mollusks were cultured with different food sources and at different water temperatures to identify which variables affect the crystallographic organization of the shell carbonate. Although shell growth is significantly altered by both parameters, microstructures do not respond in a similar way. A rise in water temperature induces a change in the crystallographic orientation of the structural units. However, different diets do not have the same effect. Furthermore, the composition and distribution of the typical pigments (polyenes) does not seem to vary in response to the food source. The results indicate that microstructure orientation can serve as a new, independent paleothermometer in this species.

Zusammenfassung

Mollusken stellen einzigartige hochauflösende Archive dar, aus denen man vergangene Umweltveränderungen ablesen kann. Durch ihr periodisches Schalenwachstum bilden sie bestimmte Wachstumsmuster aus, die wie ein Kalender genutzt werden können. Umweltbedingungen werden in den Schalen in Form von geochemischen und strukturellen Eigenschaften gespeichert und können durch Wachstumslinien und -inkremente auf den Tag, Monat oder das Jahr genau datiert werden. Es ist jedoch weiterhin eine große Herausforderung, quantitative Datensätze über Umweltparameter, wie Wassertemperatur, aus Molluskenschalen zu bestimmen. So ist beispielsweise die Wachstumsrate der Schale sowohl von der Wassertemperatur als auch von der Nahrungsverfügbarkeit abhängig. Das Sr/Ca und Mg/Ca Verhältnis in der Schale wird von der Wassertemperatur und bestimmten physiologischen Effekten beeinflusst. Ebenso ist $\delta^{18}O_{schale}$ ein dualer Proxy, der gleichzeitig die Temperatur und die isotopische Zusammensetzung des Wassers widerspiegelt. Unerkannt bleibende Fluktuationen im $\delta^{18}O_{wasser}$ treten aufgrund von Verdunstung und Frischwassereintrag häufig in Küstenregionen auf und können somit zu fehlerhaften Temperaturschätzungen führen. Diese Arbeit behandelt die Möglichkeit, die Mikrostruktur der Molluskenschale als neuen, unabhängigen Proxy für Umweltkenngrößen (insbesondere Wassertemperatur) zu verwenden. Die Ergebnisse werden in vier Manuskripten dargelegt, von denen drei in anerkannten Fachzeitschriften (peer-reviewed) publiziert sind, während eines sich derzeit im Reviewprozess befindet.

Manuskript I behandelt die Reaktion der Schalenmikrostruktur *Cerastoderma edule* auf Schwankungen der Wassertemperatur während der Wachstumssaison (Mai - September). Die Ergebnisse weisen darauf hin, dass die Form der äußeren Prismenschicht, sowie die Prismenform Temperaturveränderungen widerspiegeln. Strukturelle Prismeneinheiten werden bei höheren Temperaturen größer und

gestreckter ausgebildet. Aufgrund dieses Zusammenhanges wird ein Modell entwickelt und auf weitere Molluskenschalen angewendet, um die Nutzbarkeit dieses Proxys zu testen. Wassertemperaturen können mit einer Fehlergenauigkeit von ± 1.7 °C rekonstruiert werden. Die Analyse der Schalenmikrostruktur kann somit als vielversprechende neue Methode zur Rekonstruktion von Paläotemperaturen eingesetzt werden.

Manuskript II untersucht den Effekt von saurem Milieu auf die Schalenstruktur und -bildung bei *C. edule*. Die Ergebnisse zeigen eine verminderte Schalenbildungsrate unter erhöhtem CO_2-Druck. Weiterhin sind jüngere ontogenetische Stadien von einer Auflösung der Schale betroffen. Neugebildetes Schalenmaterial ist nicht von der Ansäuerung betroffen. Prismatische Mikrostrukturen zeigen keine signifikanten Veränderungen in Schalenhärte oder Größe und Form der einzelnen Prismeneinheiten. Daraus wird geschlossen, dass die Schalenmikrostruktur nicht sensitiv für Veränderungen im CO_2-Druck ist und somit nicht als Proxy für Hyperkapnie genutzt werden kann. Es wird jedoch ein Zusammenhang zwischen Mikrostruktur und Schalenhärte beobachtet, der darauf hinweist, dass die mechanischen Eigenschaften der Schale sowhol von der Schalenarchitektur im µm-Bereich, als auch von dem relativen Kalziumkarbonatgehalt der organischen Phase abhängig sind.

Manuskript III prüft welchen Einfluss Kochen auf die Schalenmikrostruktur *Phorcus turbinatus* ausübt. Neben generellen Veränderungen im Erscheinungsbild wird die Mikrostruktur, stabile Isotopensignatur und Mineralogie untersucht. Die Ergebnisse zeigen keine Veränderung der Schalenintegrität durch Kochen. Durch Rösten bei Temperaturen zwischen 300 und 700°C treten jedoch Veränderungen in der Färbung, eine Vergrößerung der mikrostrukturellen Einheiten, Veränderungen der chemischen Zusammensetzung, sowie die Transformation von Aragonit zu Kalzit auf. Derartige Kriterien können als Indiz zur Identifizierung von Paläokochmethoden eingesetzt werden und helfen geeignetes Schalenmaterial zur Rekonstruktion vergangener Lebensräume auszuwählen.

Manuskript IV untersucht die Empfindlichkeit der Schalenmikrostruktur von *Arctica islandica* auf bestimmte Umweltbedingungen. Die Mollusken wurden mit verschiedenen Nahrungstypen und unter unterschiedlichen Wassertemperaturen kultiviert, um zu bestimmen welche Variablen die kristallographische Organisation des Schalenkarbonats beeinflussen. Obwohl das Schalenwachstum durch beide Parameter signifikant verändert wird, reagiert die Mikrostruktur nicht gleichermaßen. Ein Anstieg der Wassertemperatur verursacht eine Veränderung der kristallographischen Organisation der einzelnen strukturellen Einheiten. Unterschiedliche Nahrungsquellen haben keinen derartigen Einfluss. Ebenso scheinen Zusammensetzung und Verteilung von typischen Schalenpigmenten (Polyenen) nicht durch die Nahrungswahl beeinflusst zu werden. Diese Ergebnisse zeigen, dass die Orientierung der mikrostrukturellen Elemente als neues unabhängiges Paläothermometer für diese Art eingesetzt werden kann.

Acknowledgements

Not displayed for reasons of data protection.

Table of contents

List of figures

Manuscript I

Manuscript II

Manuscript III

Manuscript IV

List of tables

Manuscript I

Manuscript II

Manuscript III

Manuscript IV

Chapter 1 - Introduction

1.1 Reconstructing past environments

The understanding of the climate system of the Earth has significantly progressed in the last few decades. Along with it, the ability of modeling climatic events gained remarkable importance (Edwards, 2011). In order to enhance the confidence of climate forecasts it is required to obtain reliable environmental data from the past (Annan et al., 2005; Wanamaker et al., 2007). Understanding oceanographic and atmospheric dynamics and how they influenced the climate through time is a key tool to interpret modern climate variability and predict the future climate. Furthermore, reconstructing past conditions can throw light on the complex relationship between environment and human evolution (Reitz et al., 1996). By influencing food and shelter availability, climate changes are likely to affect major human dispersal and subsistence strategies (Mannino et al., 2002; Farr et al., 2014).

To extract information about climate prior to the instrumental era, paleoclimatology studies rely on data recorded in abiogenic or biogenic archives (Jones and Mann, 2004). Ice cores (Meese et al., 1997; Svensson et el., 2008; Lemieux-Dudon et al., 2010), speleothems (Bar-Matthews et al., 1997; Hellstrom et al., 1998; Jex et al., 2011) lake and marine sediments and loess (Lamy et al., 1999; Porter, 2001; Conroy et al., 2008) are the most commonly used abiogenic archives. Examples of biogenic archives include tree-rings (Hughes et al., 1986, Sheppard et al., 2004; Siegert et al., 2014), corals (Sinclair et al., 1998; Correge, 2006; Rüggeberg et al., 2008), pollen (Peyron et al., 1998; Elenga et al., 2000), fish otoliths (Ivany et al., 2000; Elsdon and Gillanders, 2003; Reinthal et al., 2011) and mollusk shells (Mutvei et al., 2001; Schöne et al., 2004; Butler et al., 2010). Estimates of temperature, the most important climate variable, are achieved by using geochemical proxies such as isotopes ($\delta^{18}O$, δD, Δ_{47}), element ratios (i.e. Mg/Ca, Sr/Ca) and structural proxies such growth increments width and sediment layer thickness.

The archives mainly differ from each other by resolution and timescale. In general, abiogenic archives cover long time-scales with a relatively low temporal resolution. They have been successfully used to investigate long-term climatic changes (Jouzel et al., 1987; Petit et al., 1999). However, these archives cannot resolve critical short-term climatic fluctuations. Seasonal and annual climatic events and cycles such as ENSO can have important consequences on the global dynamics through teleconnections (Cobb et al., 2003; Carré et al., 2012). Other short-term events such as volcanic eruptions and anthropogenic forcing can also exert significant influence on the large-scale climate system (Robock, 2001). To understand short-term climatic variability and its impact on long time scales, high-resolution paleoclimate data are of great relevance.

1.2 Mollusk shells as high-resolution paleoenvironmental archives

Mollusks represent a valuable tool for high-resolution paleoclimate reconstructions. The formation of their shells occurs in close connection with the physical and chemical conditions of the ambient environment. For this reason, seasonal and daily environmental variations are recorded in the shells. Furthermore they are often preserved for significant amounts of time without being altered.

The production of shell carbonate (predominantly calcite and aragonite) and organic material occurs periodically (Clark, 1975; Jones, 1983). Periods of fast growth alternate with periods of slow growth resulting in the formation of distinct growth patterns, i.e., growth increments and growth lines, respectively. The periodicity is driven by internal biological clocks, which are constantly reset by the light/dark cycle, tides and temperature cycles (Pittendrigh, 1979; Richardson et al., 1979; Richardson et al., 1980. The rhythm regulating shell growth allows increments and lines to be used as calendar in the way that each shell portion can be temporally contextualized (Schöne et al., 2003b; Schöne, 2013). By quantifying specific geochemical and structural properties contained in the growth increments, environmental reconstructions with subseasonal temporal resolution can be achieved (Freitas et al., 2006; Miyaji et al., 2007).

As sessile organisms, bivalves record local environmental conditions throughout life, which can be remarkably long in some species. For instance, the freshwater mussel *Margaritifera margaritifera* can live up to 200 years (Mutvei and Westermark, 2001), and the marine clam *Arctica islandica* attains 500 years (Butler et al., 2013). With these organisms it is possible to reconstruct climate over long time intervals (Wanamaker et al., 2011; Schöne, 2013). Furthermore, bivalves are extremely widespread and live in a large number of different aquatic habitats. Their biogeographic distribution ranges from freshwater to marine, from brackish environments to the deep sea, from cold to tropical waters, ensuring an extraordinary applicability as paleoclimate archives on a global scale.

1.3 Mollusk shell proxies

Up to date, various shell geochemical and structural properties are exploited as paleoenvironmental proxies. However, physiological influences and complex biomineralization processes can make the interpretation of the record particularly challenging (Gillikin et al., 2005b; Wanamaker et al., 2008b; Schöne, 2008). In order to develop reliable climatic reconstructions, an extensive and critical knowledge of the proxies and their major limitations is required. The following paragraphs will offer an overview of the most commonly used proxies highlighting their applicability in paleoenvironmental studies.

1.3.1 Growth rate

Generally, favorable conditions result in faster growth which in turn, translates into enhanced competition abilities, greater reproduction success and ultimately to higher survival chances. Since contemporaneous specimens of the same habitat grow at similar relative rates, it is possible to combine growth increment width chronologies of individual specimens into longer stacked chronologies spanning centuries to millennia and many generations of bivalves (Scourse et al., 2006; Black et al. 2008; Butler et al., 2010; Lohmann and Schöne, 2013; Holland et al., 2014). This technique is known as crossdating and has been initially developed in dendrochronology (Fritts, 1976; Cook and Kairiukstis, 1990; Marchitto et al., 2000; Schöne et al., 2003a).

Although critical for chronology development, synchronous growth does not explicitly reveal which factors influence similar biomineralization rates. Water temperature has been suggested to play an important role in this process (i.e. Schöne et al., 2005; Wanamaker et al., 2008a; Hallmann et al., 2011). However, it is still not well resolved which factors trigger shell production rate at which proportion and why. Potential factors controlling shell formation include temperature, food availability, physiology and ontogenetic age (Jones, 1983; Witbaard et al., 1997; Butler et al., 2013; Lohmann and Schöne, 2013). The sensitivity of shell growth rate to multiple factors represents a considerable limitation of its application in paleoenvironmental reconstructions.

1.3.2 Oxygen isotope composition

The ratio between ^{18}O and ^{16}O of a shell relative to the $^{18}O/^{16}O$ ratio of a standard, defined as $\delta^{18}O_{shell}$, is widely used in paleoclimatology and archeology as a paleothermometer (e.g., Epstein et al., 1953; Grosman & Ku, 1986; Schöne et al., 2004; Surge and Barrett, 2012; Prendergast et al., 2013). At low temperatures, slightly more heavy oxygen isotopes (^{18}O) are incorporated in the crystal lattice than light isotopes (^{16}O) and vice versa. The negative quasi-linear relationship between $\delta^{18}O_{shell}$ and temperature has been experimentally determined (Epstein et al., 1953; Grossman and Ku, 1986).

Although being a relatively well-established proxy, there are some important aspects to consider when using $\delta^{18}O_{shell}$. Besides mirroring water temperature, the oxygen ratio of the shell also reflects the isotopic composition of the ambient water, resulting in a dual proxy (Schöne et al., 2013). Disentangling temperature signals from $\delta^{18}O_{water}$ fluctuations (i.e., salinity variations) can be particularly challenging, especially in nearshore environments where evaporation, freshwater influx onto the ocean and precipitation occur (Klein et al., 1996; Gillikin et al., 2005b). Furthermore, for time intervals prior to the instrumental era and at remote localities, $\delta^{18}O_{water}$ fluctuations are not known. Independent temperature estimates are then crucial (Walliser et al., 2016). Diagenetic processes represent another challenge as they can lead to mineralogical alterations which involves changes of $\delta^{18}O_{shell}$.

1.3.3 Carbonate clumped isotopes

Unlike $\delta^{18}O_{shell}$ thermometry, carbonate clumped isotope values (Δ_{47}) provide the possibility of reconstructing temperature independently from the isotopic composition of the water (Eiler, 2011). The innovative method is based on the bond formation ('clumping') between two heavy isotopes (i.e. ^{13}C and ^{18}O) into the same carbonate ion group ($^{13}C^{18}O^{16}O_2^{2-}$). In biogenic carbonates, there are twenty isotopic variations or isotopologues of the ionic group. According to number of rare isotopes contained in the each of them, they are defined as singly and multiply substituted isotopologues (Ghosh et al., 2006). Clumping of the isotopes is promoted at low temperatures increasing the abundance of multiply substituted isotopologues and allowing the use of Δ_{47} as a direct paleothermometer (Henkes et al., 2013). Furthermore, this proxy can be used to reconstruct ancient water isotopic composition of oceans and to complement $\delta^{18}O_{shell}$ information.

However, a sample size of 9-24 mg of powder carbonate material is required for the analysis (3-8 mg for each replica, at least 3 replicas are needed; Affek, 2012). Such sample amounts represent an important limitation when analyzing shells at subannual resolution or when using small specimens.

1.3.4 Element-to-calcium ratios

Trace elements are carried to the site of mineralization through active and passive (channels) transportation systems (Wheeler, 1992; Gillikin et al., 2005b; Carré et al., 2006). In particular, the incorporation of cations such as Sr^{2+}, Mg^{2+} and Ba^{2+} into the crystal lattice is promoted by similar ionic radii and electrochemical characteristics to Ca^{2+} (Kastner, 1999). In abiogenic aragonite, less strontium and magnesium are incorporated at higher temperature resulting in a negative Sr/Ca (or Mg/Ca) vs. temperature relationship (Kinsman and Holland, 1969; Dietzel et al., 2004; Gaetani and Cohen, 2006), whereas in calcite the opposite occurs (Lorens, 1981; Tesoriero and Pakow, 1996). In aragonitic bivalves the relative concentrations of strontium and magnesium have been observed to be inversely correlated to water temperature (Dodd, 1965; Klein et al., 1996; Schöne et al., 2011).

However, contrasting results suggest the relationship to be positive or not significant at all (Buchard and Fritz, 1978; Stecher et al., 1996; Hart and Blusztajn, 1998). This inconsistency suggests that a direct dependence to temperature may not be easily distinguishable. The incorporation of trace elements is likely strongly controlled by metabolic processes (Klein et al., 1996; Schöne et al., 2011, 2013), growth rate (Gillikin et al., 2005b) and kinetic effects (Lorrain et al., 2005). Due to such vital effects, it is very challenging to interpret the trace element content of shells and extract environmental information.

1.4 Shell formation

Biomineralization is an elaborate process through which mollusks and many other organisms produce minerals to protect their soft tissues. Biogenic materials are remarkably complex at the micrometer and nanometer scale, and their structural hierarchal organization distinguishes them from pure abiogenic minerals. Furthermore, biogenic carbonates are characterized by exceptional hardness, which provides effective protection against physical predation and chemical environmental threats (Jackson et al., 1988; Kamat et al., 2000). In shells, enhanced mechanical strength and material stability are achieved by a structural interplay between the two major components: the inorganic mineral and the organic matrix (Weiner and Addadi, 1997; Dashkovskiy et al., 2007; Merkel et al., 2009).

The two major precursors of the inorganic component, essential for shell formation, are calcium ions (Ca^{2+}) and the bicarbonate ions (HCO_3^-) [in the case of marine carbonates]. The latter can partly derive from diet and from metabolic pathways (McConnaughey and Gillikin, 2008). The constituents are transported into the extrapallial space, situated between the mantle epithelium and the shell (Simkiss and Wilbur, 1989; Wheeler, 1992). Ca^{2+} can be transported either by energy consuming protein systems, i.e., Ca^{2+}ATPases, or passively through channels (Klein et al., 1996; Gillikin et al., 2005b; Carré et al., 2006) whereas the transport of HCO_3^- occurs mainly through passive diffusion (Wilbur and Saleuddin, 1983). Together with the mineral phase, organic macromolecules (i.e., chitin, acidic proteins) produced by the mantle are secreted into the extrapallial space (Addadi et al., 2006). Calcium ions are temporarily stored in membrane-coated granules in the form of amorphous calcium carbonate (ACC), a transient phase of aragonite and calcite important for microstructure formation (Watabe et al., 1976; Weiner et al., 2003; Fitzer et al., 2016). At the calcification site, the vesicle membrane opens and the ACC comes into contact with the aqueous environment and becomes unstable. This destabilization sets the starting point for the crystallization (Addadi et al., 2006). The role of the organic matrix is to form the imprint for crystals, and it contains proteins that function as nucleators. To achieve a controlled crystallization, these macromolecules promote crystal formation at a specific site (Gotliv et al., 2003; Nudelman et al., 2006).

1.4.1 Shell microstructures

Shells are formed by superimposition of two or more layers of calcium carbonate with different organizations and, in some cases, different mineralogical phases. Shell microstructures are the fundamental level of the biomaterial organization, ranging between nanometer and micrometer scales in size (Bøggild, 1930; Carter et al., 1990; Carter et al., 2012). Each unit is separated from the others by thin envelopes of organic matter. In the following, the seven main types of microstructures are briefly described.

(a) **Prismatic microstructures**: Elongated units with opposite long sides parallel. Prisms do not strongly interdigitate along their boundaries. According to their size, they are defined as coarse (width > 100 μm), medium (5 μm > width > 100 μm) and fine (width < 5 μm).

(b) **Laminar microstructures**: Flat units (roths, laths, blades or tablets) mutually parallel or slightly overlapping. They include nacreous and semi-nacreous microstructures.

(c) **Crossed microstructures**: Nonprismatic, nonlaminar structures formed by basic units with different dip directions. They represent structurally complex designs, which are commonly found in bivalves and gastropods.

(d) **Spherulitic microstructures**: Spherical and subspherical aggregates formed by elongated units, which grow from the center with a radial direction.

(e) **Homogenous microstructures**: Equidimensional and irregularly shaped units arranged with no particular geometrical organization. They can be fine (width < 5 μm) or coarse grained (width >5 μm). The latter are defined as “granular” microstructures.

(f) **Helical microstructures**: Coiled helical rods with the helix axes orientated perpendicular to the depositional surface. They are rarely observed in bivalves.

(g) **Isolated spicules**: Individual regular-shapes structures sparse with the tissue layer.

1.5 Objectives of the research

This study aims to develop new environmental proxies based on shell microstructural properties. Due to their extreme diversity among mollusk species, microstructures have been extensively investigated for taxonomic classification and to reveal evolutionary change (Bøggild, 1930; Taylor, 1973; Popov, 1974; Carter et al., 2012). Besides the purely descriptive approach, a growing interest toward a deeper understanding of the biomineralization process set the basis for studies on mechanisms of microstructure formation and organization (Wada, 1961; Lowenstam and Weiner, 1989; Marin et al., 2012). It has been demonstrated that environmental conditions exert a certain degree of control on shell development. For instance, water temperature resulted correlated with the nacre unit size of *Geukensia demissa* (Lutz, 1964), with the orientation of *Viviparus viviparus* lamellae (Füllenbach et al., 2014) and with the microstructure type of *Corbicula fluminea* (Tan Tiu and Prezant, 1989). Similarly, seasonal temperature fluctuations have been associated with variations in shell architecture of *Polymesoda caroliniana* and *Scapharca broughtonii* (Tan Tiu, 1988; Nishida et al., 2012). Morphological alterations of the microstructures have been reported in *Bathymodiolus azoricus* when subjected

to different pressure conditions (Kadar et al., 2008). Likely, changes in CO_2 of the water affect the orientation of the carbonate units in *Mytilus edulis* (Hahn et al., 2012; Fitzer et al., 2014).

Although the results throw some light on the potential factors triggering shell organization, the research is still in its infancy and the processes involved are far from being completely understood. Expanding our knowledge on the relationship between shell architecture and environment can provide important insights into the structural design of new hybrid materials inspired by naturally mineralized tissues and can be applicable in tissue repair and regeneration processes. If microstructures function as independent environmental proxies, this can also further enhance the importance of mollusk shells as climate archives. In fact, microstructures may overcome some of the limitations of the existing proxies described in section 1.3. Furthermore, in contrast to geochemical proxies, microstructures have a high preservation potential and can be applied to the fossil record. Microstructures can also provide information on ancient human practices and behavior.

Each of the four projects included in the present work analyzes different mollusk species and tackle specific questions. In the following, the rationale behind each project is briefly outlined.

Manuscript I: Previous works have suggested that shell microstructure formation and organization are sensitive to the environment (Prezant et al., 1988: Nishida et al., 2012). However, the research was merely based on qualitative and descriptive approaches. The first project quantified morphological changes of biomineral units in shells of *Cerastoderma edule* (common cockle) and investigated whether these changes are related to environmental variables.

Manuscript II: Ocean acidification represents a serious threat to marine calcifiers, including bivalves (Delille et al., 2005; Ries et al., 2009). Their response to low pH not only provides useful information to predict the future effect of increased pCO_2 on benthic communities, but potentially also to reconstruct past pCO_2. Previous studies came to opposite conclusions regarding the effect of ocean acidification on mollusk shells. Some studies observed a change at the microstructural level (Hahn et al., 2012; Fitzer et al., 2014), whereas others did not (Hiebenthal et al., 2013; Stemmer et al., 2013). Microstructural characteristics and mechanical conditions of the mineral may hold the key to interpret changes of the biomineralization in acidified waters. In the second manuscript, the influence of increased pCO_2 on microstructural and mechanical properties of *C. edule* shells was tested and their possible use as proxies assessed.

Manuscript III: Human exploitation of mollusks dates back to ~ 160 ka (Marean et al., 2007). Shells can provide critical information on the relationship between humans and the environment in which they lived (Andrus et al., 2011; Prendergast et al., 2013). For instance, subsistence behaviors, settlement systems and migratory movements can be inferred by mollusk collection patterns (Colonese et al., 2009; Mannino et al., 2011; Prendergast et al., 2015). Since mollusks were part of the human diet, it is likely that they were cooked prior their consumption

(Barker et al., 2010; Hunt et al., 2011; Hill et al., 2015). Heat treatment may potentially alter the shell material. The aim of manuscript number three was to investigate the effects of food processing treatments on the marine gastropod *Phorcus turbinatus* shell and the use of microstructural and geochemical alteration for paleodiet reconstructions.

Manuscript IV: Due to its extreme longevity, the shell of the ocean quahog, *Arctica islandica* is frequently used as marine paleoclimate archive (i.e. Holland et al., 2014; Marali et al., 2015; Wanamaker et al., 2007b). However, its growing season and the factors triggering seasonal growth rate are not well understood. In this study, the influence of water temperature and diet composition on *A. islandica* shell production rate was investigated. Furthermore, the effects of the two variables on microstructural organization and pigmentation were investigated together with the possibility of using changes of the microstructure for environmental reconstructions.

1.6 References

Addadi, L., Joester, D., Nudelman, F., Weiner, S., 2006. Mollusk shell formation: a source of new concepts for understanding biomineralization processes. Chemistry 12, 980-7.

Affek, H.P., 2012. Clumped isotope paleothermometry: principles, applications, and challenges. Paleontol. Soc. Pap. 18, 101-114.

Andrus, C.F.T., 2011. Shell midden sclerochronology. Quat. Sci. Rev. 30, 2892-2905.

Annan, J.D., Hargreaves, J.C., Ohgaito, R., Abe-Ouchi, A., Emori, S., 2005. Efficiently constraining climate sensitivity with ensembles of paleoclimate simulations. Sola 1, 181-184.

Barker, G., Antoniadou, A., Armitage, S., Brooks, I., Candy, I., Connell, K., Douka, K., Drake, N., Farr, L., Hill, E., Hunt, C., Inglis, R., Jones, S., Lane, C., Lucarini, G., Meneeley, J., Morales, J., Mutri, G., Prendergast, A., Rabett, R., Reade, H., Reynolds, T., Russell, N., Simpson, D., Smith, B., Stimpson, C., Twati, M., White, K., 2010. The Cyrenaican Prehistory Project 2010: the fourth season of investigations of the Haua Fteah cave and its landscape, and further results from the 2007-2009 fieldwork. Libyan Stud. 41, 63-88.

Bar-Matthews, M., Ayalon, A., Kaufman, A., 1997. Late Quaternary paleoclimate in the Eastern Mediterranean region from stable isotope analysis of speleothems at Soreq Cave, Israel. Quat. Res. 47, 155-168.

Black, B.A., Gillespie, D.C., MacLellan, S.E., Hand, C.M., 2008. Establishing highly accurate production-age data using the tree-ring technique of crossdating: a case study for Pacific geoduck (*Panopea abrupta*). Can. J. Fish. Aquat. Sci. 65, 2572-2578.

Bøggild, O.B., 1930. The shell structure of the mollusks, in: Det Kongelige Danske Videnskabernes Selskabs Skrifter, Natruvidenskabelig Og Mathematisk. Afdeling, pp. 231-326.

Buchardt, B., Fritz, P., 1978. Strontium uptake in shell aragonite from the freshwater gastropod *Limnaea stagnalis*. Science 199, 291-292.

Butler, P.G., Wanamaker, A.D., Scourse, J.D., Richardson, C.A., Reynolds, D.J., 2013. Variability of marine climate on the North Icelandic Shelf in a 1357-year proxy archive based on growth increments in the bivalve *Arctica islandica*. Palaeogeogr. Palaeoclimatol. Palaeoecol. 373, 141-151.

Butler, P.G., Richardson, C.A., Scourse, J.D., Wanamaker, A.D., Shammon, T.M., Bennell, J.D., 2010. Marine climate in the Irish Sea: analysis of a 489-year marine master chronology derived from growth increments in the shell of the clam *Arctica islandica*. Quat. Sci. Rev. 29, 1614-1632.

Carré, M., Azzoug, M., Bentaleb, I., Chase, B.M., Fontugne, M., Jackson, D., Ledru, M.P., Maldonado, A., Sachs, J.P., Schauer, A.J., 2012. Mid-Holocene mean climate in the south eastern Pacific and its influence on South America. Quat. Int. 253, 55-66.

Carré, M., Bentaleb, I., Bruguier, O., Ordinola, E., Barrett, N.T., Fontugne, M., 2006. Calcification rate influence on trace element concentrations in aragonitic bivalve shells: evidences and mechanisms. Geochim. Cosmochim. Acta 70, 4906-4920.

Carter, J.G., Bandel, K., De Buffrenil, V., Carlson, S., Castanet, J., Dalingwater, J., Francillon-Vieillot, H., Geraudie, J., Meunier, F.J., Mutvei, H., De Ricqles, A., Sire, J.Y., Smith, A., Wendt, J., Williams, A., Zylberberg, L., 1990. Glossary of Skeletal Biomineralization, in: Carter, J.G. (Ed.), Skeletal Biomineralization: Patterns, Processes and Evolutionary Trends. New York: Van Nostrand Reinhold. pp. 337-352.

Carter, J.G., Harries, P.J., Malchus, N., Sartori, A.F., Anderson, L.C., Bieler, R., Bogan, A.E., Coan, E.V., Cope, J.C.W., Cragg, S.M., Garcia-March, J.R., Hylleberg, J., Kelley, P., Kleemann, K., Kriz, J., McRoberts, C., Mikkelsen, P.M., Pojeta, J.J., Temkin, I., Yancey, T., Zieritz, A., 2012. Illustrated glossary of the Bivalvia. Treatise Online 1. pp. 209.

Chateigner, D., Hedegaard, C., Wenk, H.R., 2000. Mollusc shell microstructures and crystallographic textures. J. Struct. Geol. 22, 1723-1735.

Clark II, G.R., 1975. Periodic growth and biological rhythms in experimentally grown bivalves. In: Rosenberg, G.D., Runcorn, S.K. (Eds.), Growth Rhythms and the history of the Earth‘s rotation. J.Wiley and Sons, New York, pp. 103-117.

Cobb, K.M., Charles, C.D., Cheng, H., Edwards, R.L., 2003. El Niño/Southern Oscillation and tropical Pacific climate during the last millennium. Nature 424, 271-276.

Colonese, A.C., Troelstra, S., Ziveri, P., Martini, F., Lo Vetro, D., Tommasini, S., 2009. Mesolithic shellfish exploitation in SW Italy: seasonal evidence from the oxygen isotopic composition of *Osilinus turbinatus* shells. J. Archaeol. Sci. 36, 1935-1944.

Conroy, J.L., Overpeck, J.T., Cole, J.E., Shanahan, T.M., Steinitz-Kannan, M., 2008. Holocene changes in eastern tropical Pacific climate inferred from a Galápagos lake sediment record. Quat. Sci. Rev. 27, 1166-1180.

Cook, E.R., Kairiukstis, L.A., 1990. Methods of dendrochronology. Applications in the Environmental Sciences. Kluwer, Dordrecht, Netherlands. pp. 394.

Correge, T., 2006. Sea surface temperature and salinity reconstruction from coral geochemical tracers. Palaeogeogr. Palaeoclimatol. Palaeoecol. 232, 408-428.

Dashkovskiy, S., Suhr, B., Tushtev, K., Grathwohl, G., 2007. Nacre properties in the elastic range: influence of matrix incompressibility. Comput. Mater. Sci. 41, 96-106.

Delille, B., Harlay, J., Zondervan, I., Jacquet, S., Chou, L., Wollast, R., Bellerby, R.G.J., Frankignoulle, M., Borges, A.V., Riebesell, U., Gattuso, J.P., 2005. Response of primary production and calcification to changes of pCO_2 during experimental blooms of the coccolithophorid *Emiliania huxleyi*. Global Biogeochem. Cycles 19(2).

Dettman, D.L., Reische, A.K., Lohmann, K.C., 1999. Controls on the stable isotope composition of seasonal growth bands in aragonitic fresh-water bivalves (unionidae). Geochim. Cosmochim. Acta 63, 1049-1057.

Dietzel, M., Gussone, N., Eisenhauer, A., 2004. Co-precipitation of Sr^{2+} and Ba^{2+} with aragonite by membrane diffusion of CO between 10 and 50 °C. Chem. Geol. 203, 139-151.

Dodd, J.R., 1965. Environmental control of strontium and magnesium in *Mytilus*. Geochim. Cosmochim. Acta 29, 385-398.

Edwards, P.N., 2011. History of climate modeling. Wiley Interdiscip. Rev. Clim. Chang. 2, 128-139

Eiler, J.M., 2011. Paleoclimate reconstruction using carbonate clumped isotope thermometry. Quat. Sci. Rev. 30, 3575-3588.

Elenga, H., Peyron, O., Bonnefille, R., Jolly, D., Cheddadi, R., Guiot, J., Andrieu, V., Bottema, S., Buchet, G., Hamilton, A.C., Maley, J., Marchant, R., Reille, M., Riollet, G., Scott, L., Straka, H., Taylor, D., Campo, E. Van, Vincens, A., Laarif, F., Jonson, H., 2000. Pollen-based biome reconstruction for southern Europe and Africa 18,000 yr BP. J. Biogeogr. 27, 621-634.

Elsdon, T.S., Gillanders, B.M., 2003. Reconstructing migratory patterns of fish based on environmental influences on otolith chemistry. Rev. Fish Biol. Fish. 13, 219-235.

Epstein, S., Buchsbaum, R., Lowenstam, H.M., Urey, H.C., 1953. Revised carbonate-water isotopic temperature scale. Bull. Geol. Soc. Am. 64, 1315-1326.

Farr, L., Lane, R., Abdulazeez, F., Bennett, P., Holman, J., Marasi, A., Prendergast, A., Al-Zweyi, M., Barker, G., 2014. The Cyrenaican Prehistory Project 2013: the seventh season of excavations in the Haua Fteah cave. Libyan Stud. 45, 163-173.

Fitzer, S.C., Chung, P., Maccherozzi, F., Dhesi, S.S., Kamenos, N.A., Phoenix, V.R., Cusack, M., 2016. Biomineral shell formation under ocean acidification: a shift from order to chaos. Sci. Rep. 6, 21076.

Fitzer, S.C., Phoenix, V.R., Cusack, M., Kamenos, N.A., 2014. Ocean acidification impacts mussel control on biomineralisation. Sci. Rep. 4.

Freitas, P.S., Clarke, L.J., Kennedy, H., Richardson, C. a., Abrantes, F., 2006. Environmental and biological controls on elemental (Mg/Ca, Sr/Ca and Mn/Ca) ratios in shells of the king scallop *Pecten maximus*. Geochim. Cosmochim. Acta 70, 5119-5133.

Fritts, H.C., 1976. Tree Rings and Climate. Academic Press, London. pp. 567.

Füllenbach, C.S., Schöne, B.R., Branscheid, R., 2014. Microstructures in shells of the freshwater gastropod *Viviparus viviparus*: a potential sensor for temperature change? Acta Biomater. 10, 3911-21.

Gaetani, G.A., Cohen, A.L., 2006. Element partitioning during precipitation of aragonite from seawater: a framework for understanding paleoproxies. Geochim. Cosmochim. Acta 70, 4617-4634.

Ghosh, P., Adkins, J., Affek, H., Balta, B., Guo, W., Schauble, E.A., Schrag, D., Eiler, J.M., 2006. 13C-18O bonds in carbonate minerals: A new kind of paleothermometer. Geochim. Cosmochim. Acta 70, 1439-1456.

Gillikin, D.P., De Ridder, F., Ulens, H., Elskens, M., Keppens, E., Baeyens, W., Dehairs, F., 2005a. Assessing the reproducibility and reliability of estuarine bivalve shells (*Saxidomus giganteus*) for sea surface temperature reconstruction: Implications for paleoclimate studies. Palaeogeogr. Palaeoclimatol. Palaeoecol. 228, 70-85.

Gillikin, D.P., Lorrain, A., Navez, J., Taylor, J.W., André, L., Keppens, E., Baeyens, W., Dehairs, F., 2005b. Strong biological controls on Sr/Ca ratios in aragonitic marine bivalve shells. Geochemistry, Geophys. Geosystems 6. doi:10.1029/2004GC000874

Gotliv, B.A., Addadi, L., Weiner, S., 2003. Mollusk shell acidic proteins: In search of individual functions. ChemBioChem 4, 522-529.

Grossman, E.L., Ku, T., 1986. Oxygen and carbon isotope fractionation in biogenic aragonite: Temperature effects. Chem. Geol. 59, 59-74.

Hahn, S., Rodolfo-Metalpa, R., Griesshaber, E., Schmahl, W.W., Buhl, D., Hall-Spencer, J.M., Baggini, C., Fehr, K.T., Immenhauser, A., 2012. Marine bivalve shell geochemistry and ultrastructure from modern low pH environments: environmental effect versus experimental bias. Biogeosciences 9, 1897-1914.

Hallmann, N., Schöne, B.R., Irvine, G.V., Burchell, M., Cokelet, E.D., Hilton, M.R., 2011. An improved understanding of the Alaska coastal current: the application of a bivalve growth-temperature model to reconstruct freshwater-influenced paleoenvironments. Palaios 26, 346- 363.

Hart, S.R., Blusztajn, J., 1998. Clams as recorders of ocean ridge volcanism and hydrothermal vent field activity. Science 280, 883-886.

Hellstrom, J., Mcculloch, M., Stone, J., 1998. A Detailed 31,000-year record of climate and vegetation change, from the isotope geochemistry of two New Zealand speleothems. Quat. Res. 50, 167-178.

Henkes, G.A., Passey, B.H., Wanamaker, A.D.J., Grossman, E.L., Ambrose, W.G.J., Carroll, M.L., 2013. Carbonate clumped isotope compositions of modern marine mollusk and brachiopod shells. Geochim. Cosmochim. Acta 106, 307-325.

Hiebenthal, C., Philipp, E.E.R., Eisenhauer, A., Wahl, M., 2013. Effects of seawater pCO2 and temperature on shell growth, shell stability, condition and cellular stress of Western Baltic Sea *Mytilus edulis* (L.) and *Arctica islandica* (L.). Mar. Biol. 160, 2073-2087.

Hill, E.A., Hunt, C.O., Lucarini, G., Mutri, G., Farr, L., Barker, G., 2015. Land gastropod piercing during the Late Pleistocene and Early Holocene in the Haua Fteah, Libya. J. Archaeol. Sci. Reports 4, 320-325.

Holland, H.A., Schöne, B.R., Marali, S., Jochum, K.P., 2014. History of bioavailable lead and iron in the Greater North Sea and Iceland during the last millennium - a bivalve sclerochronological reconstruction. Mar. Pollut. Bull. 87, 104-16.

Hughes, M., Kelly, P.M., Pilcher, J.R. and LaMarche, V.C., 1982. Climate from tree rings. Cambridge University Press, Cambridge. pp. 233.

Hunt, C.O., Reynolds, T.G., El-Rishi, H. a., Buzaian, A., Hill, E., Barker, G.W., 2011. Resource pressure and environmental change on the North African littoral: Epipalaeolithic to Roman gastropods from Cyrenaica, Libya. Quat. Int. 244, 15-26.

Ivany, L.C., Patterson, W.P., Lohmann, K.C., 2000. Cooler winters as a possible cause of mass extinctions at the Eocene/Oligocene boundary. Nature 407, 887-890.

Jackson, A.P., Vincent, J.F.V., Turner, R.M., 1988. The mechanical design of nacre. Proc. R. Soc. B Biol. Sci. 234, 415-440.

Jex, C.N., Baker, A., Eden, J.M., Eastwood, W.J., Fairchild, I.J., Leng, M.J., Thomas, L., Sloane, H.J., 2011. A 500 yr speleothem-derived reconstruction of late autumn-winter precipitation, northeast Turkey. Quat. Res. 75, 399-405.

Jones, D.S., 1983. Sclerochronology: Shell record of the molluscan shell. Am. Sci. 71, 384-391.

Jones, P.D., Mann, M.E., 2004. Climate over past millennia. Rev. Geophys. 42, 1-42.

Jouzel, J., Lorius, C., Petit, J.R., Genthon, C., Barkov, N.I., Kotlyakov, V.M., Petrov, V.M., 1987. Vostok ice core: a continuous isotope temperature record over the last climatic cycle (160,000 years). Nature 329, 403-408.

Kadar, E., Checa, A.G., Oliveira, A.N.D.P., Machado, J.P., 2008. Shell nacre ultrastructure and depressurisation dissolution in the deep-sea hydrothermal vent mussel *Bathymodiolus azoricus*. J. Comp. Physiol. B Biochem. Syst. Environ. Physiol. 178, 123-130.

Kamat, S., Su, X., Ballarini, R., Heuer, A.H., 2000. Structural basis for the fracture toughness of the shell of the conch Strombus gigas. Nature 405, 1036-1040.

Kastner, M., 1999. Oceanic minerals: their origin, nature of their environment, and significance. Proc. Natl. Acad. Sci. U. S. A. 96, 3380-3387.

Kinsman, D.J.J., Holland, H.D., 1969. The co-precipitation of cations with $CaCO_3$, -IV. The co-precipitation of Sr^{2+} with aragonite between 16 °C and 96 °C. Geochim. Cosmochim. Acta 33, 1-17.

Klein, R.T., Lohmann, K.C., Thayer, C.W., 1996. Sr/Ca and $^{13}C/^{12}C$ ratios in skeletal calcite of *Mytilus trossulus*: Covariation with metabolic rate, salinity, and carbon isotopic composition of seawater. Geochim. Cosmochim. Acta 60, 4207-4221.

Lamy, F., Hebbeln, D., Wefer, G., 1999. High-resolution marine record of climatic change in mid-latitude Chile during the last 28,000 years based on terrigenous sediment parameters. Quat. Res. 51, 83-93.

Lemieux-Dudon, B., Blayo, E., Petit, J.R., Waelbroeck, C., Svensson, A., Ritz, C., Barnola, J.M., Narcisi, B.M., Parrenin, F., 2010. Consistent dating for Antarctic and Greenland ice cores. Quat. Sci. Rev. 29, 8-20.

Lohmann, G., Schöne, B.R., 2013. Climate signatures on decadal to interdecadal time scales as obtained from mollusk shells (*Arctica islandica*) from Iceland. Palaeogeogr. Palaeoclimatol. Palaeoecol. 373, 152-162.

Lorens, R.B., 1981. Sr, Cd, Mn and Co distribution coefficients in calcite as a function of calcite precipitation rate. Geochim. Cosmochim. Acta 45, 553-561.

Lorrain, A., Gillikin, D.P., Paulet, Y.M., Chauvaud, L., Le Mercier, A., Navez, J., André, L., 2005. Strong kinetic effects on Sr/Ca ratios in the calcitic bivalve *Pecten maximus*. Geology 33, 965-968.

Lowenstam, H.A., Weiner, S., 1989. On biomineralization. New York. pp.324.

Lutz, R.A., 1984. Paleoecological implications of environmentally-controlled variation in molluscan shell microstructure. Geobios 17, 93-99.

Mannino, M.A., Thomas, K.D., Leng, M.J., Di Salvo, R., Richards, M.P., 2011. Stuck to the shore? Investigating prehistoric hunter-gatherer subsistence, mobility and territoriality in a Mediterranean coastal landscape through isotope analyses on marine mollusc shell carbonates and human bone collagen. Quat. Int. 244, 88-104.

Mannino, M.A., Thomas, K.D., 2002. Depletion of a resource? The impact of prehistoric human foraging on intertidal mollusc communities and its significance for human settlement, mobility and dispersal. World Archaeol. 33, 452-474.

Marali, S., Schöne, B.R., 2015. Oceanographic control on shell growth of *Arctica islandica* (Bivalvia) in surface waters of Northeast Iceland - Implications for paleoclimate reconstructions. Palaeogeogr. Palaeoclimatol. Palaeoecol. 420, 138-149.

Marchitto, T.M., Jones, G.A., Goodfriend, G.A., Weidman, C.R., 2000. Precise temporal correlation of Holocene mollusk shells using sclerochronology. Quat. Res. 53, 236-246.

Marean, C.W., Bar-Matthews, M., Bernatchez, J.A., Fisher, E.C., Goldberg, P., Herries, A.I.R., Jacobs, Z., Jerardino, A., Karkanas, P., Minichillo, T., Nilssen, P.J., Thompson, E., Watts, I., Williams, H.M., 2007. Early human use of marine resources and pigment in South Africa during the Middle Pleistocene. Nature 449, 906-909.

Marin, F., Roy, N. Le, Marie, B., 2012. The formation and mineralization of mollusk shell. Front. Biosci. S4 4, 1099-1125.

McConnaughey, T.A., Gillikin, D.P., 2008. Carbon isotopes in mollusk shell carbonates. Geo-Marine Lett. 28, 287-299.

Meese, D.A., Gow, A.J., Alley, R.B., Zielinski, G.A., Grootes, P.M., Ram, M., Taylor, K.C., Mayewski, P.A., Bolzan, J.F., 1997. The Greenland Ice Sheet Project 2 depth-age scale : methods and results 102, 26,411-26,423.

Merkel, C., Deuschle, J., Griesshaber, E., Enders, S., Steinhauser, E., Hochleitner, R., Brand, U., Schmahl, W.W., 2009. Mechanical properties of modern calcite- (*Mergerlia truncata*) and phosphate-shelled brachiopods (*Discradisca stella* and *Lingula anatina*) determined by nanoindentation. J. Struct. Biol. 168, 396-408.

Miyaji, T., Tanabe, K., Schöne, B., 2007. Environmental controls on daily shell growth of *Phacosoma japonicum* (Bivalvia: Veneridae) from Japan. Mar. Ecol. Prog. Ser. 336, 141-150.

Mutvei, H., Westermark, T., 2001. How environmental information can be obtained from Naiad shells, in: Springer (Ed.), Ecology and evolution of the freshwater mussels Unionoidea. Ecological Studies. Berlin & Heidelberg, pp. 367-379.

Nishida, K., Ishimura, T., Suzuki, A., Sasaki, T., 2012. Seasonal changes in the shell microstructure of the bloody clam, *Scapharca broughtonii* (Mollusca: Bivalvia: Arcidae). Palaeogeogr. Palaeoclimatol. Palaeoecol. 363-364, 99-108.

Nudelman, F., Gotliv, B.A., Addadi, L., Weiner, S., 2006. Mollusk shell formation: mapping the distribution of organic matrix components underlying a single aragonitic tablet in nacre. J. Struct. Biol. 153, 176-187.

Petit, R.J., Raynaud, D., Basile, I., Chappellaz, J., Ritz, C., Delmotte, M., Legrand, M., Lorius, C., Pe, L., 1999. Climate and atmospheric history of the past 420,000 years from the Vostok ice core, Antarctica. Nature 399, 429-413.

Peyron, O., Guiot, J., Cheddadi, R., Tarasov, P., Reille, M., de Beaulieu, J.-L., Bottema, S., Andrieu, V., 1998. Climatic Reconstruction in Europe for 18,000 YR B.P. from pollen data. Quat. Res. 196, 183-196.

Pittendrigh, C.S., 1979. Some functional aspects of circadian pacemakers, in: Suda, M., Hayaishi, O., Nakagawa, H. (Eds.), Biological rhythms and their central mechanism. Elsevier/ North-Holland Biomedical Press, pp. 3-12.

Popov, S.V., 1974. Shell microstructure and the classification of the family Cardiidae. pp. 28.

Porter, S.C., 2001. Chinese loess record of monsoon climate during the last glacial-interglacial cycle. Earth-Science Rev. 54, 115-128.

Prendergast, A.L., Azzopardi, M., O'Connell, T.C., Hunt, C., Barker, G., Stevens, R.E., 2013. Oxygen isotopes from *Phorcus* (*Osilinus*) *turbinatus* shells as a proxy for sea surface temperature in the central Mediterranean: A case study from Malta. Chem. Geol. 345, 77-86.

Prendergast, A.L., Stevens, R.E., O'Connell, T.C., Fadlalak, A., Touati, M., Al-Mzeine, A., Schöne, B.R., Hunt, C.O., Barker, G., 2015. Changing patterns of eastern Mediterranean shellfish exploitation in the Late Glacial and Early Holocene: Oxygen isotope evidence from gastropod in Epipaleolithic to Neolithic human occupation layers at the Haua Fteah cave, Libya. Quat. Int. In press.

Reinthal, P.N., Cohen, A.S., Dettman, D.L., 2011. Fish fossils as paleo-indicators of ichthyofauna composition and climatic change in Lake Malawi, Africa. Palaeogeogr. Palaeoclimatol. Palaeoecol. 303, 126-132.

Reitz, E.J., Newsom, L.A., Scudder, S.J., 1996. Issues in environmental archaeology Case Studies in Environmental Archaeology, 3-16

Richardson, C.A., Crisp, J., Runham, N.W., 1979. Tidally deposited growth bands in the shell of the common cockle, *Cerastoderma edule* (L.). Malacologia 277-290.

Richardson, C.A., Crisp, D.J., Runham, N.W., 1980. An endogenous rhythm in shell deposition in *Cerastoderma edule*. J. mar. biol. Ass UK 60, 991-1004.

Ries, J.B., Cohen, a. L., McCorkle, D.C., 2009. Marine calcifiers exhibit mixed responses to CO_2-induced ocean acidification. Geology 37, 1131-1134.

Robock, A., 2001. Volcanic eruption, Tambora. In: Munn, T. (Ed.), Encyclopedia of global environmental change, vol. 1. John Wiley and Sons, London, pp. 737-738.

Rüggeberg, A., Fietzke, J., Liebetrau, V., Eisenhauer, A., Dullo, W.-C., Freiwald, A., 2008. Stable strontium isotopes ($\delta^{88/86}$Sr) in cold-water corals - A new proxy for reconstuction of intermediate ocean water temperature. Earth Planet. Sci. Lett. 269, 569-574.

Schöne, B.R., 2008. The curse of physiology—challenges and opportunities in the interpretation of geochemical data from mollusk shells. Geo-Marine Lett. 28, 269-285.

Schöne, B.R., 2013. *Arctica islandica* (Bivalvia): a unique paleoenvironmental archive of the northern North Atlantic Ocean. Glob. Planet. Change 111, 199-225.

Schöne, B.R., Oschmann, W., Rössler, J., Freyre Castro, A.D., Houk, S.D., Kröncke, I., Dreyer, W., Janssen, R., Rumohr, H., Dunca, E., 2003a. North Atlantic Oscillation dynamics recorded in shells of a long-lived bivalve mollusk. Geology 31, 1037-1040.

Schöne, B.R., Tanabe, K., Dettman, D.L., Sato, S., 2003b. Environmental controls on shell growth rates and δ18O of the shallow marine bivalve mollusk *Phacosoma japonicum* in Japan. Mar. Biol. 142, 473-485.

Schöne, B.R., Freyre Castro, A.D., Fiebig, J., Houk, S.D., Oschmann, W., Kröncke, I., 2004. Sea surface water temperatures over the period 1884-1983 reconstructed from oxygen isotope ratios of a bivalve mollusk shell (*Arctica islandica*, southern North Sea). Palaeogeogr. Palaeoclimatol. Palaeoecol. 212, 215-232.

Schöne, B.R., Fiebig, J., Pfeiffer, M., Gleß, R., Hickson, J., Johnson, A.L.A., Dreyer, W., Oschmann, W., 2005. Climate records from a bivalved Methuselah (*Arctica islandica*, Mollusca; Iceland). Palaeogeogr. Palaeoclimatol. Palaeoecol. 228, 130-148.

Schöne, B.R., Zhang, Z., Radermacher, P., Thébault, J., Jacob, D.E., Nunn, E. V., Maurer, A.F., 2011. Sr/Ca and Mg/Ca ratios of ontogenetically old, long-lived bivalve shells (*Arctica islandica*) and their function as paleotemperature proxies. Palaeogeogr. Palaeoclimatol. Palaeoecol. 302, 52-64.

Schöne, B.R., Radermacher, P., Zhang, Z., Jacob, D.E., 2013. Crystal fabrics and element impurities (Sr/Ca, Mg/Ca, and Ba/Ca) in shells of *Arctica islandica*— Implications for paleoclimate reconstructions. Palaeogeogr. Palaeoclimatol. Palaeoecol. 373, 50-59.

Scourse, J., Richardson, C., Forsythe, G., Harris, I., Heinemeier, J., Fraser, N., Briffa, K., Jones, P., 2006. First cross-matched floating chronology from the marine fossil record: data from growth lines of the long-lived bivalve mollusc *Arctica islandica*. Holocene 16, 967-974.

Sheppard, P.R., Tarasov, P.E., Graumlich, L.J., Heussner, K.U., Wagner, M., Österle, H., Thompson, L.G., 2004. Annual precipitation since 515 BC reconstructed from living and fossil juniper growth of northeastern Qinghai Province, China. Clim. Dyn. 23, 869-881.

Siegert, N.W., Mccullough, D.G., Liebhold, A.M., Telewski, F.W., 2014. Dendrochronological reconstruction of the epicentre and early spread of emerald ash borer in North America. Divers. Distrib. 20, 847-858.

Simkiss, K., Wilbur, K.M., 1989. Biomineralization. Cell biology and mineral deposition, Academic Press, London. pp. 337.

Sinclair, D.J., Kinsley, L., McCulloch, M.T., 1998. High resolution analysis of trace elements in corals by laser ablation ICP-MS. Geochim. Cosmochim. Acta 62, 1889-1901.

Stecher, H.A., Krantz, D.E., Lord, C.J., Luther, G.W., Bock, K.W., 1996. Profiles of strontium and barium in *Mercenaria mercenaria* and *Spisula solidissima* shells. Geochim. Cosmochim. Acta 60, 3445-3456.

Stemmer, K., Nehrke, G., Brey, T., 2013. Elevated CO_2 levels do not affect the shell structure of the bivalve *Arctica islandica* from the Western Baltic. PLoS One 8. doi: 10.1371/journal.pone.0070106

Surge, D., Barrett, J.H., 2012. Marine climatic seasonality during medieval times (10^{th} to 12^{th} centuries) based on isotopic records in Viking Age shells from Orkney, Scotland. Palaeogeogr. Palaeoclimatol. Palaeoecol. 350-352, 236-246.

Svensson, A., Andersen, K.K., Bigler, M., Clausen, H.B., Dahl-Jensen, D., Davies, S.M., Johnsen, S.J., Muscheler, R., Parrenin, F., Rasmussen, S.O., Röthlisberger, R., Seierstad, I., Steffensen, J.P., Vinther, B.M., 2008. A 60,000 year Greenland stratigraphic ice core chronology. Clim. Past, Eur. Geosci. Union 4, 47-57.

Tan Tiu, A., 1988. Temporal and spatial variation of shell microstructure of *Polymesoda caroliniana* (Bivalvia: Heterodonta). Am. Malacol. Bull. 6, 199-206.

Tan Tiu, A., Prezant, R.S., 1989. Temporal variation in microstructure of the inner shell surface of *Corbicula fluminea* (Bivalvia: Heterodonta). Am. Malacol. Bull. 7, 65-71.

Taylor, J.D., 1973. The structural evolution of the bivalve shell. Paleontology 16, 519-534.

Tesoriero, A.J., Pankow, J.F., 1996. Solid solution partitioning of Sr^{2+}, Ba^{2+}, and Cd^{2+} to calcite. Geochim. Cosmochim. Acta 60, 1053-1063.

Wada, K., 1961. Crystal growth of molluscan shells. Bull. Nat. Pearl Res. Lab. 7, 703-785

Walliser, E.O., Lohmann, G., Niezgodzki, I., Tütken, T., Schöne, B.R., 2016. Response of Central European SST to atmospheric pCO_2 forcing during the Oligocene - A combined proxy data and numerical climate model approach. Palaeogeogr. Palaeoclimatol. Palaeoecol. 459, 552-569.

Wanamaker, A.D., Kreutz, K.J., Borns, H.W., Introne, D.S., Feindel, S., Funder, S., Rawson, P.D., Barber, B.J., 2007a. Experimental determination of salinity, temperature, growth, and metabolic effects on shell isotope chemistry of *Mytilus edulis* collected from Maine and Greenland. Paleoceanography 22. doi: 10.1007/s00382-007-0344-8

Wanamaker, A.D., Kreutz, K.J., Schöne, B.R., Pettigrew, N., Borns, H.W., Introne, D.S., Belknap, D., Maasch, K.A., Feindel, S., 2007b. Coupled North Atlantic slope water forcing on Gulf of Maine temperatures over the past millennium. Clim. Dyn. 31, 183-194.

Wanamaker, A.D., Heinemeier, J., Scourse, J.D., Richardson, C.A., Butler, P.G., Eiríksson, J., Knudsen, K.L., 2008a. Very long-lived mollusks confirm 17th century ad tephra-based radiocarbon reservoir ages for North Icelandic shelf waters. Radiocarbon 50, 399-412.

Wanamaker, A.D., Kreutz, K.J., Wilson, T., Borns, H.W., Introne, D.S., Feindel, S., 2008b. Experimentally determined Mg/Ca and Sr/Ca ratios in juvenile bivalve calcite for *Mytilus edulis*: Implications for paleotemperature reconstructions. Geo-Marine Lett. 28, 359-368.

Wanamaker, A.D., Kreutz, K.J., Schöne, B.R., Introne, D.S., 2011. Gulf of Maine shells reveal changes in seawater temperature seasonality during the Medieval Climate Anomaly and the Little Ice Age. Palaeogeogr. Palaeoclimatol. Palaeoecol. 302, 43-51.

Watabe, N., Meenakshi, V.R., Blackwelder, P.L., Kurtz, E.M., Dunkelberger D.G., 1976. In: Watabe, N., Wilbur, K.M. (Eds.), Mechanisms of biomineralization in the invertebrates and plants. University South Carolina Press, Columbia, pp. 283-308.

Weiner, S., Addadi, L., 1997. Design strategies in mineralized biological materials. J. Mater. Chem. 7, 689-702.

Weiner, S., Levi-Kalisman, Y., Raz, S., Addadi, L., 2003. Biologically formed amorphous calcium carbonate. Connect. Tissue Res. 44, 214-218.

Wheeler, A.P., 1992. Mechanisms of molluscan shell formation, in: Calcification in biological systems. pp. 179-216.

Wilbur, K.M., Saleuddin, A.S.M., 1983. Shell formation, in: Saleuddin, A.S.M., Wilbur, K. (Eds.), The Mollusca, Vol. 4. Physiology, Part 1. Academic Press, New York, pp. 235-287.

Witbaard, R., Franken, R., Visser, B., 1997. Growth of juvenile *Arctica islandica* under experimental conditions. Helgolaender Meeresuntersuchungen 51, 417-431.

Chapter 2 - Manuscripts

Manuscript I

Changes of shell microstructural characteristics of *Cerastoderma edule* (Bivalvia) - A novel proxy for water temperature

Published in Palaeogeography, Palaeoclimatology, Palaeoecology

Stefania Milano[1], Bernd R. Schöne[1], Rob Witbaard[2]

[1] Institute of Geosciences, University of Mainz, Joh.-J.-Becherweg 21, 55128 Mainz, Germany

[2] Royal Netherlands Institute for Sea Research, PO Box 59, 1790 AB Den Burg, Texel, The Netherlands

Author contribution

Concept: SM, BRS
Execution: SM, RW
Analysis: SM
Data interpretation: SM, BRS
Writing: SM, BRS, RW

Milano, S., Schöne, B.R., Witbaard, R., 2015. Changes of shell microstructural characteristics of *Cerastoderma edule* (Bivalvia) - A novel proxy for water temperature. Palaeogeogr. Palaeoclimatol. Palaeoecol. In press.

Abstract

Shells of bivalves potentially provide an excellent archive for high-resolution paleoclimate studies. However, quantification of environmental variables, specifically water temperature remains a very challenging task. Here, we explore the possibility to infer water temperature from changes of microstructural characteristics of shells of the common cockle, *Cerastoderma edule*. The size and elongation of individual microstructural units, i.e., prisms, in the outer shell layer of seven three to five year-old, specimens collected alive from the intertidal zone of the North Sea near Texel, The Netherlands, and Schillig, Germany, were measured by means of automatic image processing. Growth patterns (circatidal, ciralunidian and fortnightly increments and lines), shell oxygen isotope values and mark-and-recovery experiments were used to place the shell record in a precise temporal context. Irrespective of the locality and ontogenetic age, size and elongation of the prisms increased non-linearly with water temperature. Small (0.12 ± 0.05 μm^2) and round prisms (elongation: 2.42 ± 0.31) were formed at temperatures of ca. 10 °C (late April), whereas larger (0.33 ± 0.11 μm^2) and more elongated prisms (3.26 ± 0.28) occurred during hot summer (ca. 22 °C). No clear-cut or consistent correlation existed between microstructural characteristics and growth rate as well as a variety of other environmental variables such as salinity, chlorophyll a and turbidity. Based on these findings, a model was constructed from three shells at Texel that enables reconstruction of water temperature with a precision of 1.7 ± 1.0 °C from prism size and elongation: $SST = 9.02 + 17.25\ P_s + 1.10\ P_e$. This model was successfully tested at four shells from Schillig. The new temperature proxy can be of particular interest for paleoclimate studies when non-recrystallized *C. edule* shells are available. Future studies are required to verify our findings and check if other species with the same and different microstructures show similar relationships with water temperature.

Keywords: microstructure; bivalve shell; prism size; prism elongation; temperature proxy; scanning electron microscopy

Research highlights:

(1) Shell microstructural components of the marine bivalve *Cerastoderma edule* were analyzed and quantified using Scanning Electron Microscope and image processing techniques.
(2) Prismatic microstructures in the shell outer-most layer show changes during the growing season of the animals (spring to autumn).
(3) Large and elongated prisms are formed during the summer water temperature peak whereas small and rounded prisms are formed in the rest of the growing season.
(4) Water temperature reconstruction based on microstructural properties has a precision of 1.7 ± 1.0°C.
(5) Microstructures could serve as a novel temperature proxy independent from vital effects and applicable to fossil records..

1. Introduction

Bivalve mollusks serve as sensitive, high-resolution recorders of past environmental change (Jones, 1983; Marchitto et al., 2000; Richardson, 2001). Information on seasonal and inter-annual change of temperature, salinity, food availability and water quality is preserved in their shells in the form of variable growth rates and geochemical properties (Kennish and Olsson, 1975; Jones et al., 1986; Wefer and Berger, 1991). These data can be placed in a precise temporal context by using periodic shell growth patterns (Rhoads and Pannella, 1970; Evans, 1972; Goodwin et al., 2001). Furthermore, bivalves inhabit almost all aquatic environments, in particular shallowmarine and coastal settings, andwell-preserved fossil shells occur in sedimentary deposits, in particular the Cenozoic. Therefore, bivalve shells are being increasingly utilized in paleoclimatic and paleoenvironmental analyses (Schöne and Gillikin, 2013). Most of such studies focused on the reconstruction of sea surface temperature (SST) because of its coupling to a variety of other climate parameters.

One of the most frequently used proxies forwater temperature in bivalve sclerochronology is the oxygen isotope value of the shell carbonate ($\delta^{18}O_{shell}$). However, $\delta^{18}O_{shell}$ is a dual proxy that simultaneously records changes of temperature and the oxygen isotope composition of the ambientwater, $\delta^{18}O_{water}$,which is correlated to salinity. To reconstruct temperature from $\delta^{18}O_{water}$ values, the other variable ($\delta^{18}O_{water}$ or salinity) during shell formationmust be known. This information is typically not available for ancient environments and currently not possible to infer from bivalve shells. Temperature reconstructions based on $\delta^{18}O_{shell}$ are particularly challenging in coastal and intertidal areas because of large salinity fluctuations and associated variations of $\delta^{18}O_{water}$ (Gillikin et al., 2005a). Variable shell growth rates can potentially provide information on water temperature. In many poikilothermic animals, faster growth occurs in warmer waters. However, shell growth of bivalves is also controlled by food availability and quality (Ansell, 1968;Witbaard et al., 1997) and depends on preserved energy reserves from previous years (Yan et al., 2012). Therefore, the temperature information recorded in variable increment widths is often challenging to interpret. Element-to-calcium ratios such as Sr/Ca or Mg/Ca have been proposed as alternative temperature proxies. However, biological effects strongly control the incorporation of trace and minor elements into bivalve shells (Gillikin et al., 2005b; Shirai et al., 2014) and are hence difficult to interpret in terms of environmental variability (Freitas et al., 2006; Pérez-Huerta et al., 2013). A promising novel temperature proxy is the carbonate clumped isotope method (Ghosh et al., 2006). The accuracy of temperature estimates using Δ_{47} values can be as accurate as ca. ± 1.4 °C (Eagle et al., 2013). However, the low sample throughput and large amounts of sample material required for the measurements currently preclude high-resolution paleotemperature estimates.

In the present study, we explore the possibility to retrieve temperature data from changes of the shell microstructure. Few previous studies identified relationships between the shell microstructure and environmental conditions (Nishida et al., 2012; Fitzer et al., 2014) including temperature (Tan Tiu and Prezant, 1987; Prezant et al.,

1988; Tan Tiu, 1988). However, these interpretations were often based exclusively on qualitative observations. Here, we quantify shell structural changes on the µm-scale (size and elongation of individual prisms) of the common cockle, *Cerastoderma edule*, and test their possible use as an alternative, high-resolution proxy for temperature in highly dynamic, nearshore settings.

2. Materials and methods

2.1 Sample collection and preparation

Nine specimens of *Cerastoderma edule* were collected alive from two different localities in the mid intertidal zone of the North Sea (Fig. 1, Table 1). This species is a shallow burrower with very short siphons. Specimens younger than three years were visible on the sediment surface. Other specimens lived within the upper two centimeters of the substrate. Five specimens were collected ca. 300 m away from the coastline from Wanger Watt, the open tide flats north of the village of Schillig, Germany (53°42′45.68″ N, 008°01′14.88″ E; 11 March 2014). This locality belongs to the central part of the Wadden Sea. To the north (ca. 4 to 7 km away), the Wanger Watt is protected from the open sea by the islands of Wangerooge and Minsener Oog. To the east, Wanger Watt is bordered by the Jade tidal inlet channel. Another four specimens came from the open tide flats (ca. 70 m SW of the coastline) at the south coast of the island of Texel, The Netherlands (053°00′11″ N, 004°46′36″ E; 10 October 2014 and 24 November 2014; Table 1), in the westernmost part of theWadden Sea. These tide flats belong to a tidal basin drained by the Marsdiep, a deep tide-race between Den Helder in the South and the island of Texel in the North. At both localities, the bivalves lived in muddy to sandy sediments and experienced a semidiurnal tidal pattern with two approximately equal high and low tides. The average tidal range at Schillig (2.4 m) is almost twice as large as at Texel (1.4 m).During each low tide, the studied specimens were aerially exposed for approximately six hours at both localities.

To precisely determine the amount of shell that formed in a known time interval, on 19 September 2014, the specimens at Texel were immersed in a calcein solution (150 mg/l) for three hours and returned to their habitat. The fluorochrome calcein is incorporated into the shell aragonite and fluoresces bright green when viewed under a UV-light microscope (Kaehler and McQuaid, 1999). Even under the SEM, the calcein lines were easy to discern, because they were composed of larger prisms and were associated with notches in the OSL. In combination with the tidal microgrowth patterns this reference mark was used for the precise temporal alignment of the shell record. To facilitate recovery of the specimens, the shells were labeled with plastic tags and placed in PVC rings that were buried in the sediment.

After removal of soft tissues immediately after collection, single valves of the specimens were attached to a plexiglass cube and covered with a protective layer of JB KWIK epoxy resin. Two ca. two millimeter-thick sections were cut from each specimen along the axis of maximum growth using a low-speed precision saw (Buehler

Isomet 1000; Fig. 1B). These sections were embedded in Struers EpoFix resin. After 24 hours, the dry resin blocks were ground using a Buehler Metaserv 2000 grinder-polisher machine with Buehler silicon carbide papers of different grit sizes (320, 600, 1200, 2500) and subsequently polished with 3 µm diamond suspension on a Buehler VerduTex cloth. Between each of these grinding steps and after polishing, the sections were rinsed ultrasonically in de-ionized water. One slab of selected specimens was used for oxygen isotope analysis to verify the timing of major growth line formation (Table 1).

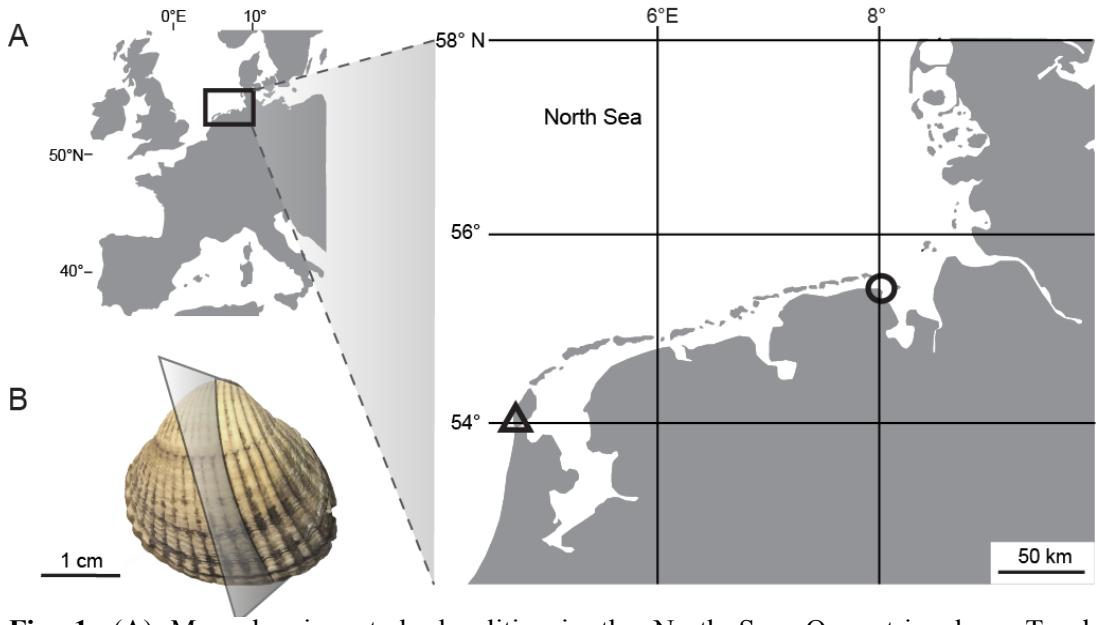

Fig. 1. (A) Map showing study localities in the North Sea. Open triangle = Texel, The Netherlands; open circle = Schillig, Germany. (B) Shell of *Cerastoderma edule*. Grey plane indicates axis of maximum growth from which shell slabs were cut.

Tab. 1. List of studied specimens of *Cerastoderma edule* and sampling details.

Sample ID	Locality	Calcein marking date	Collection date	Shell height (mm)	Age	Ontoge-netic year analyzed	Calendar year analyzed	$\delta^{18}O_{shell}$ analysis
A1	Schillig	-	11 Mar 14	16.5	3	3rd	2013	-
A2	Schillig	-	11 Mar 14	25.7	5	-	-	✓
A6	Schillig	-	11 Mar 14	18.5	3	3rd	2013	-
A24	Schillig	-	11 Mar 14	15.6	3	3rd	2013	-
A42	Schillig	-	11 Mar 14	25.3	4	-	-	✓
AJ061	Texel	19 Sep 14	10 Oct 14	27.6	5	5th	2014	✓
AJ084	Texel	19 Sep 14	10 Oct 14	25.8	4	4th	2014	-
AJ089	Texel	19 Sep 14	24 Nov 14	28.1	4	4th	2014	✓
AJ095	Texel	19 Sep 14	24 Nov 14	27.7	4	4th	2014	-

The other polished section of each specimen was first studied under a fluorescence light microscope (Zeiss Axio Imager.A1m microscope equipped with a Zeiss HBO100 mercury lamp and filter set 38: excitation wavelength, ~ 450-500 nm; emission wavelength, > 500-550 nm) to locate the calcein marks. Then, these shell slabs were etched for 15 seconds in 0.12 N HCl solution (see supplementary data S1 for various different etching durations), rinsed in deionized water, air-dried, sputter coated with a 3 nm-thick gold film. The samples were used for the analyses of microstructural characteristics and shell growth patterns under the scanning electron microscope (2^{nd} generation Phenom Pro desktop SEM).

2.2 Shell growth patterns

Like other intertidal bivalves, *C. edule* forms distinct tide-controlled growth patterns in its shell, namely fortnightly, circalunidian (24.8 hour cycles; lunar daily) and circatidal growth increments and adjoining lines (12.4 hour cycles; semidiurnal) (Ohno, 1983; Lønne and Gray, 1988; Schöne, 2008). The formation of growth increments occurs during fast periods of growth and is limited to times of immersion at high tide, whereas growth lines form shortly before or shortly after subaerial emersion when the valves are closed (Schöne, 2008). Shell growth patterns (increments and adjoining lines) were studied in the outer shell layer and used to temporally contextualize each shell portion. For this purpose, growth increments were counted and the widths of circalunidian increments measured in SEM images to the nearest 1 µm with the image processing software Panopea (© Schöne and Peinl). To identify overall growth trends and to facilitate the comparison with weekly resolved environmental data, a cubic smoothing spline ($\lambda = 0.05$) was applied to the lunar daily increment width chronologies. To constrain the timing of the major growth line formation in *C. edule,* the study areas were visited regularly and the ventral margins of the shells were assessed.

2.3 Stable isotope analysis of the shells

In order to verify the timing of major growth line formation, two specimens from Texel (AJ061 and AJ089) and two from Schillig (A2 and A42) were used for oxygen isotope analysis ($\delta^{18}O_{shell}$) (Table 1, Fig. 3). Carbonate (here aragonite) powder samples (n=60) were micromilled from the outer shell layer using a Rexim Minimo dental drill mounted to a binocular microscope and equipped with a cylindrical, diamond-coated bit (1 mm diameter; Komet/Gebr. Brasseler GmbH & Co. KG, model no. 835 104 010). The samples were processed with a Thermo Finnigan MAT 253 gas source isotope ratio mass spectrometer in continuous flow mode coupled to a GasBench II at the University of Mainz. Samples were calibrated against a NBS-19 calibrated IVA Carrara marble ($\delta^{18}O = -1.91‰$). The average internal precision (1σ) was better than 0.05‰.

2.4 Shell microstructures

Like other bivalves, the shell of *C. edule* consists of an inner (ISL), middle (MSL) and outer shell layer (OSL) (Fig. 2) [1]. Each shell layer consists of a characteristic microstructure. In this study, we adhere to the terminology of Popov (1986) and Carter et al. (2012). The ISL of *C. edule* is composed of complex crossed-lamellar microstructure (Fig. 2C). Most of the shell belongs to the MSL which is made of simple crossed-lamellar structure (Fig. 2D). The focus of this study, however, is placed on the OSL (nondenticular composite prismatic microstructure; Fig. 2E) in which the growth patterns and the microstructural units (= nanocrystal assemblages or so-called mesocrystals; Cölfen and Antonietti, 2008), i.e., individual prisms can be best studied.

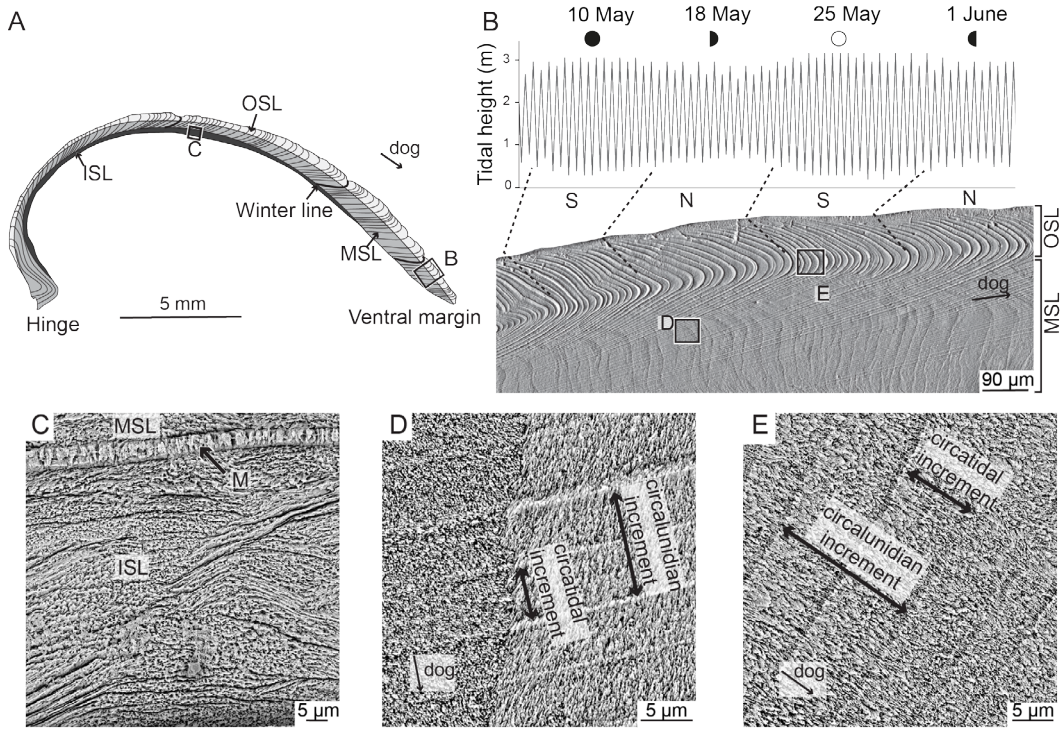

Fig. 2. Shell growth patterns and microstructures of *Cerastoderma edule*. (A) Cross-section showing shell layers. ISL = inner shell layer; MSL = middle shell layer, OSL = outer shell layer. (B-E) SEM images of shell microstructures. (B) Shell portion near outer shell surface. Lunar daily and circatidal growth patterns are arranged in fortnightly bundles. S, N = Shell portions formed during spring and neap tides, respectively. (C) Complex crossed-lamellar microstructure in the ISL. M = myostracum. (D) Simple crossed-lamellar microstructure of the MSL. Note regular changes of orientation of 1st order lamellae result in darker portion (left) and brighter shell portion (right). (E) Nondenticular composite prismatic microstructure of the OSL. dog = direction of growth

[1] In some previous works (e.g., Schöne et al., 2013), the MSL was referred to as the inner portion of the OSL (iOSL), and the remaining part of the OSL as the outer portion of the OSL (oOSL). This terminology considers the fact that the iOSL and oOSL are formed in the same outer extrapallial space,which is separated from the inner extrapallial space in which the ISL is precipitated. As a recommendation by one of the reviewers, here we follow a mere descriptive terminology (OSL,MSL, ISL).

The micro-imaging software OLYMPUS AnalySIS Pro was used to automatically detect individual prisms along the axis of maximum growth in the OSL (Fig. 4), and quantify their structural characteristics, i.e., size (area; P_s) and elongation (P_e). Elongation is defined as a dimensionless shape descriptor and calculated as the ratio between the major and minor axes. Portions of the SEM images with a fixed area of 13 ± 0.1 µm^2 were defined as "regions of interest" (ROIs). Within these ROIs (one ROI per week), automatic particle detection was applied with the grayscale threshold set to 71 (where 0 equals black and 255 equals white). All pixels of the ROIs with values above the threshold level were classified as particles, i.e. individual prisms. False detection of pixels at the prism boundaries was manually corrected. For comparison with weekly resolved time-series of environmental variables as well as shell growth rate, weekly averages of P_s and P_e were computed. The difference between the total area of the ROIs and the area occupied by the prisms, later referred as 'inter-prismatic space', was calculated and given in percentage (see supplementary data S.3).

2.5 Instrumental data

A CTD logger (HOBO U24) was anchored to a shipwreck in the intertidal zone near Schillig (c.a. 5 m from shells collection site). The logger was constantly submersed (minimum of 30 cm water coverage during low tide) and recorded water temperature between 1 April 2013 and 11 March 2014 on an hourly basis. Since conductivity measurements with the CTD logger failed, salinity was computed from sodium values using the following equation (DOE, 1994):

(1) $$S_{Na}\,(PSU) = Na^{+}\,(\mu g \cdot g^{-1}) \cdot 35/10783.7.$$

For this purpose, water samples were collected on a ca. two-weekly basis. Sodium levels were measured with a Spectro CIROS Vision^{SOP} ICP-OES system at the Institute of Geosciences, University of Mainz. Sodium was measured against a single element standard. Accuracy determined by Roth SolutionX multi element standard solution Lot R459520 was 2 RSD %.

At Texel, SST and salinity were recorded between August and November 2014 at five minute intervals by a logger (Aanderaa 3211 sensor coupled to an Aanderaa DL3634 logger; deployed ca. 1.3 km away from the shell collection site; minimum water coverage during low tide was 1 m). Logging of environmental parameters at that site was part of a long-term standard monitoring program described by van Aken (2008). Data were provided by the Royal Netherlands Institute for Sea Research (NIOZ).

Since shell growth of intertidal bivalves predominantly takes place during high tide, new time-series were calculated that only reflect (arithmetically) averaged temperature and salinity ± 1 hour around high stand. For better comparison with lower resolution data of other environmental variables, these data were then converted into

weekly resolved chronologies (Fig. 5). Weekly data of water turbidity and chlorophyll a (Chl a) concentration were obtained from satellite datasets (4 km spatial resolution, MODIS NASA, available at http://disc.sci.gsfc.nasa.gov/giovanni; last checked: January 2015) (Fig. 5).

2.6 Statistical analyses

In order to evaluate the relationship between shell architecture, environmental variables and shell growth rate, a Redundancy Analysis (RDA) was performed using the XLSTAT software (Fig. 6). ANOVA and a Kruskal-Wallis test were used to determine whether significant differences exist between the microstructures of different samples. Once the three microstructure-based models for the SST reconstruction were constructed, root mean square errors were calculated to evaluate the goodness of fit between each model and the instrumentally recorded SST (Tab. 3). The significance of each variable in the coupled model was tested using a Fisher´s F test. The strength of the linear relationship between the time-series was determined using Pearson's correlation coefficient (Tab. 3).

3. Results

3.1 Timing of shell growth and microstructures of *C. edule*

Ontogenetic age estimates were based on major dark growth lines visible on the outer shell surface and then verified by shell oxygen isotope data for selected specimens (Fig. 3, Table 1). In the three specimens from Schillig used in the microstructural analysis, these lines formed exclusively during the cold season. Each of them showed three of such 'winter' lines. However, older specimens from both localities also contained major growth lines that formed during summer (Fig. 3).

The most recently formed shell portions were studied in more detail under a fluorescence light microscope and a scanning electron microscope. The microstructure of the shell portion deposited after the calcein lines was nondenticular composite prismatic again, but individual prisms were still unusually large (see further below). Calcein lines served as absolute time markers that were used to verify the circatidal and lunar daily nature of the growth increments. For example, in samples AJ061 and AJ084 the number of circatidal increments (41 and 42, respectively) agreed with the number of tidal immersions that occurred during the 21 solar days that elapsed between 19 September (date of calcein marking) and 10 October 2014 (date of collection) (Table 2). Based on the increment counts of the specimen collected in November, the 2014 main growing season of *C. edule* at Texel ended between 11 and 14 November (Table 2).

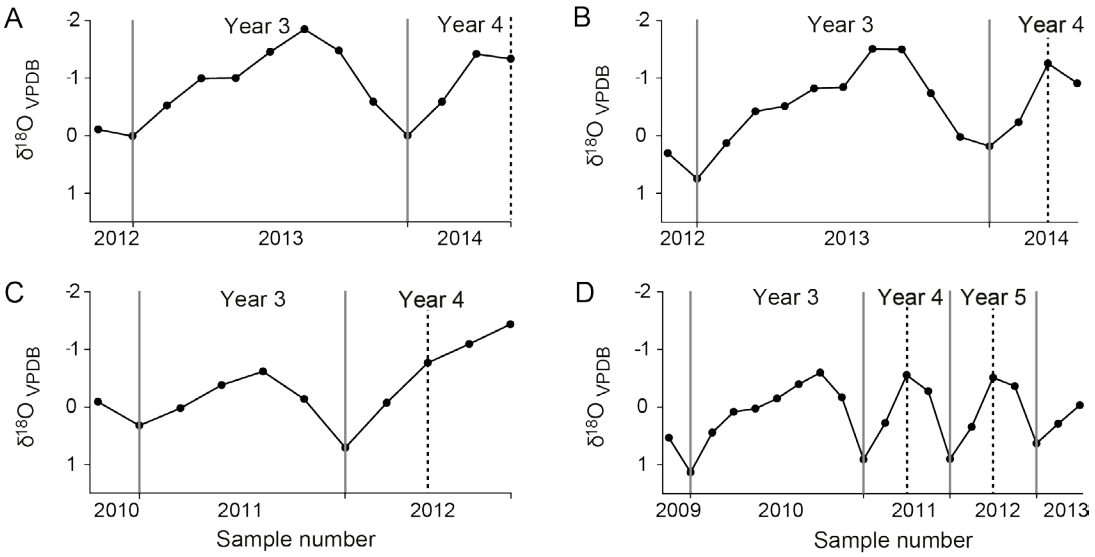

Fig. 3. $\delta^{18}O_{shell}$values of *Cerastoderma edule* from Texel (A+B) and Schillig (C+D). Grey vertical lines indicate the position of winter lines and dashed black lines denote summer lines.

All four *C. edule* shells from Texel showed a pronounced summer growth line ca. 1.4 mm before the calcein line. The shell portion between this growth line and the calcein mark contained between 87 to 95 circatidal increments suggesting that shell growth resumed after the summer growth cessation around 2 August 2014 (Tab. 2). The precise timing of shell growth before the summer line was not studied here, but according to $\delta^{18}O_{shell}$ values, shell formation took place during late spring and early summer.

Identifying the timing of seasonal shell growth of *C. edule* at Schillig was more challenging because no calcein marking was performed and therefore no hinging date was available. However, it was still possible to precisely determine when shell growth started and ended in 2013. During deployment of the logger in early April 2013, specimens of *C. edule* showed a distinct major dark line (= annual growth line) at the ventral margin, but no freshly formed shell material indicating that increment formation had not yet started. The same was true for shells collected in March 2014. However, an annual growth line was just about to form in specimens collected in the middle of September 2013 suggesting that the growing season ended shortly before. These data confirm $\delta^{18}O_{shell}$-based findings and demonstrate that shell growth was halted or at least strongly reduced during the cold season at this locality, and the annual growth line could be dubbed 'winter line'. Between the winter lines of 2012/13 and 2013/14 (= annual increment of 2013), we counted ca. 141 ± 6 lunar daily growth increments that were arranged in distinct fortnightly bundles. This places the beginning of the growing season to ca. mid-April 2013. A direct comparison of the tide calendar and the alternating lengths of the fortnightly increments (full-to-new moon period, apogee = 15 lunar days; new-to-full moon period, perigee = 13.5 lunar days; Hallmann et al., 2009; Fig. 2B) helped us to verify and further constrain the calendrical alignment of the shell growth pattern according to which the main growing season of 2013 started on ca. 19 April and ended on ca. 11 September.

Tab. 2. Timing of shell growth of *Cerastoderma edule* from Texel.

Sample ID	Calcein marking date	Collection date	# circatidal increments between summer and calcein line	Computed onset of growth after summer line	# high tides between calcein mark and death	# circatidal increments between calcein mark and death	Reconstructed date when winter line start to form
AJ061	19 Sep 14	10 Oct 14	95	01 Aug 14	42	41	10 Oct 14
AJ084	19 Sep 14	10 Oct 14	92	03 Aug 14	42	42	10 Oct 14
AJ089	19 Sep 14	24 Nov 14	95	01 Aug 14	129	103	11 Nov 14
AJ095	19 Sep 14	24 Nov 14	87	06 Aug 14	129	109	14 Nov 14

3.2 Seasonal changes of shell microstructural properties

Under the SEM, all studied specimens showed distinct seasonal changes of microstructural characteristics in the OSL. At Schillig, the size (P_s) and elongation (P_e) of the prisms gradually increased during the growing season and reached a maximum during hot summer (Fig. 4). From the beginning of the growing season of 2013 until the end of June, P_s equaled, on average (±1σ), 0.12 ± 0.05 μm² (number of prisms measured = 2170). Toward hot summer, P_s increased threefold to values of 0.33 ± 0.11 μm² (number of prisms measured = 936). During the same time intervals, the average P_e (± 1σ) values were 2.42 ± 0.31 and 3.12 ± 0.45, respectively (Fig. 5A). Microstructural properties of the winter lines differed significantly from that of the portion between adjacent winter lines (= annual growth increment) (Fig. 4) and were thus not included in further analysis.

At Texel, large prisms (0.29 ± 0.10 μm², n = 276) were observed after the summer growth line. Between ca. 21 August and 18 September 2014, P_s decreased to values of 0.10 ± 0.01 μm² (Fig. 5B; number of prisms measured = 1949). During the same time interval, average P_e values decreased from 3.26 ± 0.28 to 2.45 ± 0.16 (Fig. 5B). After the calcein line (19 September 2014), prisms (n = 501) were significantly larger again (P_s = 0.24 ± 0.02 μm²), and elongation increased slightly (P_e = 2.83 ± 0.13). Microstructural characteristics of shell portions formed after 19 September 2014 were not used in subsequent analyses, because they were apparently influenced by the calcein staining (see also Füllenbach et al., 2014).

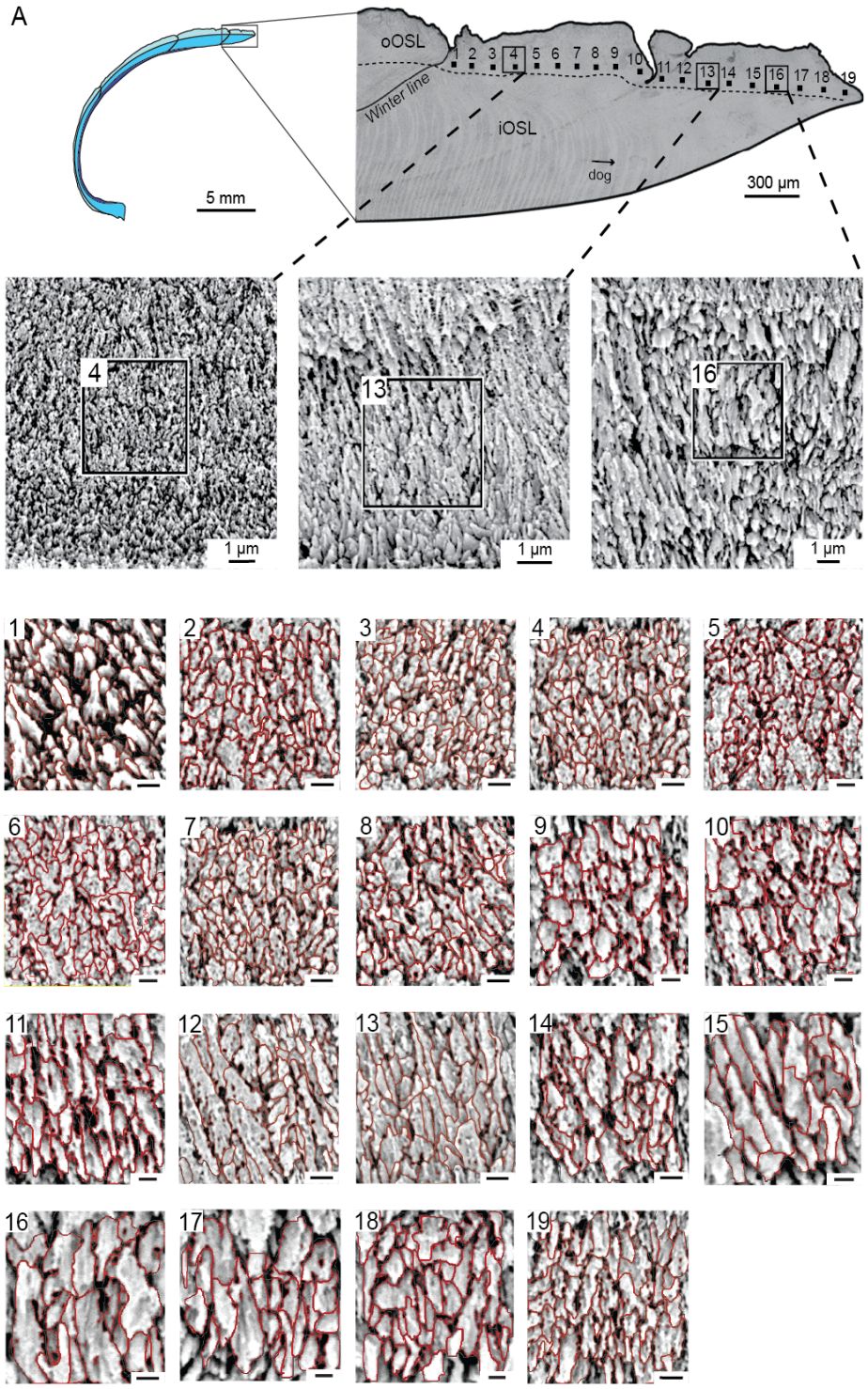

Fig. 4. Seasonally changing microstructural characteristics of *Cerastoderma edule*. (A) Shell section of *C. edule* from Schillig (specimen A24) and magnified portion near ventral margin showing the last growing season (April-September 2013) prior to death. Analyzed areas (regions of interest, ROIs) marked with numbers (1-19). (B-D) SEM images near ROIs 4, 13 and 16. (1-19) ROIs analyzed by image processing. Boundaries of individual prisms are highlighted red. Note gradual increase in size and trend toward elongated shape from 2 (spring) to 18 (hot summer). Microstructructural charactersitics of the shell portion near the winter line differ markedly from that of the main growing season (ROIs 2-19). Scale bars if not otherwise indicated = 500 nm.

3.3 Environmental variables, growth rate and microstructural characteristics

In order to analyze whether shell growth rate and microstructural characteristics (P_s, P_e) are intimately linked, the time-series were first visually compared (Fig. 5; for further information on shell growth rate see supplementary data S2). Shell portions formed during May contained small and rounded prisms, whereas large and elongated prisms occurred near the second growth peak in August (Fig. 5A). In shells from Texel, microstructural characteristics mainly changed near the first growth peak, but not near the second (Fig. 5B). Evidently, changes of the shell architecture are unrelated to changes of the shell growth rate. This finding was corroborated by redundancy analysis (RDA, Fig. 6).

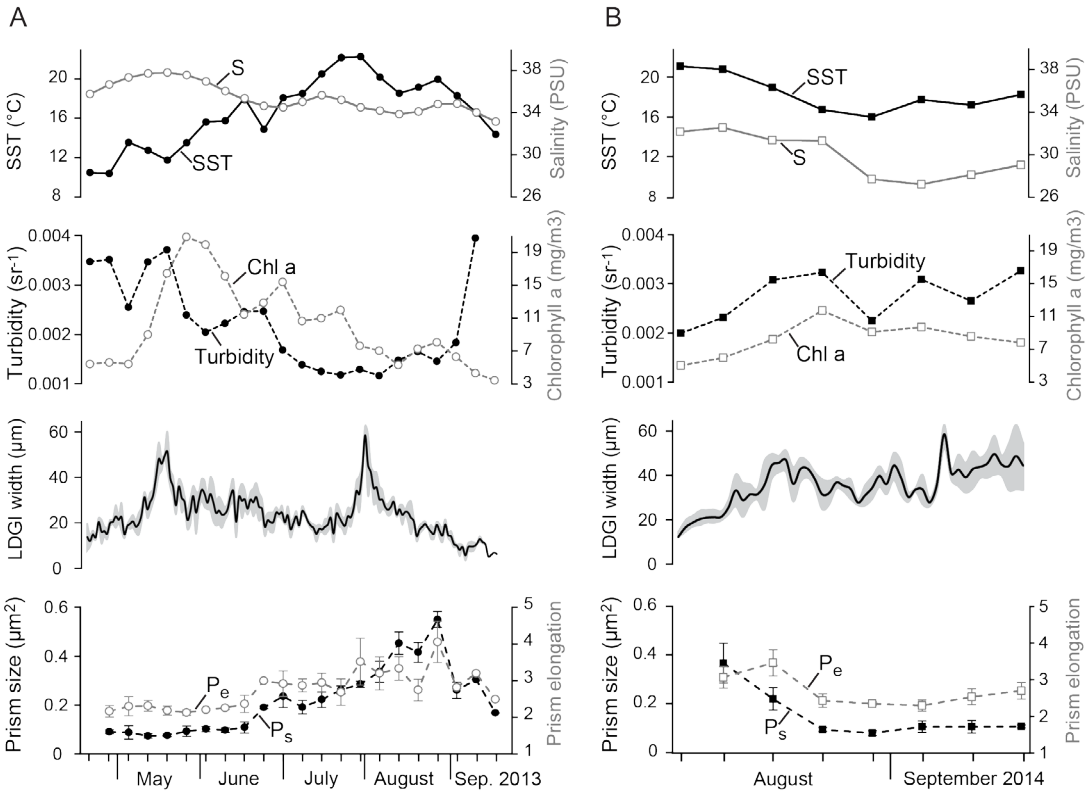

Fig. 5. Seasonal changes of prism size and elongation (P_s, P_s) of *Cerastoderma edule* from Schillig (A) and Texel (B) and their relationship with water temperature (SST), salinity (S), turbidity, chlorophyll a concentration (Chl a) and lunar daily growth increment width (LDGI width). Error bars and grey shadings indicate average standard error.

RDA also revealed that changes of microstructural characteristics were strongly linked to water temperature, but not to other environmental variables such as salinity, Chl a concentration and turbidity (Fig. 6). In *C. edule* from Schillig, data variability is mainly explained by F1 (99.57 %) and F2 (0.43 %). As shown in Figure 6A, the explanatory variable SST and the response variables P_s and P_e share a common signal. Salinity, however, is negatively correlated to P_s and P_e.

Growth rate shows ties to Chl a, but not to microstructural features. In *C. edule* from Texel, PCA extracted two factors explaining 99.78 % (F1) and 0.22% (F2) of the total variance (Fig. 6B). Strong positive correlations exist between SST, salinity, P_s and P_e. Food availability (Chl a concentration) and water turbidity are moderately related to growth rate. In all studied specimens, SST turned out to be the only environmental parameter that was consistently associated with changes of microstructural characteristics (Fig. 6).

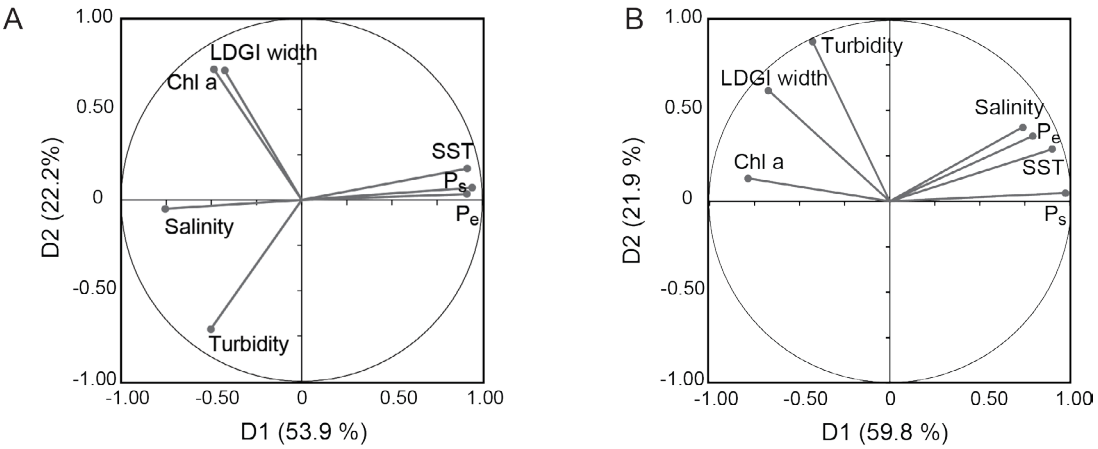

Fig. 6. Redundancy analysis of environmental and microstructural variables of *Cerastoderma edule* specimens from Schillig (A) and Texel (B). SST = sea surface temperature, Chl a = chlorophyll a concentration, P_e = average prism elongation, P_s = average prism size, LDGI width = lunar daily growth increment width. Solid circles = explanatory variables, open squares = response variables. (A) Narrow angles among the vectors show high correlations, e.g., between SST, P_e and P_s. Salinity is negatively correlated to these parameters (vector angle ~ 180°). (B) Salinity, SST, P_e and P_s, are highly correlated whereas a lower coherence is detectable between growth rate, turbidity and Chl a. Vector angles of ~ 90° between the other variables indicates absence of correlation.

3.4 Water temperature models

At both localities, larger and more elongated prisms were associated with high water temperature (SST = 19.4 ± 1.5 °C), whereas prisms were smaller and more rounded during the remainder of the growing season. ANOVA showed no significant variation between different specimens in the P_s ($p = 0.11$) and P_e ($p = 0.20$) values of the shell portions formed at elevated SST. Likewise, the Kruskal-Wallis test suggests that P_s ($p = 0.38$) and P_e ($p = 0.19$) of shell portions formed at lower SST were not significantly different between the samples.

The four shells from Texel exhibited a strong positive correlation between P_s and SST ($R = 0.80$; $R^2 = 0.64$, $p < 0.0001$) as well as between P_e and SST ($R = 0.52$; $R^2 = 0.27$; $p < 0.0001$) (Figs. 7A+B). On the basis of these empirical relationships, two regression models were developed that can be used to reconstruct SST from prism size (eq. 2) or prism elongation (eq. 3) of *C. edule*.

(2) $$SST = \ln (P_s / 0.327) / 0.0004$$

(3) $$SST = \ln (P_e / 0.727) / 0.072$$

To assess the validity of the two models, the homogeneity of variance was tested by plotting the residuals against the fitted values. Residuals calculated from both models are independent from SST and equally distributed in the range of temperature considered. The model based on P_e was applied to the three specimens of *C. edule* from Schillig. Reconstructed seasonal temperature extremes (±1σ) using equations 2 and 3 range between 16.4 ± 1.1 °C and 22.4 ± 0.3 °C and 15.1 ± 1.4 °C and 24 ± 0.4 °C, respectively. Reconstructed summer temperatures were close to instrumental records (22.3 °C), but cold temperatures during the beginning of the growing season (10.4 °C) were overestimated by 4.8 ± 0.6 °C to 6 ± 0.6 °C (Figs. 7C+D).

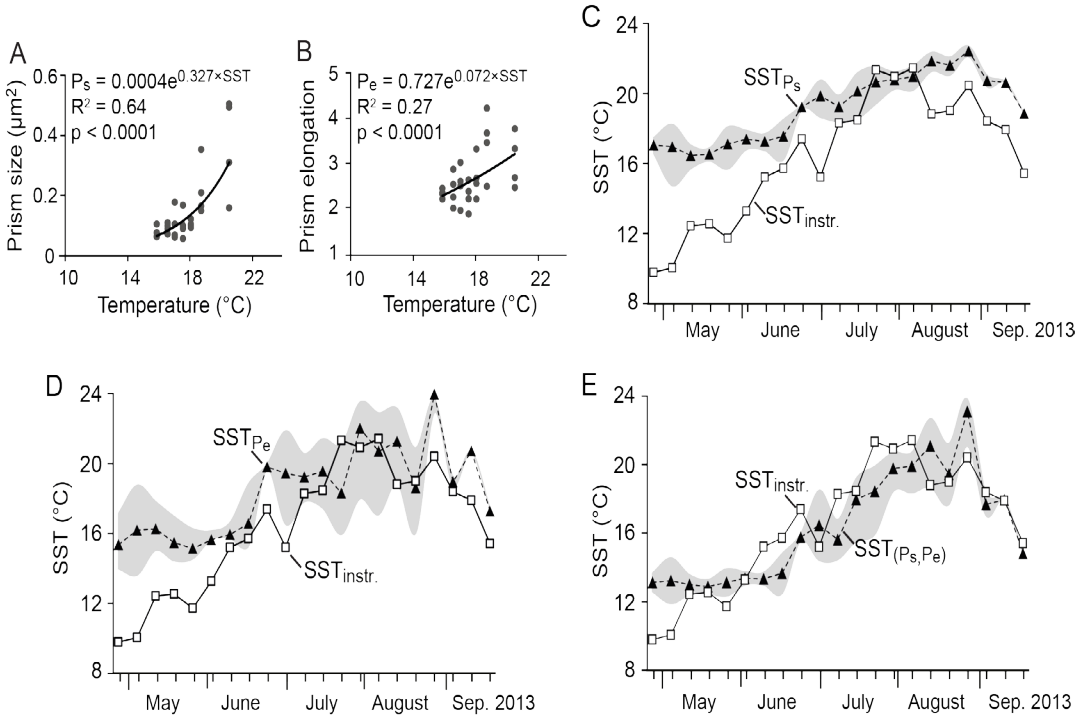

Fig. 7. Water temperature and microstructural characteristics. Relationship between water measured temperature and prism size (A) and prisms elongation (B) of *Cerastoderma edule* from Texel. (C-E) Comparison of reconstructed (open squares) and instrumentally determined (solid black triangles) water temperature at Schillig. (C) P_s model (Eq. 2), (D) P_e model (Eq. 3) and (E) coupled model using P_s and P_e (Eq. 4). Grey shadings indicate standard deviation (± 1σ).

Furthermore, a multiple regression model (eq. 4) was computed that permits reconstruction of water temperature from the combination of both microstructural variables, P_s and P_e (Fig. 7E).

(4) $$SST = 9.02 + 17.25\ P_s + 1.10\ P_e$$

The significance of each parameter in the equation was tested by a Fisher´s F Test (p (P_s) < 0.05, p (P_e) = 0.54). Thus, due to the high correlation between the two variables, P_e does not contribute significantly to explain SST variance not explained by P_s. However, temperature estimates using this coupled model are closer to instrumentally determined SST (13.3 °C and 23.3 °C) than reconstructions based on equations 2 and 3.

The average offsets between the temperature models and the instrumentally measured SST are 2.7 ± 1.9 °C (P_s model; ±1σ), 2.2 ± 1.7 °C (P_e model; ±1σ) and 1.7 ± 1.0 °C (coupled model; ±1σ). As shown in Table 3, the coupled model exhibits lower root mean square errors than the P_s and P_e models. Therefore, the coupled model can predict SST more precisely than the single model. Reconstructed and instrumental SST exhibit strong and statistically significant correlations (Table 3).

Table 3. Statistics of the SST models. RMSE = root mean square error.

Model	Average offset between measured SST and calculated SST (°C) ± 1 σ	RMSE (°C)	R	p
P_s model (Eq. 2)	2.7 ± 1.9	1.7	0.88	< 0.001
P_e model (Eq. 3)	2.2 ± 1.7	1.6	0.82	< 0.001
Coupled model (Eq. 4)	1.7 ± 1.0	1.2	0.86	< 0.001

4. Discussion

As demonstrated here, changes of the size and elongation of the prisms in the outer shell layer of *Cerastoderma edule* can serve as an independent measure of water temperature during growth. The two studied microstructural characteristics were uncorrelated to growth rate and a number of other environmental variables such as salinity, food availability (chlorophyll a levels) and water turbidity, but correlated well to changes of water temperature. The temperature models were constructed from shells of one locality (Texel) and their functioning successfully tested with specimens from another site (Schillig). The new proxy can be particularly useful for temperature estimates in nearshore, brackish environments where $\delta^{18}O_{shell}$-based temperature reconstructions tend to be imprecise because seasonal and inter-annual changes of the $\delta^{18}O_{water}$ signature (or salinity) remain unknown. Furthermore, the new temperature proxy is uncoupled to ontogenetic age of the bivalve and can therefore be applied to old and young specimens (see supplementary data S3. for microstructural individual differentiation). Unlike geochemical analyses which typically require pristine shell material, determination of the dimensions of individual prisms can even be completed in diagenetically altered fossil shells unless significant recrystallization occurred.

4.1 Bivalve shell microstructures and environment

Most of the previous studies were limited to the description of shell microstructures for taxonomic purposes and to reveal potential evolutionary relationships (Taylor, 1973; Carter and Clark, 1985; Chateigner et al., 2000; Su et al., 2002). Only a few studies focused on the possible relationship between microstructural changes and physiological or environmental conditions (Kennish, 1980; Checa et al., 2007). For example, increased predation pressure is reported to cause a thickening of the homogenous layer in the gastropod *Nucella lapillus* (Avery and Etter, 2006) and an increase in the number of crossed-lamellar layers in various gastropod species from Lake Tanganyika, east Africa (West and Cohen, 1996). In bivalves, high pCO_2 can result in unorganized crystals in the outer (calcitic) layer of *Mytilus spp.* (Hahn et al., 2012). In more acidic water, the microstructure of *Mytilus spp.* remains prismatic, but the individual prisms are no longer well-ordered. In addition, a much larger variability of the orientation of the crystallographic c-axes was observed by these authors. Apparently, such effects on the microstructure are species-specific, because the shell architecture of *Arctica islandica* was unaffected by elevated CO_2 levels (Stemmer et al., 2013). However, *A. islandic*a specimens growing in low salinity, oxygen deficient water showed a microstructure that was strongly enriched in organics and as such differed significantly from specimens collected from well-oxygenated, normal marine settings (Schöne, 2013).

As demonstrated by Tan Tiu and Prezant (1987) and Prezant et al. (1988), various kinds of artificial stress such as permanent submersion of the intertidal bivalve, *Geukensia demissa* (Tan Tiu and Prezant, 1987), or forced extended shell closure of the freshwater bivalve, *Corbicula fluminea* (Prezant et al., 1988), can evoke modifications of the shell microstructure. Similarly, decompression stress can affect the appearance of prisms and nacre platelets of the deep-sea bivalve *Bathymodiolus azoricus* (Kadar et al., 2008). Tan Tiu and Prezant (1988) also identified a relationship between the shell architecture of *C. fluminea* and water temperature. When exposed to heat stress, the typical complex crossed-lamellar microstructure was replaced by crossed-acicular crystal fabrics. Tan Tiu (1988) recognized seasonal variations of the shell microstructural type in *Polymesoda caroliniana* and hypothesized that temperature could be one of the driving factors. Likely, smaller nacre tablets formed in *G. demissa* at lower temperature (Lutz, 1984). Similar findings were recently reported by Nishida et al. (2012) who noticed seasonal changes of the relative proportions of composite prismatic and crossed-lamellar microstructures in *Scapharca broughtonii.* However, none of the previous studies has quantified changes of the characteristics of individual microstructural units and explored their potential as a proxy for water temperature.

4.2 Model for temperature-induced changes of microstructural characteristics

The present study demonstrated that large and elongated prisms are formed in warmer water (SST = 19.4 ± 1.5 °C), whereas smaller and rounded prisms occur in portions that formed during colder conditions. However, other measured physiological (ontogenetic age, growth rate) and environmental variables (salinity, food availability, turbidity) did not influence the size and habit of the microstructural units. The following hypothesis may provide an explanation for the observed changes.

Shell formation is a biologically mediated process during which fibrous proteins and acidic macromolecules form a supramolecular template for calcium carbonate precipitation (Levi-Kalisman et al., 2001). Recent advances in molecular biology have led to the identification of an increasing number of proteins forming this organic matrix and their encoding genes (Marin et al., 2008). However, the process of formation of the organic template is still not fully understood (Marie et al., 2012). This blueprint determines the characteristic size, shape and orientation of the microstructural units and becomes embedded into the biomineral as the inter-crystalline organic matrix that envelopes each mesocrystal (Wheeler, 1992; Nudelman et al., 2006). The formation of these organic macromolecules is intrinsically coupled to metabolic rate (Palmer, 1983) which in turn depends on temperature as well as food level and quality. Warmer temperatures and availability of high-quality food results in higher metabolic rates and thus, larger amounts of organic matrices being synthesized. In addition, the activity of transmembrane pumps increases when metabolic rate is higher so that larger amounts of inorganic building materials reach the site of calcification, i.e., Ca^{2+} and HCO_3^- (Carré et al. 2006). Higher temperatures also facilitate $CaCO_3$ precipitation (Coto et al., 2012). As a consequence, the individual structural units, i.e., the prisms may grow larger. However, when optimum growth temperatures are exceeded, the metabolic rate declines, shell formation rate decreases and less organic macromolecules are produced which is indicated by the decrease in inter-prismatic space (see supplementary data S3). Calcium carbonate precipitation continues at slower rates, because the activity of transmembrane pumps is reduced and the (slower) passive transmembrane ion transport mechanisms become more important. Since less organics are produced, the relative amount of $CaCO_3$ in the shell increases. To ensure that the biological control over $CaCO_3$ crystallization is maintained, larger, more elongated crystals are allowed to form. Since shell formation rates are reduced, it takes more time to form these larger crystals. Aside from kinetic effects favoring $CaCO_3$ precipitation at higher temperature, it seems very likely that temperature also influences the biomineralizing template (blueprint) which now permits the crystal to grow longer (and larger). In other words, the formation of a border (or cap) that completes a prism is delayed. The relative amount of inter-crystalline organics in shell portions with larger crystals is therefore much smaller than in shell portions with smaller prisms. The effect of temperature on crystal growth-kinetics and organic matrices has also been experimentally demonstrated (Yi et al., 2010).

It is further speculated that different organic compounds are synthesized during times of major growth line formation. For example, in contrast to growth increments, the growth lines of *Arctica islandica* are rich in polyenes (Stemmer and Nehrke, 2014). Furthermore, different microstructures contain different mixtures of organics. For example, nacre platelets and prisms of *Pinna nobilis* shells contain different fractions of polysaccharides and proteins (Cuif et al., 2013). Likewise, different prismatic microstructures of *P. nobilis* and *Pinctada margaritifera* were found to be associated with differing amounts of glycoproteins, proteoglycans and sulfated acidic polysaccharides (Dauphin et al., 2003). In addition, several previous studies noticed irregular simple prismatic microstructures or irregular spherulitic microstructures replace the otherwise dominant and typical microstructure when annual growth lines or disturbance lines are formed. In the present study, prisms near the annual lines also differ significantly from that in the portions between major growth lines.

4.3 Winter and summer lines: effect of environment and physiology

Skeletal growth of cold-blooded animals is typically controlled by combination of temperature, food availability and food quality (Kennish and Olsson 1975, Ansell, 1968; Witbaard et al., 1997). For example, fastest shell growth occurs within a species-specific optimum temperature range, whereas more extreme temperatures result in narrower increments and slower shell growth (Ivany et al., 2003; Schöne et al., 2003; Chauvaud et al., 2005). In the case of *C. edule*, shell formation is significantly slower at lower temperatures, and a winter line (Orton, 1926; Farrow, 1971; Bourget and Brock, 1990; Ponsero et al., 2009) forms below temperatures of ca. 10 °C (Kingston, 1974). Furthermore, the production of sperms and eggs is highly energy-consumptive and can result in a significant slowdown of shell growth or even the formation of a spawning line. This has extensively been studied in the veneroid bivalve, *Phacosoma japonicum* (Sato, 1999). As shown here, *C. edule* specimens under the age of three merely slowed down shell growth during hot summer, whereas older individuals formed a distinct summer growth line. Summer growth cessations in *C. edule* have previously been observed by Ramón (2003). It remains untested if the cessation of shell growth during the warm season is related to the reproductive cycle or simply the combined result of overall slower growth at higher ontogenetic age and reduced growth at higher water temperature.

4.4 Future research needs

Verification of the findings of this study could include analysis of a larger number of specimen and tank experiments during which different environmental variables can be manipulated, specifically water temperature, food supply and food quality, pH etc. Does extreme food scarcity also result in larger, more elongated crystals when the optimum growth temperature range is exceeded? Is temperature really the only variable that controls the size and elongation of individual prisms? In a subsequent step, the new method should be applied to well-preserved fossil

specimens of *C. edule*. Future studies should also investigate if the new proxy is applicable to other species with similar microstructures. Can the same statistical models be used that were developed for *C. edule* or is the relationship between water temperature and P_s or P_e species-specific? Furthermore, the technique should be adapted to other bivalve species with different microstructures.

5. Conclusions

Prism size and elongation of the marine bivalve, *Cerastoderma edule*, can serve as a novel proxy for water temperature. Both microstructural characteristics were positively correlated to water temperature, but unrelated to shell growth rate and ontogenetic age as well as salinity, chlorophyll a level and turbidity. With a coupled model that combines changes of prism size and elongation it is possible to determine water temperature with an error of ± 1.7 °C. The new temperature proxy can potentially be of particular interest for paleoclimate studies when non-recrystallized fossil shells of this species are available. Verification of the results by future studies is necessary.

6. Acknowledgements

The authors thank Dr. Klemens Seelos for his assistance with the micro-imaging software OLYMPUS AnalySIS Pro and Christoph Füllenbach for inspiring discussions and for providing shell samples. We thank Lena Gaide, Lena Nachreiner, Hans Uhlmann, Ralf Sinnig (Nationalpark-Haus Wangerland) and Michael Bremer for their help in the field at Schillig and Irene Ballesta Artero for her help in the field at Texel. We gratefully acknowledge the help of Michael Maus during isotope analysis. Funding for this study was kindly provided by the EU within the framework of the Marie Curie International Training Network ARAMACC. BRS received financial support by the DFG (SCHO793/13).

7. Supplementary data

S1. Etching technique

Etching with diluted HCl has been used in many previous studies to reveal shell microstructures in bivalves including *Cerastoderma edule* (Farrow, 1971; Richardson et al., 1979; Ohno, 1983; Lønne and Gray, 1988; Bourget and Brock, 1990). In the studies cited above, etching was more intense than in our study, e.g., 1.2 N HCl for 10 seconds, 0.01N HCl for 20-25 min, 0.1 N HCl for 30 s, 0.12 N HCl for 45 s, 1 N HCl for 30 s, respectively. We tested different exposure times with 0.12 N HCl (5 s, 8 s, 10 s, 12 s, 15 s) to determine which one provides the best result and facilitates recognition and measurability of the prisms (Fig. S1). Below 10 s etching time, the organic matrix covers the microstructures and makes quantification of prism sizes challenging and unreliable (Fig. S1). When etching lasted 12 s, prisms were better visible, but some organic remains were still present (Fig. S1). 15 s etching time turned out to provide the best results for the studied species.

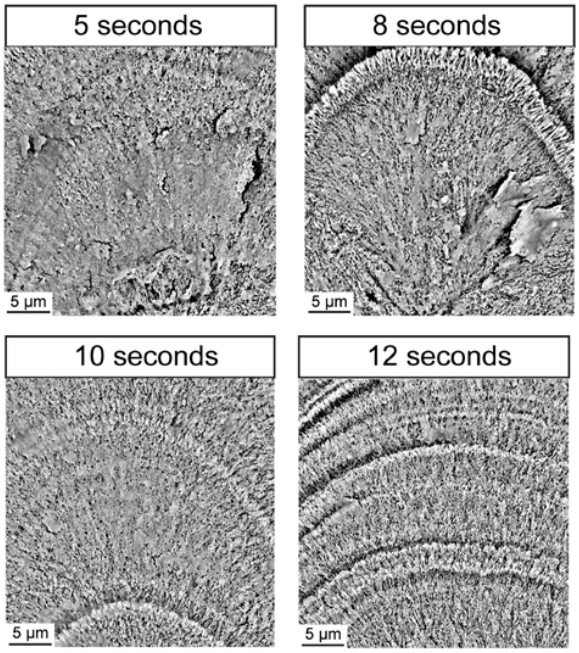

Fig. S1. SEM images of microstructures in the OSL after different etching times.

S2. Effect of ontogenetic age on temperature-induced microstructural changes

Despite different ontogenetic ages, similar changes were observed in prism size, elongation and inter-prismatic space suggesting that ontogenetic differences do not significantly affect the microstructural patterns (Fig. S2). Furthermore, only minor variations occurred between different specimens exposed to the same water temperatures (Fig. S2).

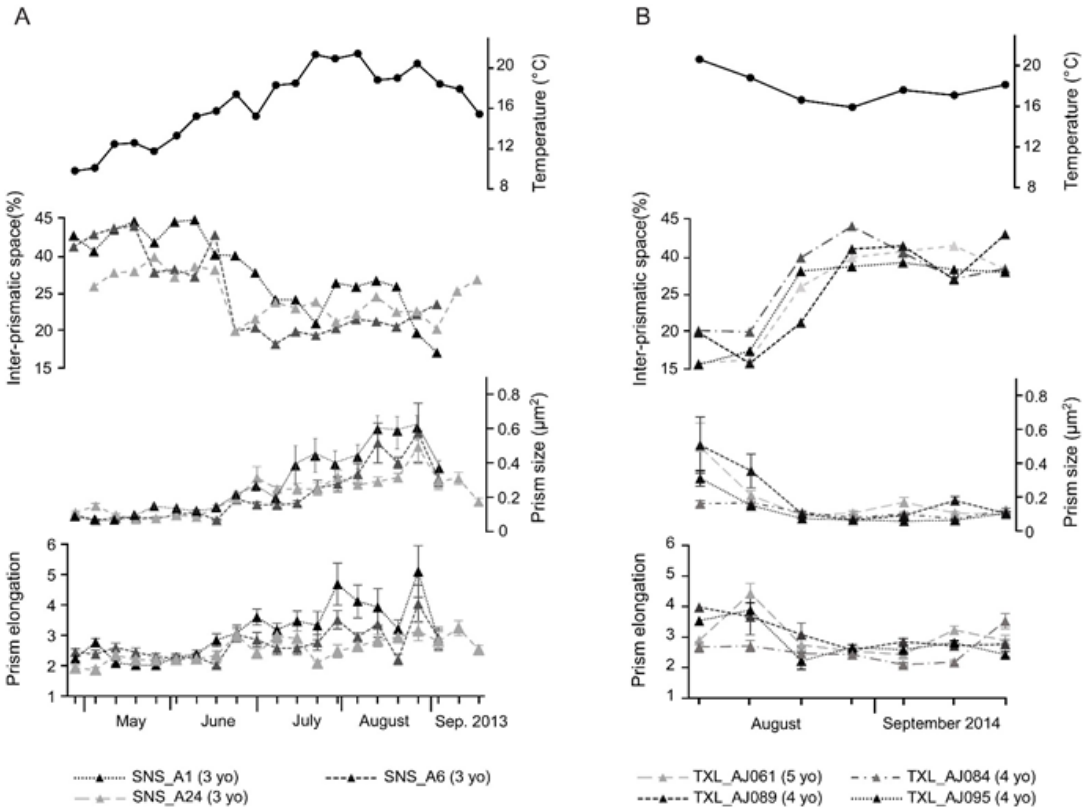

Fig. S2. Temperature-induced microstructural changes in different specimens of *Cerastoderma edule* from Schillig (A) and Texel (B). yo = years old. Error bars indicate average standard error.

S3. Seasonal changes of shell growth

Aside from periodic fluctuations caused by the spring and neap tide cycles, the lunar daily increment width curves revealed distinct seasonal changes, in particular at Schillig where the microgrowth patterns of the entire growing season were determined (Fig. 5). The widths of the lunar daily increments increased gradually during the growing season and reached a maximum of 55 ± 10 µm (measured at the axis of maximum growth within the OSL) at the end of May 2013. During summer, growth rates slowed down to values of ca. 13 ± 3 µm. A second seasonal maximum was attained at the beginning of August (60 ± 21 µm). After that, the lunar daily increment widths gradually declined toward the following 'winter' line. At Texel, increment width increased quickly after the summer line, reached a maximum in mid-August (52 ± 10 µm), declined, reached a second maximum at the end of September (70 ± 22 µm) and then declined toward the end of the main growing season of 2014.

8. References

Ansell, A.D., 1968. The rate of growth of the hard clam *Mercenaria mercenaria* (L.) throughout the geographical range. Journal du Conseil Permanent International pour l'Exploration de le Mer 31, 364-409.

Avery, R. and Etter, R., 2006. Microstructural differences in the reinforcement of a gastropod shell against predation. Marine Ecology Progress Series 323, 159-170.

Bourget, E. and Brock, V., 1990. Short-term shell growth in bivalves: individual, regional, and age-related variations in the rythym of deposition of *Cerastoderma* (= *Cardium) edule*. Marine Biology 106, 103-108.

Carré, M., Bentaleb, I., Bruguier, O., Ordinola, E., Barrett, N.T., Fontugne, M., 2006. Calcification rate influence on trace element concentrations in aragonitic bivalve shells: Evidences and mechanisms. Geochimica et Cosmochimica Acta 70, 4906-4920.

Carter, J.G. and Clark, G.R.I., 1985. Classification and phylogenetic significance of molluscan shell microstructure, in: Bottjer D.J., Hickman C.S., Ward P.D. (Eds.), Mollusks, Notes for a Short Course, University of Tennessee, 50-71.

Carter, J.G., Harries, P.J., Malchus, N., Sartori, A.F., Anderson, L.C., Bieler, R., Bogan, A.E., Coan, E.V., Cope, J.C.W., Cragg, S.M., Garcia-March, J.R., Hylleberg, J., Kelley, P., Kleemann, K., Kriz, J., McRoberts, C., Mikkelsen, P.M., Pojeta, J.J., Temkin, I., Yancey, T., Zieritz, A., 2012. Illustrated glossary of the bivalvia. Treatise Online no. 48, part N, volume 1, chapter 31.Chateigner, D., Hedegaard, C. and Wenk, H.R., 2000. Mollusc shell microstructures and crystallographic textures. Journal of Structural Geology 22, 1723-1735.

Chauvaud, L., Lorrain, A., Dunbar, R.B., Paulet, Y.-M., Thouzeau, G., Jean, F., Guarini, J.-M., Mucciarone, D., 2005. Shell of the great scallop *Pecten maximus* as a high-frequency archive of paleoenvironmental changes. Geochemistry, Geophysics, Geosystems 6. doi:10.1029/2004GC000890

Checa, A.G., Okamoto, T., Ramírez, J., 2006. Precipitation of aragonite by calcitic bivalves in Mg-enriched marine waters. Marine Biology 150, 819-827.

Coto, B., Martos, C., Peña, J.L., Rodríguez, R., Pastor, G., 2012. Effects in the solubility of $CaCO_3$: Experimental study and model description. Fluid Phase Equilibria 324. doi:10.1016/j.fluid.2012.03.020

Cölfen H. and Antonietti M., 2008. Mesocrystals and nonclassical crystallization. John Wiley & Sons,Ltd., Chichester.

Cuif, J.P., Bendounan, A., Dauphin, Y., Nouet, J., Sirotti, F., 2013. Synchrotron-based photoelectron spectroscopy provides evidence for a molecular bond between calcium and mineralizing organic phases in invertebrate calcareous skeletons. Analytical and Bioanalytical Chemistry 405, 8739-8748.

Dauphin, Y., Cuif, J.P., Doucet, J., Salomé, M., Susini, J., Willams, C.T., 2003. In situ chemical speciation of sulfur in calcitic biominerals and the simple prism concept. Journal of Structural Biology 142, 272-280.

DOE, 1994. Handbook of methods for the analysis of the various parameters of the carbon dioxide system in sea water, version 2 A. G. Dickson & C. Goyet, (Eds.), ORNL/CDIAC-74.

Eagle, R.A., Eiler, J.M., Tripati, A.K., Ries, J.B., Freitas, P.S., Hiebenthal, C., Wanamaker, A.D., Taviani, M., Elliot, M., Marenssi, S., Nakamura, K., Ramirez, P., Roy, K., 2013. Nutrient dynamics, transfer and retention along the aquatic continuum from land to ocean: towards integration of ecological and biogeochemical models. Biogeosciences 10. doi:10.5194/bg-10-1-2013

Evans, J.W., 1972. Tidal growth increments in the cockle *Clinocardium nuttalli*. Science 176, 416-417.

Farrow, G.E., 1971. Periodicity structures in the bivalve shell: experiments to establish growth controls in *Cerastoderma edule* from the Thames estuary. Paleontology 14, 571-588.

Fitzer, S.C., Cusack, M., Phoenix, V.R., Kamenos, N.A., 2014. Ocean acidification reduces the crystallographic control in juvenile mussel shells. Journal of Structural Biology 188, 39-45.

Freitas, P.S., Clarke, L.J., Kennedy, H., Richardson, C.A., Abrantes, F., 2006. Environmental and biological controls on elemental (Mg/Ca, Sr/Ca and Mn/Ca) ratios in shells of the king scallop *Pecten maximus*. Geochimica et Cosmochimica Acta 70, 5119-5133.

Füllenbach, C.S., Schöne, B.R. and Branscheid, R., 2014. Microstructures in shells of the freshwater gastropod *Viviparus viviparus*: a potential sensor for temperature change? Acta biomaterialia 10, 3911-3921.

Ghosh, P., Adkins, J., Affek, H., Balta, B., Guo, W., Schauble, E.A., Schrag, D., Eiler, J.M., 2006. ^{13}C-^{18}O bonds in carbonate minerals: a new kind of paleothermometer. Geochimica et Cosmochimica Acta 70, 1439-1456.

Gillikin, D.P., De Ridder, F., Ulens, H., Elskens, M., Keppens, E., Baeyens, W., Dehairs, F., 2005a. Assessing the reproducibility and reliability of estuarine bivalve shells (*Saxidomus giganteus*) for sea surface temperature reconstruction: implications for paleoclimate studies. Palaeogeography, Palaeoclimatology, Palaeoecology 228, 70-85.

Gillikin, D.P., Lorrain, A., Navez, J., Taylor, J.W., André, L., Keppens, E., Baeyens, W., Dehairs, F., 2005b. Strong biological controls on Sr/Ca ratios in aragonitic marine bivalve shells. Geochemistry, Geophysics, Geosystems 6. doi:10.1029/2004GC000874

Goodwin, D.H., Flessa, K.W., Schöne, B.R., Dettman, D.L., 2001.Cross-calibration of daily growth increments, stable isotope variation, and temperature in the Gulf of California bivalve mollusk *Chione cortezi*: implications for paleoenvironmental analysis. Palaios 16, 387-398.

Hahn, S., Rodolfo-Metalpa, R., Griesshaber, E., Schmahl, W.W., Buhl, D., Hall-Spencer, J.M., Baggini, C., Fehr, K.T., Immenhauser, A., 2012. Marine bivalve shell geochemistry and ultrastructure from modern low pH environments: environmental effect versus experimental bias. Biogeosciences 9, 1897-1914.

Hallmann, N., Burchell, M., Schöne, B.R., Irvine, G. V., Maxwell, D., 2009. High-resolution sclerochronological analysis of the bivalve mollusk *Saxidomus gigantea* from Alaska and British Columbia: techniques for revealing environmental archives and archaeological seasonality. Journal of Archaeological Science 36, 2353-2364.

Ivany, L.C., Wilkinson, B.H. and Jones, D.S., 2003. Using stable isotopic data to resolve rate and duration of growth throughout ontogeny: an example from the surf clam, *Spisula solidissima*. Palaios 18, 126-137.

Jones, D.S., 1983. Sclerochronology : shell record of the molluscan shell. American Scientist 71, 384-391.

Kadar, E., Checa, A.G., Oliveira, A.N.D.P., Machado, J.P., 2008. Shell nacre ultrastructure and depressurisation dissolution in the deep-sea hydrothermal vent mussel *Bathymodiolus azoricus*. Journal of Comparative Physiology B: Biochemical, Systemic, and Environmental Physiology 178, 123-130.

Kaehler, S. and McQuaid, C.D., 1999. Use of the fluorochrome calcein as an in situ growth marker in the brown mussel *Perna perna*. Marine Biology 133, 455-460.

Kelley, R.O., Dekker, R. A. F. and Bluemink, J.G., 1973. Ligand-mediated osmium binding: its application in coating biological specimens for scanning electron microscopy. Journal of Ultrastructure Research 45, 254-258.

Kennish, M.J., 1980. Skeletal growth of aquatic organisms, in: Rhoads D.C. and Lutz R.A. (Eds.) Skeletal growth of aquatic organisms: biological records of environmental changes. Plenum Press, 255-292.

Kennish, M.J. and Olsson, R.K., 1975. Effects of thermal discharges on the microstructural growth of *Mercenaria mercenaria*. Environmental Geology 1, 41-64.

Kingston, P., 1974. Some observations on the effects of temperature and salinity upon the growth of *Cardium Edule* and *Cardium Glaucum* larvae in the laboratory. Journal of the Marine Biological Association of the United Kingdom 54, 309-317.

Levi-Kalisman, Y., Falini, G., Addadi, L., Weiner, S., 2001. Structure of the nacreous organic matrix of a bivalve mollusk shell examined in the hydrated state using cryo-TEM. Journal of Structural Biology 135, 8-17.

L**ø**nne, O.J. and Gray, J.S., 1988. Influence of tides on migrogrowth bands in *Cerastoderma edule* from Norway. Marine Ecology Progress Series 42, 1-7.

Lutz, R.A., 1984. Paleoecological implications of environmentally-controlled variation in molluscan shell microstructure. Geobios 17, 93-99

Marchitto, T.M., Jones, G.A., Goodfriend, G.A., Weidman, C.R., 2000. Precise temporal correlation of holocene mollusk shells using sclerochronology. Quaternary Research 53, 236-246.

Marie, B., Joubert, C., Tayalé, A., Zanella-Cléon, I., Belliard, C., Piquemal, D., Cochennec-Laureau, N., Marin, F., Gueguen, Y., Montagnani, C., 2012. Different secretory repertoires control the biomineralization processes of prism and nacre deposition of the pearl oyster shell. Proceedings of the National Academy of Sciences of the United States of America 109, 20986-20991.

Marin, F., Pokroy, B., Luquet, G., Layrolle, P., De Groot, K., 2007. Molluscan shell proteins:primary structure, origin and evolution. Current Topics in Developmental Biology 80, 209-276.

Nishida, K., Ishimura, T., Suzuki, A., Sasaki, T., 2012. Seasonal changes in the shell microstructure of the bloody clam, *Scapharca broughtonii* (Mollusca: Bivalvia: Arcidae). Palaeogeography, Palaeoclimatology, Palaeoecology 363-364, 99-108.

Ohno, T., 1983. A note on the variability of growth increment formation in the shell of the common cockle *Cerastoderma edule*. In: Brosche P., Sünderman J. (Eds). Tidal friction and the earth's rotation. Springer, 222-228.

Orton, J.H., 1926. On the rate of growth of *Cardium edule*. Part I. Experimental observations. Journal of the Marine Biological Association of the United Kingdom 14, 239-279.

Palmer, A.R., 1983. Relative cost of producing skeletal organic matrix versus calcification: evidence from marine gastropods. Marine Biology 75, 287-292.

Pérez-Huerta, A., Etayo-Cadavid, M.F., Andrus, C.F.T., Jeffries, T.E., Watkins, C., Street, S.C., Sandweiss, D.H., 2013. El Niño impact on mollusk biomineralization-implications for trace element proxy reconstructions and the paleo-archeological record. PloS ONE 8. doi:10.1371/journal.pone.0054274

Ponsero, A., Daboudineau, L. and Allain, J., 2009. Modelling of the common European cockle (*Cerastoderma edule* L.) fishing grounds aimed at sustainable management of traditional harvesting. Fisheries Science 75, 839-850.

Popov, S.V., 1986. Composite prismatic structure in bivalve. Acta Palaeontologica 31, 3-26.

Prezant, R.S., Tan Tiu, A. and Chalermwat, K., 1988. Shell microstructure and color changes in stressed *Corbicula fluminea*. The Veliger 31, 236-243.

Ramón, M., 2003. Population dynamics and secondary production of the cockle *Cerastoderma edule* (L .) in a backbarrier tidal flat of the Wadden Sea. Scientia Marina 67, 429-443.

Rhoads, D.C. and Pannella, G., 1970. The use of molluscan shell growth patterns in ecology and paleoecology. Lethaia 3, 143-161.

Richardson, C.A., 2001. Molluscs as archives of environmental change. In: Gibson R.N., Barnes M. and Atkinson R.J.A. (Eds.) Oceanography and Marine Biology: an Annual Review, 39, CRC Press, 103-164.

Sato, S., 1999. Temporal change of life-history traits in fossil bivalves: An example of *Phacosoma japonicum* from the Pleistocene of Japan. Palaeogeography, Palaeoclimatology, Palaeoecology 154, 313-323.

Schöne, B.R., 2008. The curse of physiology— Challenges and opportunities in the interpretation of geochemical data from mollusk shells. Geo-Marine Letters 28, 269-285.

Schöne, B.R., 2013. *Arctica islandica* (Bivalvia): A unique paleoenvironmental archive of the northern North Atlantic Ocean. Global and Planetary Change 111, 199-225.

Schöne, B.R. and Gillikin, D.P., 2013. Unraveling environmental histories from skeletal diaries — Advances in sclerochronology. Palaeogeography, Palaeoclimatology, Palaeoecology 373. doi:10.1016/j.palaeo.2012.11.026

Schöne, B.R., Tanabe, K., Dettman, D.L., Sato, S., 2003. Environmental controls on shell growth rates and $\delta^{18}O$ of the shallow marine bivalve mollusk *Phacosoma japonicum* in Japan. Marine Biology 142, 473-485.

Schöne, B.R., Radermacher, P., Zhang, Z., Jacob, D.E., 2013. Crystal fabrics and element impurities (Sr/Ca, Mg/Ca, and Ba/Ca) in shells of *Arctica islandica*—Implications for paleoclimate reconstructions. Palaeogeography, Palaeoclimatology, Palaeoecology 373, 50-59.

Shirai, K., Schöne, B.R., Miyaji, T., Radarmacher, P., Krause, R.A., Tanabe, K., 2014. Assessment of the mechanism of elemental incorporation into bivalve shells (*Arctica islandica*) based on elemental distribution at the microstructural scale. Geochimica et Cosmochimica Acta 126, 307-320.

Stemmer, K., Nehrke, G. and Brey, T., 2013. Elevated CO_2 levels do not affect the shell structure of the bivalve *Arctica islandica* from the Western Baltic. PloS ONE 8. doi:10.1371/journal.pone.0070106

Stemmer, K. and Nehrke, G., 2014. The distribution of polyenes in the shell of Arctica islandica from North Atlantic localities: a confocal Raman microscopy study. Journal of Molluscan Studies 80, 365-370.

Su, X., Belcher, A.M., Zaremba, C.M., Morse, D.E., Stucky, G.D., Heuer, A.H., 2002. Structural and microstructural characterization of the growth lines and prismatic microarchitecture in red abalone shell and the microstructures of abalone "flat pearls." Chemistry of Materials 14, 3106-3117.

Tan Tiu, A., 1988. Temporal and spatial variation of shell microstructure of *Polymesoda caroliniana* (Bivalvia: Heterodonta). American Malacological Bulletin 6, 199-206.

Tan Tiu, A. and Prezant, R.S., 1987. Shell microstructural responses of *Geukensia demissa granosissima* (Mollusca: Bivalvia) to continual submergence. American Malacological Bulletin 5, 173-176.

Taylor, J.D., 1973. The structural evolution of the bivalve shell. Paleontology 16, 519-534.

van Aken, H.M., 2008. Variability of the water temperature in the western Wadden Sea on tidal to centennial time scales. Journal of sea Research 60, 227-234

Wefer, G. and Berger, W.H., 1991. Isotope paleontology: growth and composition of extant calcareous species. Marine Geology 100, 207-248.

West, K. and Cohen, A., 1996. Shell microstructure of gastropods from Lake Tanganyika, Africa: adaptation, convergent evolution, and escalation. Evolution 50, 672-681.

Wheeler, A.P., 1992. Mechanisms of molluscan shell formation. In: Bonucci E. (Ed.) Calcification in biological systems, CRC Press, 179-216.

Witbaard, R., Franken, R. and Visser, B., 1997. Growth of juvenile *Arctica islandica* under experimental conditions. Helgolaender Meeresuntersuchungen 51, 417-431.

Yan, L., Schöne, B.R. and Arkhipkin, A., 2012. *Eurhomalea exalbida* (Bivalvia): A reliable recorder of climate in southern South America? Palaeogeography, Palaeoclimatology, Palaeoecology 350-352, 91-100.

Yi, W., Yan, C. and Ma, P., 2010. Crystallization kinetics of Li_2CO_3 from $LiHCO_3$ solutions. Journal of Crystal Growth 312, 2345-2350.

Manuscript II

Impact of high pCO_2 on shell structure of the bivalve *Cerastoderma edule*

Published in Marine Environmental Research

Stefania Milano[1], Bernd R. Schöne[1], Schunfeng Wang[2], Werner E. Müller[2]

[1] Institute of Geosciences, University of Mainz, Joh.-J.-Becherweg 21, 55128 Mainz, Germany

[2] Institute of Physiological Chemistry, University of Mainz, Duesbergweg 6, 55099 Mainz, Germany

Author contribution

Concept: SM, BRS, WEM
Execution: SM, SW
Analysis: SM
Data interpretation: SM, BRS, SW
Writing: SM, BRS, WEM, SW

Milano, S., Schöne, B.R., Wang, S., Müller, W.E., 2016. Impact of high pCO_2 on shell structure of the bivalve *Cerastoderma edule*. Mar. Environ. Res. 119, 144-155.

Abstract

Raised atmospheric emissions of carbon dioxide (CO_2) result in an increased ocean pCO_2 level and decreased carbonate saturation state. Ocean acidification potentially represents a major threat to calcifying organisms, specifically mollusks. The present study focuses on the impact of elevated pCO_2 on shell microstructural and mechanical properties of the bivalve *Cerastoderma edule*. The mollusks were collected from the Baltic Sea and kept in flow-through systems at six different pCO_2 levels from 900 µatm (control) to 24,400 µatm. Extreme pCO_2 levels were used to determine the effects of potential leaks from the carbon capture and sequestration sites where CO_2 is stored in sub-seabed geological formations. Two approaches were combined to determine the effects of the acidified conditions: (1) Shell microstructures and dissolution damage were analyzed using scanning electron microscopy (SEM) and (2) shell hardness was tested using nanoindentation. Microstructures of specimens reared at different pCO_2 levels do not show significant changes in their size and shape. Likewise, the increase of pCO_2 does not affect shell hardness. However, dissolution of ontogenetically younger portions of the shell becomes more severe with the increase of pCO_2. Irrespective of pCO_2, strong negative correlations exist between microstructure size and shell mechanics. An additional sample from the North Sea revealed the same microstructural-mechanical interdependency as the shells from the Baltic Sea. Our findings suggest that the skeletal structure of *C. edule* is not intensely influenced by pCO_2 variations. Furthermore, our study indicates that naturally occurring shell mechanical property depends on the shell architecture at µm-scale.

Keywords: mollusc shell; acidification; carbon dioxide capture and sequestration; microstructure; shell hardness; scanning electron microscopy; nanoindentation

1. Introduction

Growing emission of anthropogenically-derived CO_2 to the atmosphere and its subsequent uptake by the oceans are leading to climate change and ocean acidification (Caldeira and Wickett, 2003; Feely et al., 2004; Raven et al., 2005). The addition of CO_2 to the ocean is followed by an increase in bicarbonate and H^+ ions concentrations and a decrease in carbonate ions concentration (Orr et al., 2005; Feely et al., 2004). These changes are predicted to have severe potential environmental and ecological repercussions on regional and global scales (Orr et al., 2005; Kleypas et al., 2006; Fabry et al., 2008; Dupont et al., 2010). Since the pre-industrial period, CO_2 atmospheric concentration increased from 280 to over 400 ppm (IPCC, 2007; data available from www.esrl.noaa.gov/gmd/ccgg/trends/) and ocean surface pH decreased by 0.1 units (Raven et al., 2005). According to the IS92a ocean acidification scenario, pH is predicted to further decrease by 0.3-0.4 units by 2100 (Meehl et al., 2007). In order to mitigate the emissions of CO_2, a new strategy of carbon dioxide capture and sequestration (CCS) has been introduced (Steeneveldt et al., 2006). For this technology CO_2 from the industrial processes is secured, injected and permanently stored it in sub-seabed geological formations providing a long-term isolation from the atmosphere. Even though the benefits of CCS have been demonstrated (IEA, 2010), stocking large volumes of CO_2 below the ocean floor generates apprehension about potential leaks and the consequent extreme acidification of the surrounding waters (IPCC, 2005).

In the past, great interest has been addressed to the effects of ocean acidification on marine calcifying organisms (Delille et al., 2005; Ries et al., 2009; Dupont et al., 2010; Ragazzola et al., 2012; Xu et al., 2016). Low pH leads to a decrease of CO_3^{2-} which in turn affects seawater saturation state (Ω). Undersaturated conditions ($\Omega < 1$) occurring in acidified water cause $CaCO_3$ to dissolve. Under these conditions, the ability of organisms to build $CaCO_3$ skeletons can decrease (Pörtner et al., 2005; Guinotte and Fabry, 2008; Doney et al., 2009), resulting in growth slowdown and potentially delayed sexual maturity (Kooijman and Metz, 1984). Furthermore, hypercapnia (high pCO_2 levels) can cause shell dissolution, jeopardizing the protection against the external threats as predation (Green et al., 2004). Despite the large number of studies on the effects of acidification, the consequences on biominerals formation are still not well understood. For instance, some species of gastropods, urchins, coralline and calcareous algae respond with an increased net calcification (Ries et al., 2009) whereas certain bivalves are not affected at all (Nieuhuis et al., 2010; Stemmer et al., 2013; Fitzer et al., 2014b). Furthermore, specific scenarios and threats of CCS on endemic marine communities have been explored in few studies (Neumann, 2012; Klok et al., 2014). Abundance and reproductive success of some bivalves such as *C. edule* and the families *Yoldiidae* and *Thyasiridae* were shown to be compromised by extreme levels of pCO_2 (Neumann, 2012; Klok et al., 2014). In order to implement future CCS projects, more assessments on potential ecosystemic responses are needed, with a particular focus on benthic organisms.

Given the high abundance of *C. edule* among the bivalve macrobenthic community of our study area (Western Baltic Sea) and its wide geographical

distribution from Norway to north-western Africa coasts, this mollusk was used as model species in the present study (De-Bastos and Tyler-Walters, 2007; Thomsen et al., 2010). Possible alteration of *C. edule* population due to acidification may have severe ecological implications. For instance, a lower abundance may lead to an unbalanced settlement success of other competitive species.

In turn, this could lead to a change of the meiofaunal and microbial communities in the area (Flach, 1996). Our aim is to investigate the impact of extremely acidified conditions, possibly occurring in case of a CCS leakage, on the shell material. CCS systems are built in deep waters, whereas *C. edule* is commonly found in shallow waters. However, the threat for onshore habitats is represented by potential transport pipeline failures caused, for example, by pipeline corrosion (Cole et al., 2011). Microstructural alterations and changes of mechanical properties of the shell may affect the survival of the organisms. Furthermore, these changes may represent useful tools for future environmental monitoring and reconstructions of past acidified conditions. The evaluation of shell architecture and hardness as potential CO_2 proxies rises the necessity to better understand the biomineralization processes that control the architecture and mechanical properties of shells. For this reason, our study also examines the influence of the size of the microstructural units on the mechanical behavior of *C. edule* shells.

2. Materials and Methods

A total of fifteen shells of *C. edule* were analyzed. Fourteen two year-old animals were collected from Falckenstein (Kiel Fjord, Baltic Sea) on 21 November 2011 along with sediment. The latter was used to simulate natural environment during the acidification experiment conducted at the GEOMAR Helmholtz Centre for Ocean Research Kiel (Fig. 1). The animals were collected with a Van Veen grab at a water depth of 1-2 m where they lived constantly submersed. In addition, one three-year-old *C. edule* was collected alive from the tide flat north of Schillig, North Sea on 11 March 2014 (Fig. 1A). This locality is characterized by a large tidal range (approx. 2.4 m), and the animal was aerially exposed for ca. six hours during each low tide. The specimen from Schillig was used to verify the results obtained during the tank studies at Kiel.

2.1 Tank experiment

The experiment started on 17 December 2011 and ended on 6 March 2012. Prior to the start of the experiment, bivalves were kept for 25 days in holding tanks at 9 °C. At the end of the acclimation period, the animals immersed in calcein for ca. 24 hours. Calcein is a non-toxic marker which is incorporated into growing carbonate structures and it is visible as bright green mark when observed using a UV-light microscope (Kaehler and McQuaid, 1999). Marking provides a precise estimation of the amount of shell formed during the experimental phase. Six different levels of pCO_2 were set: 900 µatm (control), 1,500 µatm, 2,900 µatm, 6,600 µatm, 12,800 µatm and 24,400

µatm (Fig. 1B). The corresponding pH values ranged between 7.8 and 6.4. For each level, one header tank was connected to six replicate tanks. Each of the latter (12.5 l) contained 20 cm of sediment, 10 cm of water and 40 *C. edule*, resembling the natural population density. The pCO_2 levels were chosen to mimic potential CCS leakage scenarios. According to the models, seepages could release between 8 and 800 CO_2 tons/day in shallow water areas decreasing the pH value by as much as 1.0 unit (Blackford et al., 2008; Blackford et al., 2009). Given that the average pH in the Baltic Sea ranges between 7.4 and 8.4 (Havenhand, 2012), seepages could cause a dramatic decrease of pH down to 6.4. The pCO_2 levels were maintained constant throughout the experiment in the header tanks by using a pH feedback computerized system (IKS Aquastar).

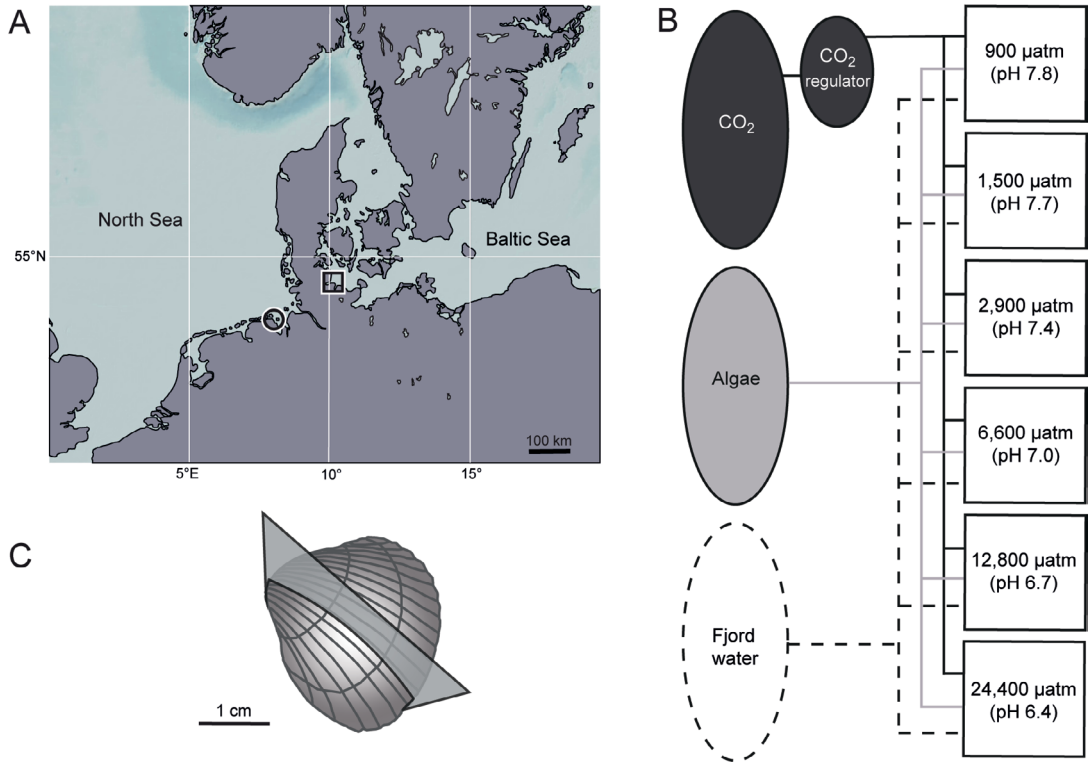

Fig. 1. (A) Study sites of Schillig, North Sea (circle) and Kiel Fjord, Baltic Sea (square). (B) Acidification experiment setup. (C) Sketch of *Cerastoderma edule* shell with the cutting plane along the axis of maximum growth.

Water in the tanks was constantly pumped from Kiel Fjord by a flow-through system. A flow rate of 100 ml min^{-1} was channeled to each replicate tank. Food was provided by constantly pumping and maintaining a stable concentration of 3,500 - 4,000 cells ml^{-1} of *Rhodomonas sp*. algae in the header tanks that supply the replicate tanks via a peristaltic pump. Temperature, salinity and pH were measured on a daily basis during the experiment using a pH meter (WTW SenTix 81 Plus) and a salinometer (WTW Cond315i). Carbonate chemistry was measured weekly.

Dissolved inorganic carbon was measured using an Automated Infrared Inorganic Carbon Analyzer (Marianda AIRICA). Aragonite saturation state and pCO_2 were calculated from pH_{NBS}, dissolved inorganic carbon, temperature, salinity and and first and second dissociation constants of carbonic acid in seawater using the software CO2SYS (Tab. 1). At the end of the experiment the soft tissues of the animals were removed with a scalpel. Then, the shells were washed, air-dried and stored in plastic bags. The experimental set up is further described by Schade et al. (in prep).

Table 1. Summary of the water chemistry parameters during the acidification experiment. Data are presented as means ± SD. TA = total alkalinity, Ω Arg = aragonite saturation state.

pCO_2 level (µatm)	Temperature (°C)	Salinity	pCO_2 (µatm)	pH	TA (µmol kg^{-1} SW)	Ω Arg
900	6.2 ± 1.1	17.6 ± 2.1	923.7 ± 58.3	7.8 ± 0.03	2032.4 ± 133.2	0.5 ± 0.06
1,500	6.2 ± 1.1	17.7 ± 2.0	1461.9 ± 195.2	7.4 ± 0.05	2049.9 ± 156.6	0.3 ± 0.04
2,900	6.4 ± 1.0	17.8 ± 2.0	2882.5 ± 360.5	7.4 ± 0.06	2028.4 ± 126.9	0.2 ± 0.02
6,600	6.3 ± 1.2	17.8 ± 2.0	6630.1 ± 775.8	7.0 ± 0.03	2020.4 ± 130.3	0.1 ± 0.01
12,800	6.3 ± 1.1	17.8 ± 2.0	12783.5 ± 1583.3	6.7 ± 0.03	1936.9 ± 170.9	0.04 ± 0.01
24,400	6.3 ± 1.2	17.8 ± 2.0	24381.1 ± 2103.3	6.4 ± 0.03	1848.9 ± 94.3	0.02 ± 0.00

2.2 Sample preparation

Fourteen specimens used in the acidification experiment were prepared for SEM analysis. SEM was used to measure shell growth, dissolution and microstructural properties. Three replicas were selected from the control (900 µatm) and highest pCO_2 level (24,400 µatm), respectively. Two replicas were selected from each intermediate pCO_2 level. Nanoindentation analysis was conducted on six specimens (one shell per treatment). The shell from Schillig was used for SEM and nanoindentation analyses (Tab. 2). The right valve of each sample (including the shell collected in Schillig) was glued to a plexiglass cube and covered with a layer of JB KWIK epoxy resin. A low-speed precision saw (Buehler Isomet 1000) was used to cut ca. two millimeter-thick sections from each specimen along the axis of shell maximum growth (Fig. 1C).

When used for both analyses, one shell slab was prepared for SEM analysis and a second one for nanoindentation study. Slabs for SEM were embedded in Struers EpoFix resin, whereas slabs for nanoindentation were glued to glass slides using a thin layer JB KWIK epoxy resin. After being air-dried overnight, the surface of all samples were ground using a Buehler Metaserv 2000 grinder-polisher machine equipped with Buehler silicon carbide papers of different grit sizes (320, 600, 1200, 2500). Subsequently, the slabs were polished with 3 µm diamond suspension on a Buehler VerduTex cloth. Samples were ultrasonically cleaned with deionized water after each grinding step and after polishing. Shell slabs used for SEM were etched for

15 seconds in 1 vol% HCl, rinsed in deionized water, air-dried, sputter coated with a 3 nm-thick gold film. Subsequently, the slabs were analyzed under the scanning electron microscope (LOT Quantum Design 2nd generation Phenom Pro desktop SEM) using a backscattered electron detector and a 10kV accelerating voltage. Slabs for nanoindentation were further polished for ca. three hours with a 1 µm Al_2O_3 suspension in a Buehler VibroMet 2 vibratory polisher. Afterward, the calcein marks were located under a fluorescence light microscope (Zeiss Axio Imager.A1m microscope equipped with a Zeiss HBO100 mercury lamp and filter set 38: excitation wavelength, ~ 450 - 500 nm; emission wavelength, ~ 500 - 550 nm).

2.3 *C. edule* microstructures

Shell architecture of *C. edule* has been previously described by Carter et al. (2012) and Milano et al. (2015). The shell consists of three aragonitic layers, each with a characteristic microstructure (Fig. 4B-D). A complex crossed-lamellar microstructure dominates the inner shell layer (ISL), simple crossed-lamellar microstructure forms the inner portion of the outer shell layer (iOSL; also referred to as middle shell layer) and a non-denticular composite prismatic microstructure is found in the outer portion of outer shell layer (oOSL). The oOSL was in the focus of the present study.

2.4 Image processing

Three different image processing software products were used to evaluate shell growth patterns, microstructural properties and dissolution damage. To precisely align the growth record, tidal growth increments (Ohno, 1983; Schöne, 2008) were counted and measured in the oOSL to the nearest 1 µm with the software Panopea (© Schöne and Peinl).

Olympus Analysis Pro was used to automatically detect individual prisms in the oOSL. Automated image processing was completed in regions of interest (ROIs) with a fixed area of 13 ± 0.1 μm^2. In samples from Kiel, an average of six ROIs were analyzed in each of the two shell portions formed prior to ($oOSL_{wild}$) and during the acidification experiment ($oOSL_{tank}$). In total, the size and elongation of 4,263 individual prisms was determined. In the shell from Schillig, a total of nine ROIs and 484 individual prisms were investigated in shell portions formed during spring-autumn 2013.

To properly detect individual prisms, the greyscale threshold was set to 71. This value turned out to be most suitable to reliably identify the spaces between individual crystal units. False detection of pixels at the prism boundaries was manually corrected. Given the presence of part of the organic matrix in the inter-crystalline space (Nudelman et al., 2006), the latter was used to indirectly quantify the organic compound. Quantitative assessment of the inter-prismatic space was carried out by

calculating the difference between the ROI total area and the sum of the single prism areas. It was then expressed as percentage.

Quantification of dissolution damage in the shells from Kiel was achieved by using Fiji, a platform of the open-source imaging software ImageJ. Four regions in each sample were selected starting from the hinge towards the ventral margin every ca. 4.4 mm. SEM images of the oOSL were taken (Fig. 3A). Within these images, visibly altered zones (i.e. holes) were manually marked. In order to quantify the damage, dissolved areas were expressed as percentage of the studied oOSL portion. The results from the four regions of each sample were then averaged.

2.5 Nanoindentation

Shell hardness was determined by means of a NanoTest Vantage nanoindenter (Institute of Physiological Chemistry; University of Mainz). An average of 107 nanoindentations were performed in the oOSL of each sample. The number of indentations on the oOSLwild and oOSLtank portions of the samples from Kiel ranged from 36 to 108 and from 16 to 65, respectively (Tab. 2). Test direction was perpendicular to the shell slabs. Nanoindentation was carried out by a loading rate of 3 mN/s. The maximum depth of the indenter in the material was set to 1 µm. The Berkovich indenter tip used during the test had a three-sided pyramidal shape with a geometry factor of 1.034.

Table 2. Basic data on studied *Cerastoderma edule* specimens along with microstructural and nanoindentation analyses.

Sample ID	Locality	Shell height (mm)	Age	pCO_2 level (µatm)	# prisms		# nanoindentations	
					$oOSL_{wild}$	$oOSL_{tank}$	$oOSL_{wild}$	$oOSL_{tank}$
B14_A1	Kiel	19.1	2	900	204	300	50	65
B17_A1	Kiel	18.6	2	900	191	200	-	-
B22_A1	Kiel	18.9	2	900	205	193	-	-
B3_A1	Kiel	18.2	2	1,500	111	131	86	32
B12_A1	Kiel	17.4	2	1,500	100	108	-	-
B29_A5	Kiel	19.3	2	2,900	95	91	-	-
B31_A1	Kiel	18.9	2	2,900	216	129	76	40
B25_A3	Kiel	17.1	2	6,600	394	496	108	32
B25_A9	Kiel	17.5	2	6,600	253	239	-	-
B18_A1	Kiel	18.8	2	12,800	51	55	-	-
B36_A6	Kiel	19.8	2	12,800	50	42	76	24
B1_A13	Kiel	19.6	2	24,400	52	55	-	-
B9_A1	Kiel	17.2	2	24,400	56	58	-	-
B9_A5	Kiel	16.1	2	24,400	106	82	36	16
A1	Schillig	16.5	3	-	484	-	108	-

2.6 Shell growth and temporal alignment

In *C. edule* shell, the formation of growth increments is controlled by tides. Shell growth largely occurs during high tide and results in the formation of a circatidal increment. During low tide, a circatidal growth line is deposited. Two couplets of circatidal increments and lines represent a lunar (= circalunidian) day (24.8 hours). By counting circalunidian increments and measuring their width along the axis of maximum growth in the oOSL, it was possible to determine the timing and rate of shell growth.

In order to evaluate potential seasonal changes in hardness in the sample from Schillig, the shell portion corresponding to the last growing season was temporally aligned. On the basis of field observations, shell stable isotope analysis ($\delta^{18}O$) and growth increment analysis, the onset and ending of the growing season 2013 was determined (Milano et al., 2015).

2.7 Statistical analyses

ANOVA, Kruskal-Wallis and Tukey´s HSD post hoc test were performed on the samples from Kiel to investigate whether significant differences exist in microstructural and mechanical properties between shell portions deposited under pCO_2 of 900 µatm in nature and in tanks as well as under elevated CO_2 levels ($pCO_2 \geq 1{,}500$ µatm). Once the relationships between structural and mechanical variables were identified, the regression slopes of Kiel and Schillig samples were compared using ANCOVA.

3. Results

3.1 Shell growth and dissolution in acidified conditions

With increasing pCO_2, the time interval during which shell growth occurred decreased significantly (ANOVA $p < 0.05$). For example, the animals kept in the control tank grew for 22 ± 1 days, while those exposed to 24,400 µatm pCO_2 grew for only 8 ± 2 days (Fig. 2A). Tukey´s post hoc test showed significant differences between the specimens growing at the two highest pCO_2 levels (12,800 and 24,400 µatm) and the rest of the shells. Furthermore, at higher CO_2 levels, a lower net calcification occurred. Bivalves kept at pCO_2 of 900 µatm grew 0.5 ± 0.1 mm of shell during the experiment, whereas those exposed to the highest CO_2 concentration grew 0.2 ± 0.1 mm (Fig. 2B). However, this decrease in growth was not significant from a statistical point of view (ANOVA $p = 0.05$). Furthermore, the daily growth rates did not show significant changes with increasing pCO_2 (ANOVA $p = 0.15$). At 900 µatm, *C. edule* grew in average by 21.3 ± 5.1 µm/day, and by 22.5 ± 4.5 µm/day at 24,400 µatm (Fig. 2C).

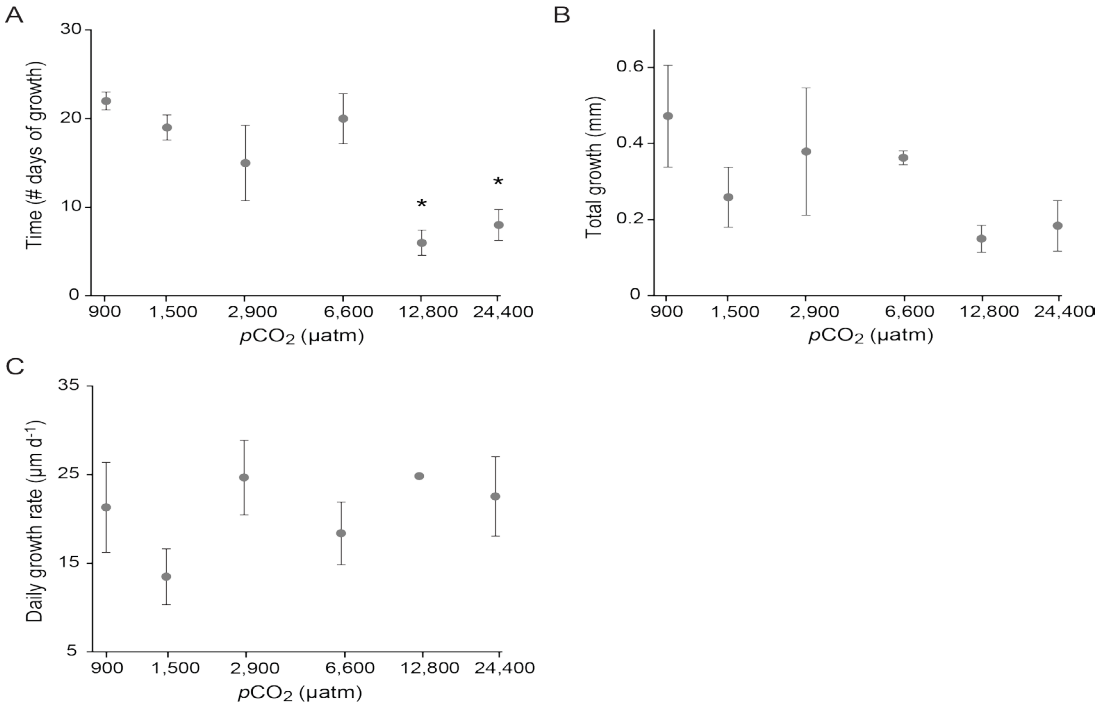

Fig. 2. Shell growth of the samples from Kiel reared at different pCO_2 levels in terms of (A) number of growing days, (B) total amount of aragonite deposited during the experiment and (C) daily growth rate. A logarithmic scale was applied to the x-axes. Error bars indicate standard deviation (±1σ). Asterisks indicate significant differences (Tukey´s post hoc test, $p < 0.05$). N = 2-3.

Shell dissolution was discernible in ontogenetically older shell portions, in particular near the hinge region, whereas no damage was detected in the portions used for the microstructural analysis (Fig. 3C-H). Furthermore, shell damage was limited to the oOSL, and did not occur in the iOSL or ISL. As shown in Figure 3B, the percentage of damaged area in the control specimens equaled 1.9 %, whereas it was 4.6 % and 6.6 % from the 1,500 µatm and 2,900 µatm treatments, respectively. Hypercapnia at 6,600 µatm and 12,800 µatm dissolved 37.0 % and 39.2 % of the oOSL, respectively. This sudden increase in damage was due to a complete dissolution of one of the four regions analyzed (100 % damage). The sample kept at 24,400 µatm showed complete dissolution of the two most umbonal regions considered with a total oOSL damage of 73.3 %.

3.2 Effects of increased pCO_2 on shell microstructure and hardness

In comparison with the natural environment, microstructural and mechanical properties of *C. edule* did not change significantly in artificial conditions and at elevated pCO_2 levels (Figs. 4+5). To analyze the effect of acidification, the measurements were grouped into three classes: (1) measurements conducted on shell portions formed prior to the experiment (n = 14 for microstructures; n = 6 for hardness), (2) measurements of portions formed during the experiment at control level (n = 3 for microstructures; n = 1 for hardness), (3) measurements of portions formed during the experiment in acidified conditions (n =11 for microstructures; n = 5 for hardness). Although prisms were slightly smaller in the specimen that grew in the 900 µatm tank than specimens exposed to elevated pCO_2, no statistical differences were found between the size of the prisms formed in natural and artificial conditions (Kruskal-Wallis p = 0.06; Fig. 5A). Similarly, prism elongation did not vary considerably (Kruskal-Wallis p = 0.15; Fig. 5B). In addition, no significant differences were observed in the shell hardness (ANOVA p = 0.56; Fig. 5C).

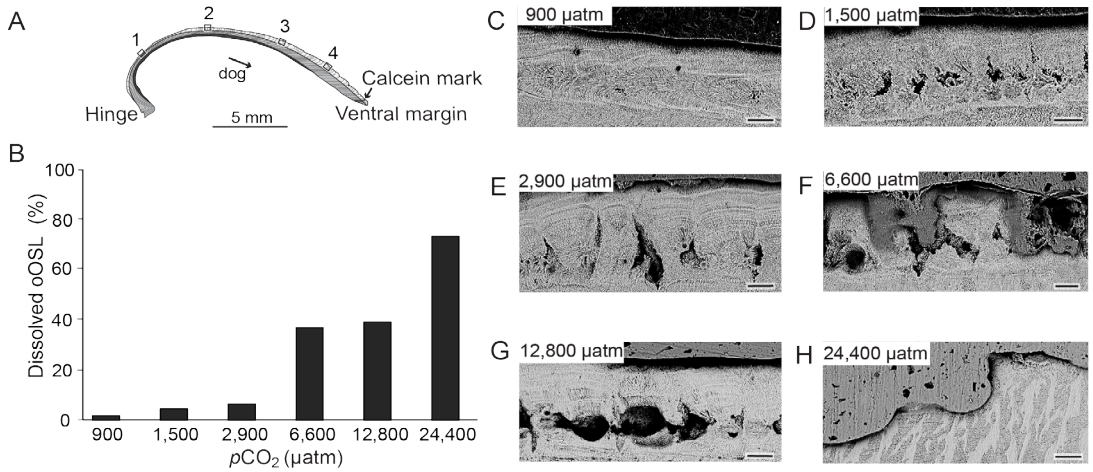

Fig. 3. Shell dissolution during the acidification experiment. (A) Shell sketch showing the four areas analyzed. (B) Percentage of damaged oOSL shell of the fourteen samples used in the experiment. (C-G) SEM images showing the increasing damage to the oOSL (second areas from the hinge) due to the rising acidification level. (H) SEM image showing complete dissolution of the area 2 at 24,400 µatm. The remaining shell portion in the image represents the iOSL. dog = direction of growth. Scale bars = 20 µm.

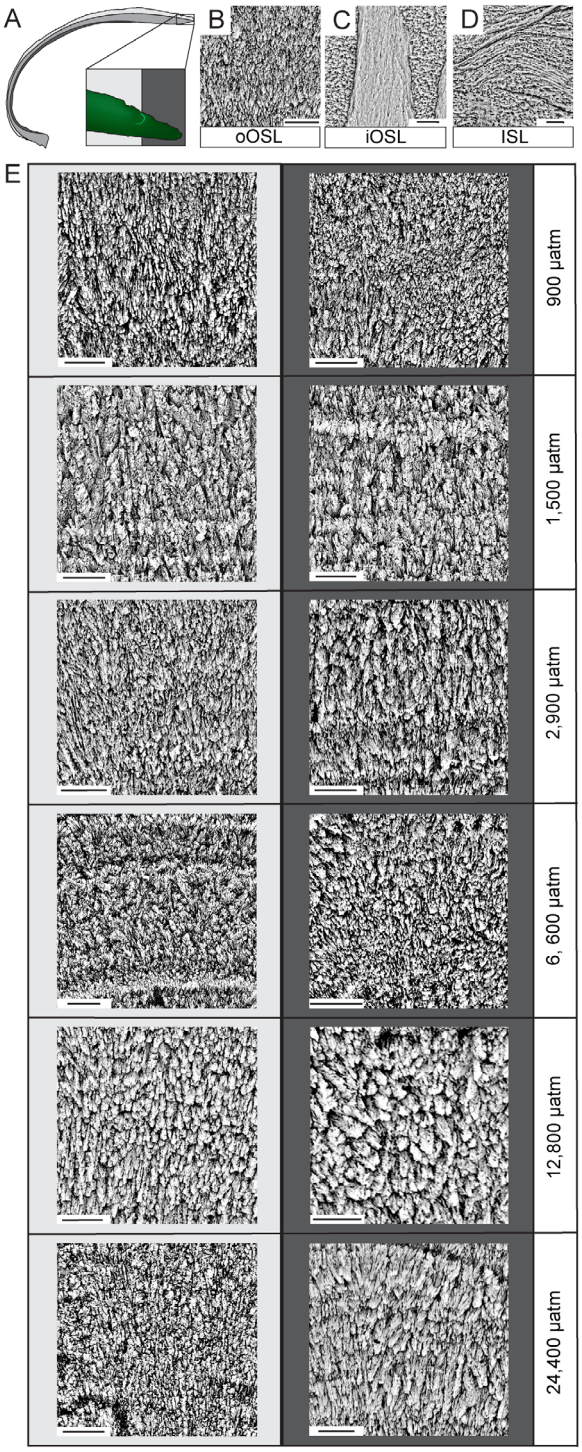

Fig. 4. *C. edule* microstructures. (A) Shell sketch showing the three-layered shell organization and the calcein mark indicating the start of the acidification experiment. (B) SEM image of the characteristic non-denticular composite prismatic microstructure of the outer portion of outer shell layer (oOSL). (C) SEM image of the simple crossed-lamellar microstructure of the inner portion of the outer shell layer (iOSL). (D) SEM image of the complex crossed-lamellar microstructure of the inner shell layer (ISL). (E) Microstructures of the oOSL of the shells from Kiel reared at different pCO_2. Light grey boxes include SEM images of shell portions formed prior the experiment ($oOSL_{wild}$). Dark grey box include images of microstructures formed during the experiment ($oOSL_{tank}$). Scale bars = 5 µm.

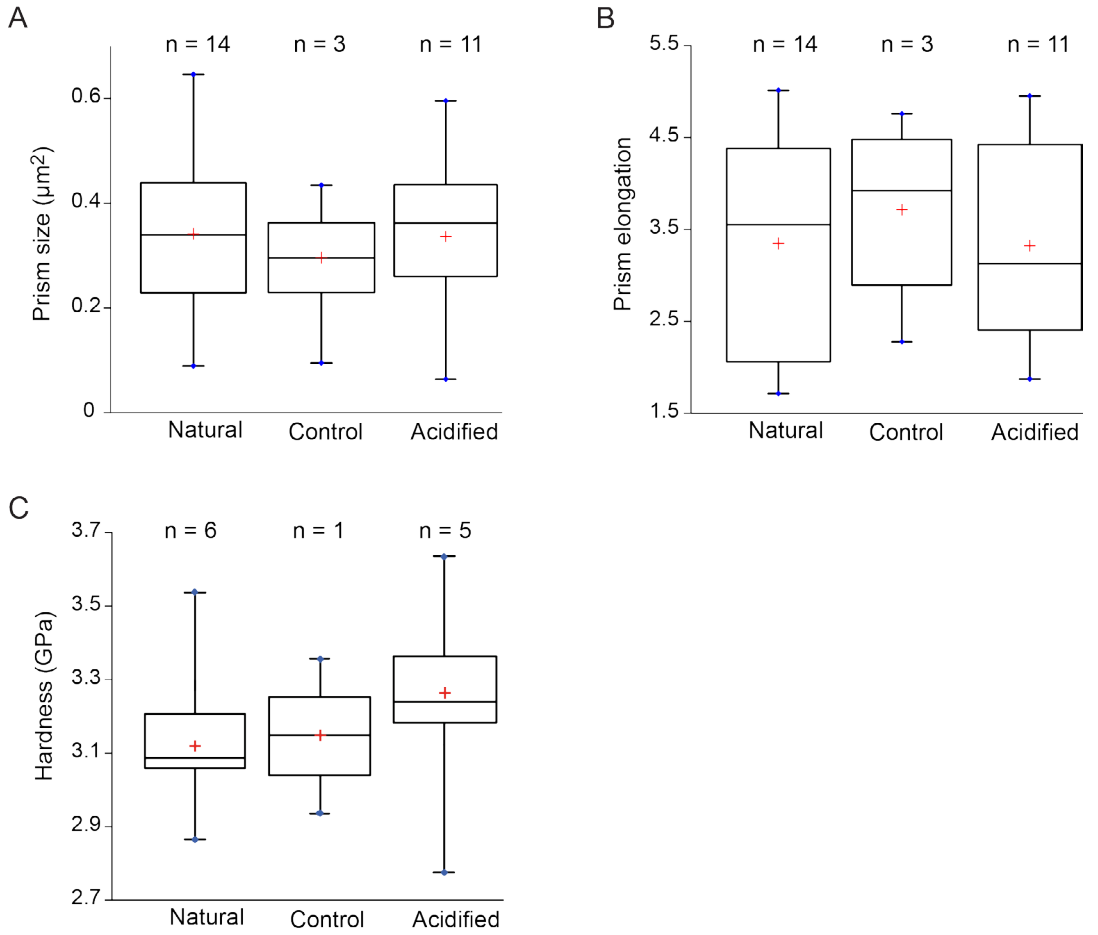

Fig. 5. Shell microstructures and hardness in portions formed in the natural, artificial (control) and artificial and acidified conditions. Effects of acidification on (A) prism size, (B) prism elongation and (C) shell hardness.

3.3 Relationship between shell microstructural and mechanical properties

Irrespective to pCO_2, the six replicas collected from Kiel and the one shell from Schillig showed a strong negative correlation between hardnessand prism size and a strong positive relationship between mechanical property and inter-prismatic space. In specimens from Kiel, hardness of shell portions formed in the natural environment was highly correlated to prism size ($R = -0.80$; $R^2 = 0.64$; $p < 0.0001$; Fig. 6A). Likewise, hardness of shell portions formed during higher CO_2 levels correlated to prism size ($R = -0.68$; $R^2 = 0.46$; $p < 0.0001$). A similar relationship was seen in the sample from Schillig ($R = -0.89$; $R^2 = 0.80$; $p < 0.01$). The regression slopes were not significantly different between the three data sets (ANCOVA $p = 0.85$). The hardness of $oOSL_{wild}$ showed strong linear correlations with the percentage of inter-prismatic space ($R = 0.68$; $R^2 = 0.46$; $p < 0.0001$; Fig. 6C). The same applied to the $oOSL_{tank}$ portions ($R = 0.72$; $R^2 = 0.52$; $p < 0.0001$) and the shell from Schillig ($R = 0.77$; $R^2 = 0.60$; $p < 0.0001$). The regression slopes were not significantly different between the three data sets (ANCOVA $p = 0.69$).

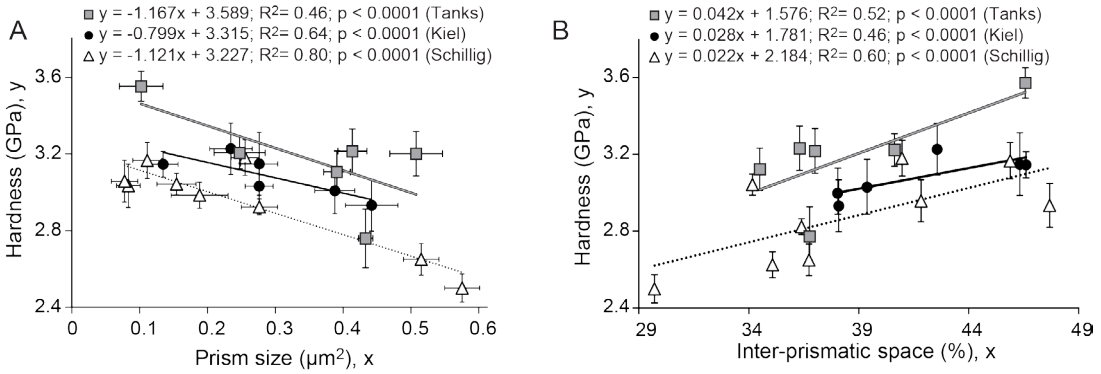

Fig. 6. Relationships between microstructure and mechanical property. Correlation between shell hardness (A) prism size and (B) inter-prismatic space. Grey squares refer to portions of the shells from Kiel formed during the acidification experiment. Black circles refer to portions of the shells from Kiel formed in the natural environment. Open triangles refer to the shell from Schillig grown in the natural environment. Error bars = 1σ.

3.4 Seasonal changes in shell hardness during the growing season

According to growth pattern analysis, the growing season 2013 of the Schillig specimen started on 19th April and ended on 11th September. During this time interval, the shell exhibited seasonal variations in hardness (Fig. 7). Furthermore, the size of individual prisms in the oOSL increased during the growing season as a result of increasing water temperature. As shown in Figure 7, an increase in prism size was associated with a decrease in shell hardness. As a consequence, a strong negative correlation was observed between the two variables ($R = - 0.89$; $R^2 = 0.80$; $p < 0.0001$). The amount of inter-prismatic space was negatively correlated with prism size ($R = - 0.69$; $R^2 = 0.48$; $p < 0.0001$) and positively correlated with shell hardness. Larger prims were thus associated with lower amounts of organics and greater shell hardness. Furthermore, a negative correlation existed between SST and hardness ($R = - 0.37$; $R^2 = 0.13$; $p < 0.0001$), so that shell material formed during summer was softer than that formed at colder temperatures.

4. Discussion

In accordance with Klok et al. (2014), our results indicate that *C. edule* grow less shell in a given time interval at elevated pCO_2. Acidified water induces a severe dissolution of ontogenetically youger shell portions (Fig. 3). However, despite hypercapnic conditions, microstructural architecture remain largely unaffected (Fig. 4). None of the six specimens shows any significant change in the mechanical property due to acidification. However, our study shows that, irrespective to acidification, *C. edule* shell microstructural organization plays an important role in determining shell hardness. Seasonal microstructural changes are indeed reflected in variations in shell hardness.

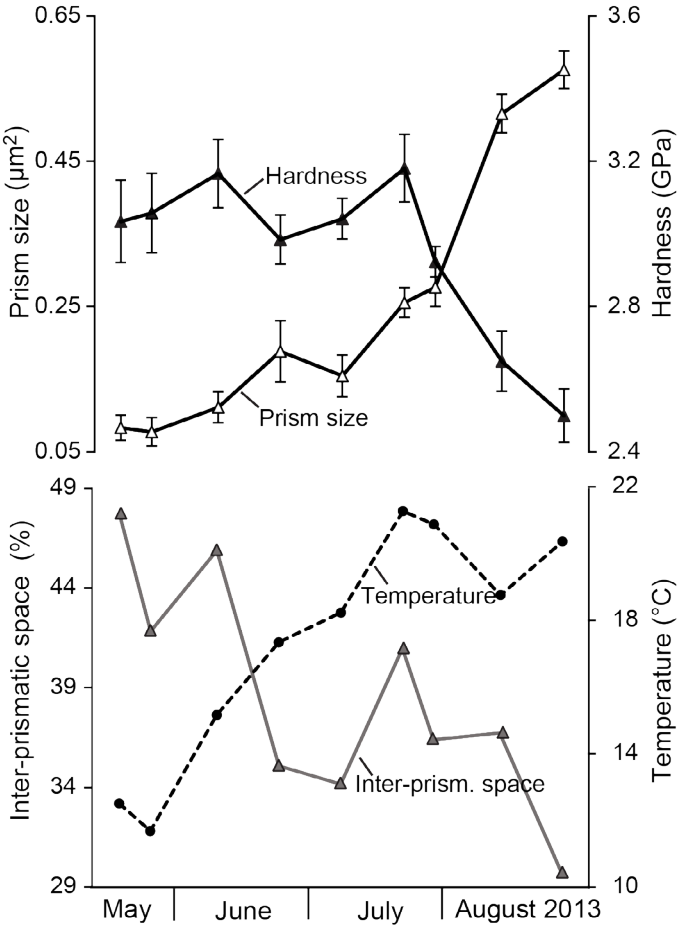

Fig. 7. Seasonal variations in microstructure (prism size and inter-prismatic space) and mechanical (shell hardness) properties of *C. edule* from Schillig. Error bars = 1σ.

4.1 Shell growth and dissolution under hypercapnic conditions

During the experiment, all studied cockles grew at a similar rate. However, the specimens reared at higher pCO_2 grew for less time. Therefore, the total shell material deposited decreased with increasing pCO_2. Acidified conditions have been previously reported to induce divergent responses in exoskeleton production of marine calcifying organisms (Orr et al., 2005; Iglesias-Rodriguez et al., 2008; Bechmann et al., 2011). High pCO_2 can induce increased calcification rates. For instance, the ophiuroid *Amphiura filiformis* responded with an upregulation of metabolism and calcification to compensate the adverse conditions (Wood et al., 2008). On the contrary, low shell growth rate was confirmed in the vent mussel *Bathymodiolus brevior* (Tunnicliffe et al., 2009). Natural populations living in extremely acidified waters showed a reduced daily growth rate when compared to populations from unaffected sites (Tunnicliffe et al., 2009). Similar observations were recorded in specimen of *Mytilus galloprovincialis* cultured under hypercapnic conditions (Michaelidis et al., 2005). Contrastingly, shell deposition of *Arctica islandica* was not affected by acidification (Hiebental et al., 2013; Stemmer et al., 2013). In the first experiment the animals were

kept at pCO_2 up to ~ 1,600 µatm and weekly growth rate was not affected by any treatment (Hiebenthal et al., 2013). The same applies to the study by Stemmer et al., 2013, where *A. islandica* maintained unaltered its daily growth rate. Also, production rate of shell material by the intertidal gastropod *Nucella lamellosa* was not affected by high pCO_2 (Nienhuis et al., 2010). In accordance to the latter findings, our results indicate that daily shell growth rate of *C. edule* remains substantially unaltered in hypercapnic conditions.

However, alterations in growth are not always reflected in a corresponding trend in net calcification. In fact, growth rate and net calcification only match when the temporal duration of growth is not influenced by the experimental conditions and all samples grow for the same period of time. In the present study, *C. edule* cultured at high pCO_2 grew shell only during a few days. Despite unaltered growth rate, this results in fewer amounts of material deposited over the time of the experiment. With regards to the total shell growth, our results are in accordance with previous studies. The same trend was observed in controlled tank experiments with *M. edulis* kept at pCO_2 up to 4,000 µatm (Thomsen et al., 2010; Melzner et al., 2011). Bamber (1990) observed a reduction in growth of *Crassostrea gigas* when cultured for 30 days at pH < 7. Another example was shown by Beniash et al., (2010). *Crassostrea virginica* cultured at pCO_2 up to 3,400 µatm showed a loss of shell mass with increasing pCO_2 indicating a negative effect on shell growth (Beniash et al., 2010).

With respect to growth, organisms react differently to acidified and undersaturated waters. Different responses may depend on the specific capacities of the organisms to regulate their internal pH (Ries et al., 2009). Some species are able to maintain an elevated pH at the site of calcification and use the increased amount of dissolved inorganic carbon in their fluid for calcification by converting HCO_3^- to CO_3^{2-} via proton regulation or by direct use of HCO_3^- for shell production (Ries at al., 2009). On the basis of this explanation, our results indicate that *C. edule*, like other organisms, is potentially unable to control its pH and therefore, acidified water induces a decrease in carbonate production. Shell growth suppression is also potentially related to altered metabolic pathways. This, in turn, can cause a delay in reaching the sexual maturity which, in this species, is suggested to be size-dependent (Klok et al., 2014). Therefore, reduced shell size can lower the reproduction rate and expose the animals to a higher predation pressure causing alterations in the population dynamics.

When exposed to acidified conditions, mollusk shell surfaces can also be affected by a certain magnitude of dissolution (Gazeau et al., 2013). Dissolution is potentially caused by the corrosiveness of the surrounding medium (Waldbusser et al., 2011). CO_2 is an "acidic molecule" that forms carbonic acid (H_2CO_3) when reacting with water (Chierici and Fransson, 2009). As a consequence, carbonate ion concentration decreases as well as carbonate saturation state ($\Omega < 1$; Chierici and Fransson, 2009). In these conditions of undersaturation and corrosiveness, the chemical processes set the stage for the stability of biogenic carbonates (Waldbusser et al., 2011). Biological factors are possibly involved in this process (Powell et al., 2011). However, our results do not provide certainty on the nature and mechanism

of the process. The present study indicates that increasing pCO_2 intensifies *C. edule* shell dissolution. However, damaged portions are limited to the oOSL and to shell portions formed during early ontogeny. oOSL more direct exposure to ambient water may be the reason for its additional sensitivity to acidification (Booth et al., 1984; Nienhuis et al., 2010). A sharp increase in the percentage of dissolved shell portion is recorded at pCO_2 6,600 µatm and higher, suggesting a threshold level beyond which severe damage can occur in the shells of *C. edule*. Our study is in accordance with previous findings that suggest a strong cause-effect relationship between hypercapnia and shell dissolution in different species of mollusks (Kuwatani and Nishii, 1969; Bamber et al., 1990; Green et al., 2004; Michaelidis et al., 2005; McClintock et al., 2009; Melzer et al., 2011).

4.2 Shell microstructure and hardness

The analysis conducted on fourteen shells shows that prismatic structures of the oOSL formed under natural conditions and in the control tank do not significantly differ in shape or size from those deposited at higher pCO_2. This is in good agreement with findings by Beniash et al. (2010) and Stemmer et al. (2013) where no changes were reported in the crystallinity of the foliated layer (calcite) of *C. virginica* and in the homogenous microstructure (aragonite) of *A. islandica*. However, a different response was recorded in *M. edulis* where microstructures in the outer calcitic layer showed an enhanced crystallographic misorientation during juvenile and adult stages of life (Hahn et al., 2012; Fitzer et al., 2014a, b).

The six specimens analyzed by nanoindentation show that there is no change in hardness between shell portions deposited under natural and acidified conditions. Likewise, uniformity in shell hardness was previously described in *M. edulis* and *A. islandica* by Hiebenthal et al. (2013) and Mackenzie et al. (2014). A decrease in the hardness was reported in *C. virginica* and *M. mercenaria* when exposed to hypercapnia combined with elevated temperature (27 °C; Ivanina et al., 2013). However, high pCO_2 alone did not result in significant changes (Ivanina et al., 2013). Likely, juvenile *C. virginica* respond with a lower shell hardness only when grown in a combination of hyposaline and acidified waters (Dickinson et al., 2012). In contrast, the combination of high temperature and high CO_2 seems to reduce the impact on shell hardness in both calcitic and aragonitic layers of *M. edulis* (Fitzer et al., 2015). In general, the effect caused by acidification on microstructural architecture seems to be strongly biased by the combination with other environmental parameters.

According to published data and our findings, structural integrity is maintained under hypercapnic conditions, at the cost of reduced shell growth. This may indicate the capacity by which the organisms resist predation, endolithic boring and abrasion due to burrowing. Unaltered microstructures and hardness suggest that these shell properties cannot be used as proxies for reconstruction of past acidification events or environmental monitoring.

4.3 Structural and mechanical relationships

It is well known that biogenic $CaCO_3$ from which shells are formed is much harder than its geological counterpart (Jackson et al., 1988; Smith et al., 1999; Kamat et al. 2000). This strength is due to the biomaterial complexity, its hierarchical organization and critically depends on the different factors e.g. anisotropy of the crystal units (Pokroy et al., 2004; Pokroy et al., 2006), matrix incompressibility (Dashkovskiy et al., 2007) and Van-der-Waals forces (Smith et al., 1999). However, a major role is played by the interaction between mineral and organic phases (Weiner and Addadi, 1997; Merkel et al., 2009). In fact, these two components are characterized by complementary mechanical features (Dashkovskiy et al., 2007). The mineral phase provides rigidity against mechanical failure and abrasion. However, this alone would result in a stiff but brittle material (Huber et al., 2015). The organic matrix, although present in small quantities (1-5 wt %) (Kawaguchi and Watabe, 1993), provides the flexibility and cohesive strength necessary to significantly improve the hardness of the shell (Meyers et al., 2006). A complex assemblage of organic macromolecules (proteins, glycoproteins, chitin and acidic polysaccharides; Marin et al., 2008) is mainly present as an intercrystalline envelope around individual crystal units (Harper, 2000). The organics enhance the fracture toughness by energy dissipation (Currey, 1999; Kamat et al., 2004; Weaver et al. 2010). Crack propagation in the shell is lowered as a result of a reduction and redistribution of the indentation energy (Dashkovskiy et al., 2007; Fratzl et al. 2007; Merkel et al., 2007; Tushtev et al., 2008).

Our results show that areas containing smaller prisms and a higher percentage of inter-prismatic space are characterized by greater hardness. Although the quantification of the inter-prismatic space is not a direct measurement of the inter-prismatic organic matrix content, we assumed a certain correlation between the two. In fact, the inter-prismatic space is the void left after the etching process. Given the anisotropic nature of the shell architecture, our results are limited to the test direction.

Although there are slight differences in hardness between the material formed in the tanks and in natural environments at Kiel and Schillig, these differences are not statistically significant (Fig. 5). Small prisms have a greater surface-to-volume ratio than large prisms. This, in turn, translates into a potential increase in inter-prismatic space and hence, inter-prismatic organics (Harper, 2000; Rodriguez-Navarro et al. 2006). Higher amounts of organics between small microstructural units may improve mechanical resistance and explain the relationship between the two properties (Merkel et al., 2007; Liang et al., 2008; Zhang et al., 2010). Likely, Taylor and Layman (1972) agreed that small structural units provide a reduction in crack propagation compared to larger units. In the latter case, the cracks can travel much farther along the unit boundaries. Another example of mechanical- microstructural size dependency is represented by the results by Ji et al. (2014) investigating *Clinocardium californiense* shell. Large prismatic microstructures of the shell outer portion resulted in a more deformable material than the complex crossed lamella of the two inner layers. Furthermore, the hardness in the inner portion was particularly low where thick third-order lamellae were present.

4.4 Seasonal changes in hardness and microstructures

The importance of the relationship between microstructure and mechanical properties can be appreciated in the light of previous findings. As described by Milano et al. (2015), prisms size of *C. edule* shells increases during the growing season. Along with this variation, a seasonal change in shell hardness is visible. Both properties can represent potential proxies for reconstructing water temperatures. During the summer temperature peak, (i) prisms tend to become larger, (ii) the inter-prismatic space decreases and, as a result, (iii) shell material is less resistant to deformation. Warm temperatures beyond the optimum temperature can cause a decline in metabolism (Ansell, 1968; Schöne et al., 2006; Hiebenthal et al., 2013) that, in turn, can lower the production of organic matrix leading to a decrease in shell hardness. From an energetic perspective, four molecules of ATP are needed to form a single peptide bond in a protein chain (Lehninger, 1975). Instead, only one molecule of ATP is required to actively transport two Ca^{2+} through the mitochondria (Schatzmann, 1973). Although some additional cost is needed to transport HCO_3^- that becomes shell carbonate, the synthesis of proteins remains more costly that the precipitation of the mineral phase (Palmer, 1983; Wilbur and Saleuddin, 1983; Palmer, 1992). Moreover, seasonal variations of calcium and glucose concentration were observed by Pekkarinen (1997) in the hemolymph, extrapallial fluid and mantle cavity fluid of *Anodonta anatina*. During the summer months, concurrently with the temperature peak, calcium concentration rises whereas glucose content decreases. In accordance with our findings, low availability of glucose during summer could indicate a decrease in carbohydrate metabolism (Ivanina et al., 2013) leading to a decrease in the synthesis of polysaccharides forming the organic matrix and therefore, a reduced shell hardness. At the same time, the greater availability of calcium transported to the biomineralization site could potentially be related to the larger size of the prisms. This suggest that, although shell architecture and hardness are not sensitive to acidification, they may successfully record temperature variations.

5. Conclusions and further studies

Extreme acidified water conditions only marginally affect the shells of the marine bivalve *Cerastoderma edule*. The newly-formed shell material displays microstructural and mechanical stability. However, growth is reduced and dissolution damage increases in acidified conditions. Even if the reduced energy investment in shell growth may trigger the ability of maintaining material integrity, dissolution of the exoskeleton may prove lethal for the mollusks on a longer time scale.

Our findings show that *C. edule* shell microstructure and hardness are not sensitive to changes in pCO_2 and hence do not serve as proxies for acidification. However, the strong relationship between the two plays an important role in the evaluation of shell architecture and mechanics as paleotemperature proxies. In

addition, our results lend additional insight into the importance of mineral and organic phase interplay in the mechanics of biominerals.

Nanoindentation is an extremely time-consuming analytical technique. In order to verify the present results, it is suggested to increase the number of specimens analyzed. Additional acidification tank experiments including temperature-controlled conditions would be suitable to study the combination of hypercapnia and temperature on mollusk shells. Further investigations on the mechanical and microstructural interdependencies in biogenic carbonate materials are needed. Better understanding of the role of the organic matrix and the size of microstructural units can provide useful insights for biomimetics and material sciences. For this purpose, direct measurements on the organic content are recommended. Bivalve species with large prismatic microstructures, i.e. *Mytilus sp.*, are preferred. When decalcified, the organic matrix is better visible and measurable than in small prismatic or crossed-lamellar microstructures.

6. Acknowledgements

The authors thank Dr. Frank Melzner and Hanna Schade (Helmholtz Centre for Ocean Research Kiel, GEOMAR) for conducting the acidification experiment and for providing shell material. We acknowledge the help of Dr. Klemens Seelos (Institute of Geosciences, University of Mainz) for his support with the software OLYMPUS AnalySIS Pro. Funding for this study was kindly provided by the EU within the framework of the Marie Curie International Training Network ARAMACC (604802) and by the DFG (SCHO793/13).

7. References

Ansell, A.D., 1968. The rate of growth of the hard clam *Mercenaria mercenaria* (L) throughout the geographic range. Journal du Conseil Permanent International pour l'Exploration de le Mer 31, 364-409.

Bamber, R.N., 1990. The effects of acidic seawater on three species of lamellibranch mollusc. Journal of Experimental Marine Biology and Ecology 143, 181-191. doi:10.1016/0022-0981(90)90069-O

Bechmann, R.K., Taban, I.C., Westerlund, S., Godal, B.F., Arnberg, M., Vingen, S., Ingvarsdottir, A., Baussant, T., 2011. Effects of ocean acidification on early life stages of shrimp (*Pandalus borealis*) and mussel (*Mytilus edulis*). Journal of Toxicology and Environmental Health A 74, 424-438. doi:10.1080/15287394.2011.550460

Beniash, E., Ivanina, A., Lieb, N.S., Kurochkin, I., Sokolova, I.M., 2010. Elevated level of carbon dioxide affects metabolism and shell formation in oysters *Crassostrea virginica*. Marine Ecology Progress Series 419, 95-108. doi:10.3354/meps08841

Blackford, J.C., Jones, N., Proctor, R., Holt, J., 2008. Regional scale impacts of distinct CO_2 additions in the North Sea. Marine Pollution Bulletin, 56, 1461-1468. http://doi.org/10.1016/j.marpolbul.2008.04.048

Blackford, J.C., Jones, N., Proctor, R., Holt, J., Widdicombe, S., Lowe, D., Rees, A., 2009. An initial assessment of the potential environmental impact of CO_2 escape from marine carbon capture and storage systems. Journal of Power and Energy 223, 269-280. doi:10.1243/09576509JPE623

Booth, C.E., McDonald, D.G., Walsh, P.J., 1984. Acid-base balance in the sea mussel, *Mytilus edulis*. I. Effects of hypoxia and air exposure on intracellular acid-base status. Marine Biology Letters 5, 347-358.

Caldeira, K. and Wickett, M.E., 2003. Oceanography: anthropogenic carbon and ocean pH. Nature 425, 365. doi:10.1038/425365a

Carter, J.G., Harries, P.J., Malchus, N., Sartori, A.F., Anderson, L.C., Bieler, R., Bogan, A.E., Coan, E.V., Cope, J.C.W., Cragg, S.M., Garcia-March, J.R., Hylleberg, J., Kelley, P., Kleemann, K., Kriz, J., McRoberts, C., Mikkelsen, P.M., Pojeta, J.J., Temkin, I., Yancey, T., Zieritz, A., 2012. Illustrated glossary of the bivalvia. Treatise Online no. 48, part N, volume 1, chapter 31.

Chierici, M. and Fransson, A., 2009. Calcium carbonate saturation in the surface water of the Arctic Ocean: undersaturation in freshwater influenced shelves. Biogeosciences Discussions, 6, 4963-4991. doi:10.5194/bgd-6-4963-2009

Cole, I.S., Corrigan, P., Sim, S., Birbilis, N., 2011. Corrosion of pipelines used for CO_2 transport in CCS: Is it a real problem? International Journal of Greenhouse Gas Control 5, 749-756. doi:10.1016/j.ijggc.2011.05.010

Currey, J.D., 1999. The design of mineralised hard tissues for their mechanical functions. The Journal of Experimental Biology 202, 3285-3294.

Dashkovskiy, S., Suhr, B., Tushtev, K., Grathwohl, G., 2007. Nacre properties in the elastic range: influence of matrix incompressibility. Computational Materials Science 41, 96-106. doi:10.1016/j.commatsci.2007.03.015

De-Bastos, E., Tyler-Walters, H., 2007. *Cerastoderma edule* Common cockle. In Tyler-Walters H. and Hiscock K. (eds.) Marine life information network: biology and sensitivity key information reviews (on-line). Plymouth: Marine Biological Association of the United Kingdom. Available from: http://www.marlin.ac.uk/species/detail/1384

Delille, B., Harlay, J., Zondervan, I., Jacquet, S., Chou, L., Wollast, R., Bellerby, R.G.J., Frankignoulle, M., Borges, A.V., Riebesell, U., Gattuso, J.P., 2005. Response of primary production and calcification to changes of pCO_2 during experimental blooms of the coccolithophorid *Emiliania huxleyi*. Global Biogeochemical Cycles 19. doi:10.1029/2004GB002318

Dickinson, G.H., Ivanina, A. V, Matoo, O.B., Pörtner, H.O., Lannig, G., Bock, C., Beniash, E., Sokolova, I.M., 2012. Interactive effects of salinity and elevated CO_2 levels on juvenile eastern oysters, *Crassostrea virginica*. The Journal of Experimental Biology 215, 29-43. doi:10.1242/jeb.061481

Doney, S.C., Fabry, V.J., Feely, R.A., Kleypas, J.A., 2009. Ocean acidification: the other CO_2 problem. Annual Review of Marine Science 1, 169-192. doi:10.1146/annurev.marine.010908.163834

Dupont, S., Ortega-Martínez, O., Thorndyke, M., 2010. Impact of near-future ocean acidification on echinoderms. Ecotoxicology 19, 449-462. doi:10.1007/s10646-010-0463-6

Fabry, V.J., Seibel, B.A., Feely, R.A., Orr, J.C., 2008. Impacts of ocean acidification on marine fauna and ecosystem processes. ICES Journal of Marine Science 65, 414-432.

Feely, R.A., Sabine, C.L., Lee, K., Berelson, W., Kleypas, J., Fabry, V.J., Millero, F.J., 2004. Impact of anthropogenic CO_2 on the $CaCO_3$ system in the oceans. Science 305, 362-366. 10.1126/science.1097329

Fitzer, S.C., Cusack, M., Phoenix, V.R., Kamenos, N.A., 2014a. Ocean acidification reduces the crystallographic control in juvenile mussel shells. Journal of Structural Biology 188, 39-45. doi:10.1016/j.jsb.2014.08.007

Fitzer, S.C., Phoenix, V.R., Cusack, M., Kamenos, N.A., 2014b. Ocean acidification impacts mussel control on biomineralisation. Scientific Reports 4. doi: 10.1038/srep06218

Fitzer, S.C., Zhu, W., Tanner, K.E., Phoenix, V.R., Nicholas, A.K., Cusack, M., 2015. Ocean acidification alters the material properties of *Mytilus edulis* shells. Journal of the Royal Society Interface 12. doi: 10.1098/rsif.2014.1227Published

Flach, E.C., 1996. The influence of the cockle, *Cerastoderma edule*, on the macrozoobenthic community of tidal flats in the Wadden Sea. Mar. Ecol. 17, 87-98. doi:10.1111/j.1439-0485.1996.tb00492.x

Fratzl, P., Gupta, H.S., Fischer, F.D., Kolednik, O., 2007. Hindered crack propagation in materials with periodically varying Young's modulus - lessons from biological materials. Advanced Materials 19, 2657-2661. doi:10.1002/adma.200602394

Gazeau, F., Parker, L.M., Comeau, S., Gattuso, J., O'Connor, W.A., Martin, S., Pörtner, H., Ross, P.M., 2013. Impacts of ocean acidification on marine shelled molluscs. Marine Biology 160, 2207-2245. doi:10.1007/s00227-013-2219-3

Green, M.A., Jones, M.E., Boudreau, C.L., Moore, R.L., Westman, B.A., 2004. Dissolution mortality of juvenile bivalves in coastal marine deposits. Limnology and Oceanography

49, 727-734. doi:10.4319/lo.2004.49.3.0727

Guinotte, J.M. and Fabry, V.J., 2008. Ocean acidification and its potential effects on marine ecosystems. Annals of the New York Academy of Sciences 1134, 320-342. doi:10.1196/annals.1439.013

Hahn, S., Rodolfo-Metalpa, R., Griesshaber, E., Schmahl, W.W., Buhl, D., Hall-Spencer, J.M., Baggini, C., Fehr, K.T., Immenhauser, A., 2012. Marine bivalve shell geochemistry and ultrastructure from modern low pH environments: environmental effect versus experimental bias. Biogeosciences 9, 1897-1914. doi:10.5194/bg-9-1897-2012

Harper, E.M., 2000. Are calcitic layers an effective adaptation against shell dissolution in the Bivalvia? Journal of Zoology 251, 179-186. doi:10.1017/S095283690000604X

Havenhand, J.N., 2012. How will ocean acidification affect Baltic Sea ecosystems? An assessment of plausible impacts on key functional groups. Ambio 41, 637-644. doi:10.1007/s13280-012-0326-x

Hiebenthal, C., Philipp, E.E.R., Eisenhauer, A., Wahl, M., 2013. Effects of seawater pCO_2 and temperature on shell growth, shell stability, condition and cellular stress of Western Baltic Sea *Mytilus edulis* (L.) and *Arctica islandica* (L.). Marine Biology 160, 2073-2087. doi:10.1007/s00227-012-2080-9

Huber, J., Griesshaber, E., Nindiyasari, F., Schmahl, W.W., Ziegler, A., 2015. Functionalization of biomineral reinforcement in crustacean cuticle: Calcite orientation in the partes incisivae of the mandibles of *Porcellio scaber* and the supralittoral species *Tylos europaeus* (Oniscidea, Isopoda). Journal of Structural Biology 190, 173-191. doi:10.1016/j.jsb.2015.03.007

IEA, 2010. Energy technology perspectives: 2010. Scenarios & strategies to 2050. International Energy Agency.

Iglesias-Rodriguez, M.D., Halloran, P.R., Rickaby, R.E.M., Hall, I.R., Colmenero-Hidalgo, E., Gittins, J.R., Green, D.R.H., Tyrrell, T., Gibbs, S.J., von Dassow, P., Rehm, E., Armbrust, E.V., Boessenkool, K.P., 2008. Phytoplankton calcification in a high-CO_2 world. Science 320, 336-340. doi:10.1126/science.1154122

IPCC, 2005. IPCC Special report on carbon dioxide capture and storage. doi:10.1021/es200619j

IPCC, 2007. IPCC Fourth assessment report: Climate change 2007

Ivanina, A.V., Dickinson, G.H., Matoo, O.B., Bagwe, R., Dickinson, A., Beniash, E., Sokolova, I.M., 2013. Interactive effects of elevated temperature and CO_2 levels on energy metabolism and biomineralization of marine bivalves *Crassostrea virginica* and *Mercenaria mercenaria*. Comparative Biochemistry and Physiology 166, 101-111. doi:10.1016/j.cbpa.2013.05.016

Jackson, A.P., Vincent, J.F.V., Turner, R.M., 1988. The mechanical design of nacre. Proceedings of the Royal Society B: Biological Sciences 234, 415-440.

Ji, H.M. and Li, X.W., 2014. Microstructural characteristic and its relation to mechanical properties of *Clinocardium californiense* shell. Journal of the American Ceramic Society 8. doi: 10.1111/jace.13246

Kaehler, S., McQuaid, C.D., 1999. Use of the fluorochrome calcein as an in situ growth

marker in the brown mussel *Perna perna*. Marine Biology 133, 455-460. doi:10.1007/s002270050485

Kamat, S., Su, X., Ballarini, R., Heuer, A.H., 2000. Structural basis for the fracture toughness of the shell of the conch *Strombus gigas*. Nature 405, 1036-1040. doi:10.1038/35016535

Kamat, S., Kessler, H., Ballarini, R., Nassirou, M., Heuer, A.H., 2004. Fracture mechanisms of the *Strombus gigas* conch shell: II-micromechanics analyses of multiple cracking and large-scale crack bridging. Acta Materialia 52, 2395-2406. doi:10.1016/j.actamat.2004.01.030

Kawaguchi T. and Watabe N., 1993. The organic matrices of the shell of the American oyster *Crassostrea virginica* Gmelin Journal of Experimental Marine Biology and Ecology 170, 11-28.

Kleypas, J.A., Feely, R.A., Fabry, V.J., Langdon, C., Sabine, C.L., Robbins, L.L., 2006. Impacts of ocean acidification on coral reefs and other marine calcifiers: a guide for future research, report of a workshop sponsored by NSF, NOAA, USGS.

Klok, C., Wijsman, J.W.M., Kaag, K., Foekema, E., 2014. Effects of CO_2 enrichment on cockle shell growth interpreted with a dynamic energy budget model. Journal of Sea Research 94, 111-116. doi:10.1016/j.seares.2014.01.011

Kooijman, S.A.L.M. and Metz, J.A.J., 1984. On the dynamics of chemically stressed populations: the deduction of population consequences from effects on individuals. Ecotoxicology and Environmental Safety 8, 254-274. doi:10.1007/BF02255198

Kuwatani, Y. and Nishii, T., 1969. Effects of pH of culture water on the growth of the Japanese pearl oyster. Bulletin of the Japanese Society of Scientific Fisheries 35, 342-350.

Lehninger, A.L., 1975. Biochemistry. Worth Publishers, Inc., New York.

Liang, Y., Zhao, J., Wang, L., Li, F., 2008. The relationship between mechanical properties and crossed-lamellar structure of mollusk shells. Materials Science and Engineering A 483-484, 309-312. doi:10.1016/j.msea.2006.09.156

Mackenzie, C.L., Ormondroyd, G. A., Curling, S.F., Ball, R.J., Whiteley, N.M., Malham, S.K., 2014. Ocean warming, more than acidification, reduces shell strength in a commercial shellfish species during food limitation. PLoS One 9, doi:10.1371/journal.pone.0086764

Marin, F., Luquet, G., Marie, B., Medakovic, D., 2008. Molluscan shell proteins: primary structure, origin, and evolution. Current Topics in Developmental Biology 80, 209-276. doi:10.1016/S0070-2153(07)80006-8

McClintock, J.B., Angus, R.A., Mcdonald, M.R., Amsler, C.D., Catledge, S.A., Vohra, Y.K., 2009. Rapid dissolution of shells of weakly calcified antarctic benthic macroorganisms indicates high vulnerability to ocean acidification. Antarctic Science 21, 449-456. doi:10.1017/S0954102009990198

Meehl, G.A., Stocker, T.F., Collins, W.D., Friedlingstein, P., Gaye, A.T., Gregory, J.M., Kitoh, A., Knutti, R., Murphy, J.M., Noda, A., Raper, S.C.B., Watterson, I.G., Weaver, A.J., Zhao, Z., 2007. Global Climate Projections, Climate Change 2007: Contribution of working group I to the fourth assessment report of the intergovernmental panel on climate change. doi:10.1080/07341510601092191

Melzner, F., Stange, P., Trübenbach, K., Thomsen, J., Casties, I., Panknin, U., Gorb, S.N.,

Gutowska, M.A., 2011. Food supply and seawater pCO_2 impact calcification and internal shell dissolution in the blue mussel *Mytilus edulis*. PLoS One 6, doi: 10.1371/journal.pone.0024223

Merkel, C., Deuschle, J., Griesshaber, E., Enders, S., Steinhauser, E., Hochleitner, R., Brand, U., Schmahl, W.W., 2009. Mechanical properties of modern calcite- (*Mergerlia truncata*) and phosphate-shelled brachiopods (*Discradisca stella* and *Lingula anatina*) determined by nanoindentation. Journal of Structural Biology 168, 396-408. doi:10.1016/j.jsb.2009.08.014

Merkel, C., Griesshaber, E., Kelm, K., Neuser, R., Jordan, G., Logan, A., Mader, W., Schmahl, W.W., 2007. Micromechanical properties and structural characterization of modern inarticulated brachiopod shells. Journal of Geophysical Research 112, doi: 10.1029/2006JG000253

Meyers, M.A., Lin, A.Y.M., Seki, Y., Chen, P.Y., Kad, B.K., Bodde, S., 2006. Structural biological composites: An overview. Biological Materials Mechanics 58, 35-41. doi:10.1007/s11837-006-0138-1

Michaelidis, B., Ouzounis, C., Paleras, A., Pörtner, H.O., 2005. Effects of long-term moderate hypercapnia on acid-base balance and growth rate in marine mussels *Mytilus galloprovincialis*. Marine Ecology Progress Series 293, 109-118. doi:10.3354/meps293109

Milano, S., Schöne, B.R., Witbaard, R., 2015. Changes of shell microstructural characteristics of *Cerastoderma edule* (Bivalvia) - A novel proxy for water temperature. Paleogeography, Paleoclimatology, Paleoecology. http://dx.doi.org/10.1016/j.palaeo.2015.09.051

Neumann, J., 2012. Effect of high CO_2 and low pH on benthic communities of the deep sea.

Nienhuis, S., Palmer, A.R., Harley, C.D.G., 2010. Elevated CO_2 affects shell dissolution rate but not calcification rate in a marine snail. Proceedings of the Royal Society B: Biological Sciences 277, 2553-2558. doi:10.1098/rspb.2010.0206

Nudelman, F., Gotliv, B.A., Addadi, L., Weiner, S., 2006. Mollusk shell formation: Mapping the distribution of organic matrix components underlying a single aragonitic tablet in nacre. Journal of Structural Biology 153, 176-187. doi:10.1016/j.jsb.2005.09.009

Ohno, T., 1983. A note on the variability of growth increment formation in the shell of the common cockle *Cerastoderma edule*. In: Tidal Friction and the Earth's Rotation II. Springer Berlin Heidelberg, 222-228.

Orr, J.C., Fabry, V.J., Aumont, O., Bopp, L., Doney, S.C., Feely, R. a, Gnanadesikan, A., Gruber, N., Ishida, A., Joos, F., Key, R.M., Lindsay, K., Maier-Reimer, E., Matear, R., Monfray, P., Mouchet, A., Najjar, R.G., Plattner, G.-K., Rodgers, K.B., Sabine, C.L., Sarmiento, J.L., Schlitzer, R., Slater, R.D., Totterdell, I.J., Weirig, M.-F., Yamanaka, Y., Yool, A., 2005. Anthropogenic ocean acidification over the twenty-first century and its impact on calcifying organisms. Nature 437, 681-686. doi:10.1038/nature04095

Palmer, A.R., 1983. Relative cost of producing skeletal organic matrix versus calcification: evidence from marine gastropods. Marine Biology 75, 287-292.

Palmer, A.R., 1992. Calcification in marine molluscs: How costly is it? Proceedings of the National Academy of Sciences USA 89, 1379-1382.

Pekkarinen, M., 1997. Seasonal changes in calcium and glucose concentrations in different

body fluids on *Anodonta anatina* (Bivalvia: Unionidae). Netherlands Journal of Zoology 47, 31-45.

Pokroy, B., Fitch, A.N., Lee, P.L., Quintana, J.P., Caspi, E.N., Zolotoyabko, E., 2006. Anisotropic lattice distortions in the mollusk-made aragonite: A widespread phenomenon. Journal of Structural Biology 153, 145-150. doi:10.1016/j.jsb.2005.10.009

Pokroy, B., Quintana, J.P., Caspi, E.N., Berner, A., Zolotoyabko, E., 2004. Anisotropic lattice distortions in biogenic aragonite. Nature Materials 3, 900-902. doi:10.1038/nmat1263

Powell, E.N., Staff, G.M., Callender, W.R., Ashton-Alcox, K.A., Brett, C.E., Parsons-Hubbard, K. M., Walker, S.E., Raymond, A., 2011. Taphonomic degradation of molluscan remains during thirteen years on the continental shelf and slope of the northwestern Gulf of Mexico. Palaeogeography, Palaeoclimatology, Palaeoecology, 312, 209-232. doi:10.1016/j.palaeo.2010.12.006

Pörtner, H.O., Langenbuch, M., Michaelidis, B., 2005. Synergistic effects of temperature extremes, hypoxia, and increases in CO_2 on marine animals: from earth history to global change. Journal of Geophysical Research 110, doi: 10.1029/2004JC002561

Ragazzola, F., Foster, L.C., Form, A., Anderson, P.S.L., Hansteen, T.H., Fietzke, J., 2012. Ocean acidification weakens the structural integrity of coralline algae. Global Change Biology 18, 2804-2812. doi:10.1111/j.1365-2486.2012.02756.x

Raven, J., Caldeira, K., Elderfield, H., Hoegh-Guldberg, O., Liss, P., Riebesell, U., Shepherd, J., Turley, C., Watson, A., 2005. Ocean acidification due to increasing atmospheric carbon dioxide. Royal Society, London p. 57

Ries, J.B., Cohen, A.L., McCorkle, D.C., 2009. Marine calcifiers exhibit mixed responses to CO_2-induced ocean acidification. Geology 37, 1131-1134. doi:10.1130/G30210A.1

Rodríguez-Navarro, A.B., CabraldeMelo, C., Batista, N., Morimoto, N., Alvarez-Lloret, P., Ortega-Huertas, M., Fuenzalida, V.M., Arias, J.I., Wiff, J.P., Arias, J.L., 2006. Microstructure and crystallographic-texture of giant barnacle (*Austromegabalanus psittacus*) shell. Journal of Structural Biology 156, 355-362. doi:10.1016/j.jsb.2006.04.009

Schatzmann, H.J., 1973. Dependence on calcium concentration and stoichiometry of the calcium pump in human red cells. Journal of Physiology 235, 551-569.

Schöne, B.R., 2008. The curse of physiology—challenges and opportunities in the interpretation of geochemical data from mollusk shells. Geo-Marine Letters 28, 269-285. doi:10.1007/s00367-008-0114-6

Schöne, B.R., Rodland, D.L., Fiebig, J., Oschmann, W., Goodwin, D., Flessa, K.W., Dettman, D., 2006. Reliability of multitaxon, multiproxy reconstructions of environmental conditions from accretionary biogenic skeletons. The Journal of Geology 114, 267-285. doi: 10.1086/501219

Smith, B.L., Schaffer, T.E., Viani, M., Thompson, J.B., Frederick, N. a, Kindt, J., Belcher, A.M., Stucky, G.D., Morse, D.E., Hansma, P.K., 1999. Molecular mechanistic origin of the toughness of natural adhesives, fibres and composites. Nature 399, 761-763. doi:10.1038/21607

Steeneveldt, R., Berger, B., Torp, T.A., 2006. CO_2 Capture and storage: closing the knowing-doing gap. Chemical Engineering Research and Design 84, 739-763. doi:10.1205/cherd05049

Stemmer, K., Nehrke, G., Brey, T., 2013. Elevated CO_2 levels do not affect the shell structure of the bivalve *Arctica islandica* from the Western Baltic. PLoS One 8, doi: 10.1371/journal.pone.0070106

Taylor, J.D., Layman, M., 1972. The mechanical properties of bivalve (Mollusca) shell structure. Paleontology 15, 73-87

Thomsen, J., Gutowska, M.A., Saphörster, J., Heinemann, A., Trübenbach, K., Fietzke, J., Hiebenthal, C., Eisenhauer, A., Körtzinger, A., Wahl, M., Melzner, F., 2010. Calcifying invertebrates succeed in a naturally CO_2-rich coastal habitat but are threatened by high levels of future acidification. Biogeosciences 7, 3879-3891. doi:10.5194/bg-7-3879-2010

Tunnicliffe, V., Davies, K.T.A., Butterfield, D.A., Embley, R.W., Rose, J.M., Chadwick, W.W.Jr., 2009. Survival of mussels in extremely acidic waters on a submarine volcano. Natural Geoscience 2, 344-348. doi:10.1038/ngeo500

Tushtev, K., Murck, M., Grathwohl, G., 2008. On the nature of the stiffness of nacre. Materials Science and Engineering C 28, 1164-1172. doi:10.1016/j.msec.2007.10.039

Waldbusser, G.G., Steenson, R.A., Green, M.A., 2011. Oyster shell dissolution rates in estuarine waters: Effects of pH and shell legacy. Journal of Shellfish Research, 30, 659-669. doi:10.2983/035.030.0308

Weaver, J.C., Wang, Q., Miserez, A., Tantuccio, A., Stromberg, R., Bozhilov, K.N., Maxwell, P., Nay, R., Heier, S.T., DiMasi, E., Kisailus, D., 2010. Analysis of an ultra hard magnetic biomineral in chiton radular teeth. Materials Today 13, 42-52. doi:10.1016/S1369-7021(10)70016-X

Weiner, S. and Addadi, L., 1997. Design strategies in mineralized biological materials. Journal of Materials Chemistry 7, 689-702. doi:10.1039/a604512j

Wilbur, K. and Saleuddin, A.S., 1983. Shell formation. In: Physiology, Part 1. The Mollusca, Vol. 4. Saleuddin, A.S., Wilbur, K. (Eds.), Academic Press, New York, 235-287.

Wood, H.L., Spicer, J.I., Widdicombe, S., 2008. Ocean acidification may increase calcification rates, but at a cost. Proceedings of the Royal Society B 275, 1767-1773. doi:10.1098/rspb.2008.0343

Xu, X., Zhao, L., Yan, X., 2016. Seawater acidification affects the physiological energetics and spawning capacity of the Manila clam *Ruditapes philippinarum* during gonadal maturation. Comparative Biochemistry and Physiology Part A 196, 20-29. doi:10.1016/j.cbpa.2016.02.014

Zhang, J.Y., Liu, G., Zhang, X., Zhang, G.J., Sun, J., Ma, E., 2010. A maximum in ductility and fracture toughness in nanostructured Cu/Cr multilayer films. Scripta Materialia 62, 333-336.

Manuscript III

Effects of cooking on mollusk shell structure and chemistry: Implications for archeology and paleoenvironmental reconstruction

Published in Journal of Archaeological Science: Reports

Stefania Milano, Amy L. Prendergast, Bernd R. Schöne

Institute of Geosciences, University of Mainz, Joh.-J.-Becherweg 21, 55128 Mainz, Germany

Author contribution

Concept: SM, ALP
Execution: SM, ALP
Analysis: SM
Data interpretation: SM, BRS, ALP
Writing: SM, ALP, BRS

Milano, S., Prendergast, A.L., Schöne, B.R., 2016. Effects of cooking on mollusk shell structure and chemistry: Implications for archeology and paleoenvironmental reconstruction. J. Archaeol. Sci. Reports 7, 14-26.

Abstract

Mollusk shells excavated from archeological sites have been used to reconstruct paleoenvironment, human foraging, and migratory patterns. To retrieve information on past environment or human behavior, chemical signatures such as oxygen stable isotopes ($\delta^{18}O_{shell}$) are analyzed. Shell archeological remains usually represent food waste. Thermal treatments such as boiling and roasting may influence shell structure and biochemical composition. However, little is known about the relationship between changes at macro-, microstructural and chemical levels. This work is a calibration study on modern *Phorcus* (*Osilinus*) *turbinatus* shells. A simulation of two different cooking methods (boiling and roasting) was carried out at four temperatures (100 °C, 300 °C, 500 °C and 700 °C) for two durations (20 min and 60 min). The structure and biochemistry of shells boiled at 100 °C did not significantly change. However, treatments at higher temperatures strongly affected both the structure and the biochemistry of the shells. At 300 °C the external coloration, as well as nacre iridescence, were altered. Raman spectroscopy revealed that, at this temperature, the aragonite-calcite polymorphic transformation starts. Scanning Electron Microscope (SEM) analysis showed drastic changes in the microstructural organization also beginning at 300 °C. Furthermore, the isotopic $\delta^{18}O_{shell}$ values were significantly affected. Increasing cooking temperatures resulted in an enhancement of the above-mentioned alterations. These results provide a set of temperature-related morphological, structural and biochemical characteristics for investigating the thermal behavior of biocarbonates and for estimating different cooking treatments in archeological record.

Keywords: microstructure; Raman; paleotemperature reconstruction; heating; *Phorcus* (*Osilinus*) *turbinatus*; Mediterranean; archeology

1. Introduction

The contribution of shellfish to prehistoric Mediterranean subsistence has been demonstrated by the recovery of marine mollusk shells from numerous archeological sites along the coasts of the Mediterranean Sea (Erlandson, 2001; Aura et al., 2009; Colonese et al., 2011; Hunt et al., 2011; Barker et al., 2012; Colonese et al., 2014; Bosch et al., in press). Evidence of visibly burnt shells in archeological middens supports the hypothesis that shellfish diets could include a certain level of cooking (Stringer et al., 2008; Taylor et al., 2011; Douka et al., 2014). In fact, despite the evidence of a terrestrial-centered diet (Garcia Guixe et al., 2006; Craig et al., 2010), these prehistoric populations integrated marine resources as a protein supplement to their diets (Lubell et al., 1994; Richards and Hedges, 1999). In particular, shells of the gastropod *Phorcus* (*Osilinus*) *turbinatus* are commonly found in Mediterranean archeological deposits (Mannino et al. 2007; Mannino et al., 2008; Colonese et al. 2011; Prendergast et al., 2013; Bosch et al., in press; Prendergast et al. in press).

These remains offer a valuable source of information on the ancient environment and human-environment interactions. Shell carbonate is deposited periodically (resulting in the formation of growth increments and lines, e.g., Clark, 1975; Jones, 1980; Schöne et al., 2007) and generally in oxygen isotopic equilibrium with ambient water (Epstein et al. 1951; Wefer and Berger 1991; Lécuyer et al. 2004). This allows the preservation of environmental signatures (Shackleton, 1974; Schöne et al., 2004). The shell $\delta^{18}O_{shell}$ value is commonly used as paleothermometer to reconstruct sea surface temperature at the time of shell deposition (Epstein et al., 1953; Schöne et al., 2003; Ferguson et al., 2011; Surge and Barrett, 2012). Furthermore, the $\delta^{18}O_{shell}$ composition of the last deposited shell material can be used to determine the season of shellfish foraging (Shackleton, 1973; Andrus and Crowe, 2000; Mannino et al., 2003; Burchell et al., 2013a; Prendergast et al. in press). Another method used by Milner (2001) in order to evaluate season of death of *Ostrea edulis* is based on shell growth patterns. By measuring the growth between the last annual line and the ventral margin it is possible to determine the moment of death with an error of ± 1 month (Milner, 2001). Ancient subsistence practices and site occupation can be interfered from the seasonality of shellfish foraging, leading to information about prehistoric feeding habits, settlement patterns and human movements (Mannino and Thomas, 2002; Mannino et al., 2011; Burchell et al., 2013b; Bosch et al., in press; Prendergast et al. in press). Furthermore, the stable carbon isotopic signature of mollusk shells ($\delta^{13}C_{shell}$) contains valuable information on the environment during lifetime of the organism and its physiology. The origin of the carbon of the $CaCO_3$ and the proper interpretation of this signal have been long debated (Klein et al., 1996; Dettman et al., 1999; Gillikin et al., 2007; McConnaughey and Gillikin, 2008). In land organisms, as snails, it is established that δ^{13}Cshell reflects dietary habits (Stott, 2002; Metref et al., 2003; McConnaughey and Gillikin, 2008; Prendergast et al., in press b). However, in aquatic shells, the carbon isotopic record is still not fully understood. In fact, it can be linked to numerous variables such as water salinity, environmental level of CO_2, DIC content and physiological processes (McConnaughey and Gillikin, 2008; Schöne et al., 2011).

Stable isotope signatures preserved in shells may be sensitive to post-mortem alterations. In particular, shells preserved in archeological sites may have been subject to alterations such as cooking. In *P. turbinatus*, the portion of the shell used for isotopic analysis is composed of biogenic aragonite, which is prone to recrystallization into calcite when heated (Lécuyer et al., 1996; Balmain et al., 1999; Dauphin et al., 2006). Processes like cooking by boiling or roasting may alter shell mineralogy and isotopic composition (Andrus and Crowe, 2002). Therefore, the isotopic signature may no longer accurately reflect ambient environmental conditions at the time of shell deposition, leading to erroneous reconstructions. To avoid this, fossil samples from archeological middens to be used in paleoenvironmental studies are usually selected based on the consistency of their external appearance (Larsen, 2015). However, very little is known about the thermal alterations on shell structure due to cooking procedures. Therefore, altered shells may not be easily identifiable at first sight. For instance, boiling, roasting at moderate temperatures and indirect fire exposure may not necessarily alter the shell surface as much as roasting at elevated temperatures where a drastic surface blackening occurs.

This study investigates the effects of different cooking methods and temperatures on shell morphology, mineralogy, microstructure and isotopic composition ($\delta^{18}O_{shell}$ and $\delta^{13}C_{shell}$) in modern specimens of the topshell, *P. turbinatus*, and discusses their implications for archeological research and paleoenvironmental reconstruction. Furthermore, the present study provides a more rigorous toolkit than simply relying on external shell appearance for the selection of shell material for the use on paleoenvironmental reconstruction and seasonal shellfish foraging research.

2. Background

2.1 *P. turbinatus* ecology and distribution

P. turbinatus, previously known as *Osilinus turbinatus, Monodonta turbinata* and *Trochocochlea turbinata*, is a marine gastropod found along the coasts of the Mediterranean Sea (Benedetti-Cecchi et al., 2003; Katsanevakis et al., 2008; Caruso and Chemello, 2009; Donald et al., 2012; Prendergast et al., 2013). This species is commonly found in the intertidal zone of rocky shorelines. It generally inhabits the middle to lower intertidal zone as it has a high sensitivity to subaerial exposure, elevated temperatures and desiccation (Menzies et al., 1992). An important adaptation against extreme environmental fluctuations is the strong foot muscle which allows the colonization of high energy areas where daily temperature and salinity conditions are more stable (Menzies et al., 1992). This species has been reported to spawn twice a year, during spring and autumn (Schifano, 1983). The wide distribution of *P. turbinatus* in modern and archeological settings, its limited subaerial exposure and its high sensitivity to environmental variations such as water temperature make this species a highly suitable candidate for paleoenvironmental and paleoseasonalinity reconstructions (Schifano and Censi, 1983; Mannino et al., 2008).

2.2 *P. turbinatus* shell growth and structure

Adult *P. turbinatus* shell diameter ranges between 15 and 38 mm (Poppe and Goto, 1991). Adults can weigh up to 15 g (Žmak et al., 2015). Shell deposition occurs throughout the year with temporary slowdowns and brief cessations, which are identified by growth lines parallel to the shell lip (Schifano, 1983; Mannino et al. 2008; Colonese et al., 2009). The mean annual growth rate was described by Mannino et al. (2008) to range between 17-19 mm with a decrease related to ontogeny. Furthermore, seasonal variations in shell growth rates have been previously recorded (Mannino et al., 2008). Depending on the different geographical localities, autumn/winter can correspond to the period of fastest shell growth (Mannino et al., 2008) or to a period of growth slowdown (Regis, 1972).

P. turbinatus shell is characterized by a slightly conical shape with a patterned surface. Pigmented blotches (black, olive green, purple) on a cream background are organized in bands perpendicular to the growth direction (Crothers, 2001; Fig. 2). The shell is divided into two layers (inner and outer shell layer) with different microstructural organizations (Mannino et al., 2008). The inner layer consists of nacreous aragonite, which occupies about 90% of the shell volume (Žmak et al., 2015). Generally, nacre formed by gastropods differs from nacre in bivalves in arrangement and growth process (Nakahara, 1991; Checa et al., 2009). The specific arrangement of nacre in gastropods is known as “towered nacre” (Checa et al., 2009). The outer layer formed by aragonite organized in prismatic microstructures (Mannino et al., 2008). According to the author´s observations and to the terminology from Carter et al. (2012), the microstructure can be classified as spherulitic prismatic (Fig. 2A). First-order prisms contain elongated units (second-order prisms), which radiate from a nucleation site and are disposed in a fan-like pattern.

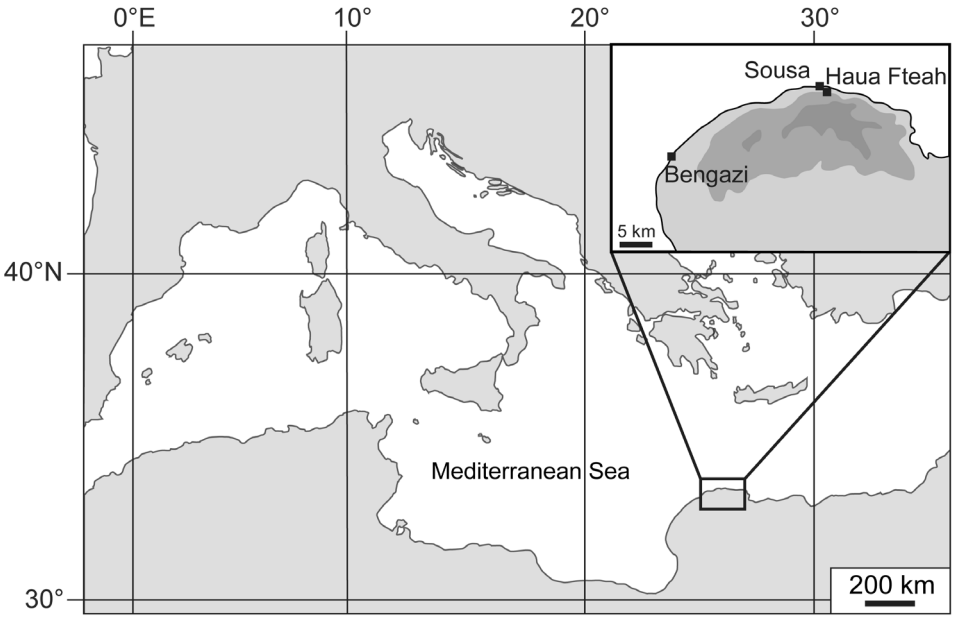

Fig. 1. Map showing the study localities along the Libyan coast. In inset, details of Sousa and the archeological site of Haua Fteah.

3. Materials and methods

3.1 Collection site

In this study, eighteen shells of *P. turbinatus* were analyzed. All specimens were collected alive from the intertidal zone of two close-by localities along the rocky coast of Sousa, Libya (Fig. 1). Immediately after collection they were sacrificed by soft tissue removal. Eight shells were collected in April 2010 from locality M03 (32.797168°N, 22.545482°E, WGS84). Ten shells were collected from locality ML06 (32.907994°N, 22.044392°E, WGS84) on a monthly basis from May to September 2012 (Prendergast et al. in press). The distance between the two sites is approximately 40 km.

3.2 Experimental setup

Sixteen shells were subject to different cooking treatments, two shells were left uncooked and used as control specimens. Each treatment was conducted with two different durations: 20 min and 60 min, with two shells for each different temperature and duration. Four shells were boiled in freshwater at 100 °C (two shells for 20 minutes and two shells for 60 minutes) using a yellow MAG HS 7 hot plate with integrated thermometer to maintain a constant water temperature. Twelve shells were roasted in a Nabertherm High Temperature Tube Furnace at 300 °C, 500 °C and 700 °C, respectively.

3.3 Sample preparation

After treatment, each shell was covered in a layer of JB KWIK epoxy resin for protection during the cutting process. A low-speed precision saw (Buehler Isomet 1000) was used to cut two slabs from each specimen (1.5 and 2 mm thick) across the outer whorl perpendicular to the direction of growth. In preparation for SEM and Raman analyses, the 1.5 mm-thick sections were embedded in Struers EpoFix resin. The 2 mm-thick sections used for stable isotopes analysis were mounted on microscope slides using JB KWIK epoxy resin. All samples were dried overnight and ground using a Buehler Metaserv 2000 grinder-polisher with Buehler silicon carbide papers of different grit sizes (320, 600, 1200, 2500). Subsequently, they were polished with 3 µm diamond suspension on a Buehler VerduTex cloth. An ultrasonic bath was performed between each of the grinding and polishing steps. Embedded slabs were additionally polished for ca 3 hrs with a 1 µm Al_2O_3 suspension in a Buehler VibroMet 2 vibratory polisher. Furthermore, in order to enhance the visibility of the microstructures for the SEM analysis, they were etched in 1 vol% HCl for 5 s and bleached in 6 vol% NaClO for 30 min. Afterwards the embedded samples were sputter coated with a 3 nm-thick gold film and examined under the scanning electron microscope (2nd generation LOT Quantum Design Phenom Pro desktop SEM).

3.4 Raman spectroscopy analysis

After SEM analysis, the embedded slabs were ground and polished again following the same procedure as described above (Section 3.3). Raman measurements were recorded using a Horiba Jobin Yvon LabRam 800 spectrometer equipped with Olympus BX41 optical microscope (University of Mainz). It employed a 532.21 nm laser wavelength, a 400 µm confocal hole, a grating with 1800 grooves/mm, an entrance slit width of 100 µm and 50× long-distance objective lens. The data were acquired with a time window between 3 and 5 seconds. For each sample, two measurements were taken in each shell layer.

3.5 Stable isotopes analysis

In order to assess thermal and diagenetic effects on $\delta^{18}O_{shell}$ and $\delta^{13}C_{shell}$, the inner nacreous layers were micromilled using a Rexim Minimo dental drill mounted to a binocular microscope and equipped with a cylindrical, diamond-coated bit (1 mm diameter; Komet/Gebr. Brasseler GmbH & Co. KG, model no. 835 104 010). The powdered samples (n = 500) were processed with a Thermo Finnigan MAT 253 gas source isotope ratio mass spectrometer in continuous flow mode coupled to a GasBench II at the University of Mainz. Samples were calibrated against an NBS-19 calibrated IVA Carrara marble ($\delta^{18}O$ = - 1.91‰). The average internal precision (1σ) was better than 0.05 ‰.

The $\delta^{18}O$ values of shell aragonite were not adjusted for differences in acid fractionation factors of aragonite and calcite. Using the acid fractionation factors of Kim et al. (2007) for a reaction temperature of 72 °C, actual $\delta^{18}O$ values of aragonite would be 0.38 ‰ more negative than reported here. However, this correction was not applied, because we used paleotemperature equations (Grossman and Ku, 1986; O'Neil, 1969) that assumed no differences in acid fractionation factors for the two $CaCO_3$ polymorphs. Furthermore, this equation did not consider temperature-induced changes of the acid fractionation factors. For example, Grossman and Ku (1986) reacted their carbonate samples at 50 and 60 °C and, accordingly, their $\delta^{18}O$ values of aragonite would require a correction by only - 0.34 ‰ and - 0.36 ‰, respectively (using acid fraction factors from Kim et al, 2007). In order to compute temperatures with the equation of Grossman & Ku (1986), $\delta^{18}O$ values of aragonite processed at 72 °C would therefore require a correction of - 0.02 to - 0.04 ‰. Since this difference is smaller than the precision uncertainty of the mass spectrometer (see below), our data were not adjusted.

The $\delta^{18}O_{shell}$ values were used to calculate sea surface temperature (SST) using the equation of Grossman and Ku (1986) with a scale correction of - 0.27 ‰ (Dettman et al., 1999):

(1) $$SST\ °C = 20.60 - 4.34 \cdot (\delta^{18}O_{shell} - (\delta^{18}O_{water} - 0.27))$$

For samples in which aragonite has been transformed into calcite, SST was also calculated using the equation of O'Neil (1969):

(2) $SST\ (ºC) = 16.9 - 4.38 \cdot (\delta^{18}O_{shell} - \delta^{18}O_{water}) + 0.1 \cdot (\delta^{18}O_{shell} - \delta^{18}O_{water})$

A mean annual $\delta^{18}O_{water}$ value of 1.5‰ was used in the SST calculations. This value was measured on the basis of monthly water collection during the period from February to September 2012 as described in Prendergast et al. (in press). For the missing months, $\delta^{18}O_{water}$was derived from water salinity data according to the following equation by Pierre, 1999:

(3) $\delta^{18}O_{water} = (0.25 \cdot S) - 8.2$

where S = salinity.

3.6 Environmental data and statistical analysis

Monthly salinity data for Sousa were obtained from the dataset EN4 SSS (1° spatial resolution, KNMI Climate Explorer at http://climexp.knmi.nl; last checked: 30 November 2015). Monthly SSTs were retrieved from the Advanced Very High Resolution Radiometer (AVHRR) aboard NOAA polar-orbiting satellites. This instrument estimates water temperatures with a spatial resolution of 4 km by measuring infrared and microwave thermal emission from the ocean surface (Minnett et al., 2002). Both temperature and salinity data refer to the last entire years before collection (2009 and 2011) and partially to 2012 (Tab. 1). In order to evaluate the influence of different cooking temperatures on the isotopic composition of the shells, ANOVA and Kruskal-Wallis test were performed by using the statistical software PAST (version 3.05; http://folk.uio.no/ohammer/past/; last checked: 30 November 2015). The significance level was set to $\alpha = 0.05$.

4. Results

4.1 Thermal effect on shell macro- and microstructures

Shell appearance is drastically altered by increasing cooking temperatures (Fig. 2). Boiled shells maintain their original external and internal appearance with defined pigmented blotches in the outer layer and a gray/iridescent nacre (Fig. 2B - D). At 300 °C (Fig. 2E + F), the patterns of the outer shell surface are no longer clearly distinguishable and the entire surface takes on a light brown shade. The nacre loses its typical iridescence appearing patchy (white and brown). Interestingly, growth lines are more easily discerned. At 500 °C (Fig. 2G + H), shells exhibit a darker gray external coloration. The outer layer becomes brittle and tends to detach from the rest of the shell. The nacre acquires a homogenous gray coloration, although with growth lines still clearly visible. At 700 °C (Fig. 2I + J), shells present a homogenous cream coloration. The outer shell layer is almost totally lost. After 20 min, the nacre looks dark gray and porous. After 60 min, it exhibits a cream coloration with the exception of a gray portion still visible in the mid- inner portion of the nacre itself. This area is particularly brittle and inconsistent. The samples roasted at 700 °C are extremely crumbly with remainders not in section almost entirely turned to powder. It is unlikely that such samples would survive in the archeological record.

Microstructural alterations of both shell layers are detectable in some of the cooking treatments. For boiled shells (100 °C), no visible changes are present in the outer shell layer when compared to the unheated shell (Fig. 3A - C). On the other hand, nacre platelet organization appears slightly altered in the sample boiled for 60 min (Fig. 3C), where the inter-platelet space is less regular than in the control. Shells roasted at 300 °C clearly show changes in both inner and outer layer microstructures (Fig. 3D + E). When roasted for 20 min (Fig. 3D), the shell presents thin sheets between first-order prisms, whereas second-order prisms do not seem altered. In addition, the nacre platelets lose their geometric definition, with irregular edges and nanometric pores appearing of the surfaces. The duration of the treatment can play an important role as shown in Fig. 3E, where the samples heated at 300 °C for 60 min present more drastic alterations than those heated only for 20 mins. Prisms in the outer layer predominantly join/agglomerate in significantly larger spherical-shaped units characterized by a porous appearance. However, small portions of the prismatic microstructures are still visible. Furthermore, a sheet of organics partially covers portions of the nacreous inner layer. At 500 °C, prisms are completely replaced by a new type of microstructure (Fig. 3F + G). Meanwhile, nacre platelets lose their individual brick-like forms and start to fuse together. In particular, in the sample roasted for 60 min, new boundaries appear defining irregular-shaped assemblages made of several single platelets (Fig. 3G). Roasting at 700 °C causes considerable detachment of the outer shell layer. The microstructures in the remaining portions of the outer layer seem to undergo another drastic transformation. They appear irregular-shaped and branched after 20 min (Fig. 3H) and poorly-defined after 60 min (Fig. 3I). A great change occurs in the nacre, where the platelets are completely replaced by much larger irregular and blocky microstructures. Their size increases dramatically with the duration of the cooking.

Tab. 1. Monthly environmental data from 2009 to 2012 at Sousa. Salinity, obtained by KNMI Climate Explorer, was used to calculate most of $\delta^{18}O_{water}$ data. Values in bold indicates $\delta^{18}O_{water}$ directly measured from water samples (Prendergast et al., in press).

Month	Salinity (psu)			$\delta^{18}O_{water}$ (‰)			Instrumental SST (°C)		
	2009	2011	2012	2009	2011	2012	2009	2011	2012
January	38.8	38.8	38.5	1.5	1.5	1.4	17.2	17.7	17.0
February	38.8	38.8	38.4	1.5	1.5	**1.4**	16. 4	16.6	16.4
March	38.7	38.7	38.4	1.5	1.5	**1.3**	15.9	16.6	16.1
April	38.7	38.7	38.4	1.5	1.5	**1.2**	16.9	17.4	17.2
May	38.7	38.7	38.5	1.5	1.5	**1.5**	19.6	19.3	20.0
June	38.7	38.7	38.5	1.5	1.5	**1.2**	23.5	22.7	23.5
July	39.0	38.8	38.7	1.6	1.5	**1.2**	25.4	25.7	26.6
August	39.3	38.5	39.0	1.6	1.4	**1.0**	26.6	26.8	27.4
September	39.3	38.6	39.0	1.6	1.5	**1.5**	25.7	26.6	26.2
October	39.2	38.6	39.0	1.6	1.5	1.6	24.3	23.8	25.3
November	38.9	38.6	39.1	1.5	1.4	1.6	21.4	21.1	23.0
December	38.8	38.6	39.0	1.5	1.4	1.5	19.1	18.8	19.4
Average	38.9	38.7	38.7	1.5	1.5	1.4	21.0	21.1	21.5

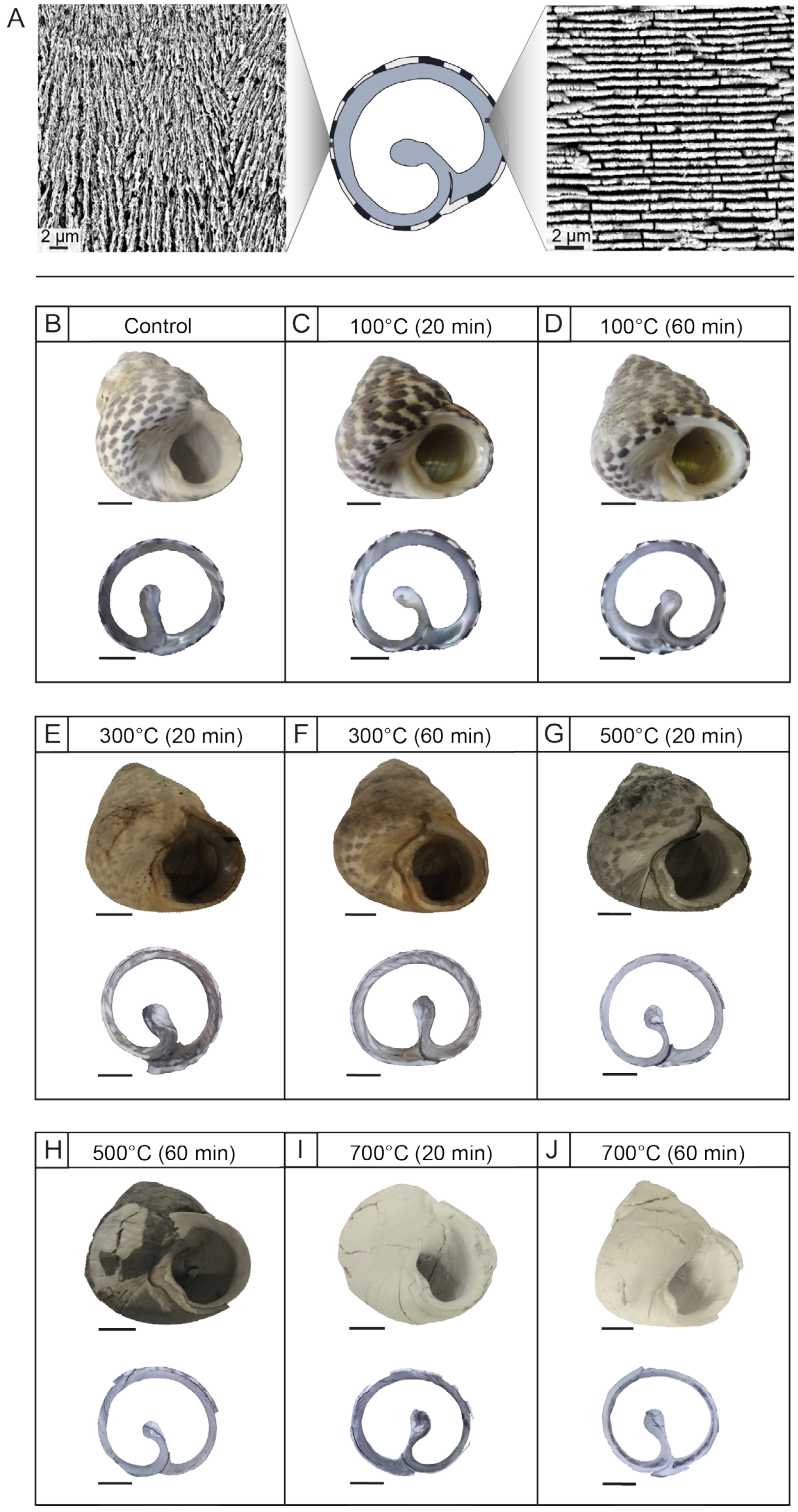

Fig. 2. *Phorcus turbinatus* shell structure and changes induced by cooking. (A) Sketch of a cross-section showing the two shell layers and SEM images of their microstructural organization. Left SEM image = inner shell layer (nacre, aragonite platelets); right SEM image = outer shell layer (aragonite spherulitic prisms). (B) External and cross-section appearance of an untreated shell (control). (C-J) Cooking effects on the external and cross-section appearance of *Phorcus turbinatus* shells. Scale bars if not otherwise indicated = 5 mm.

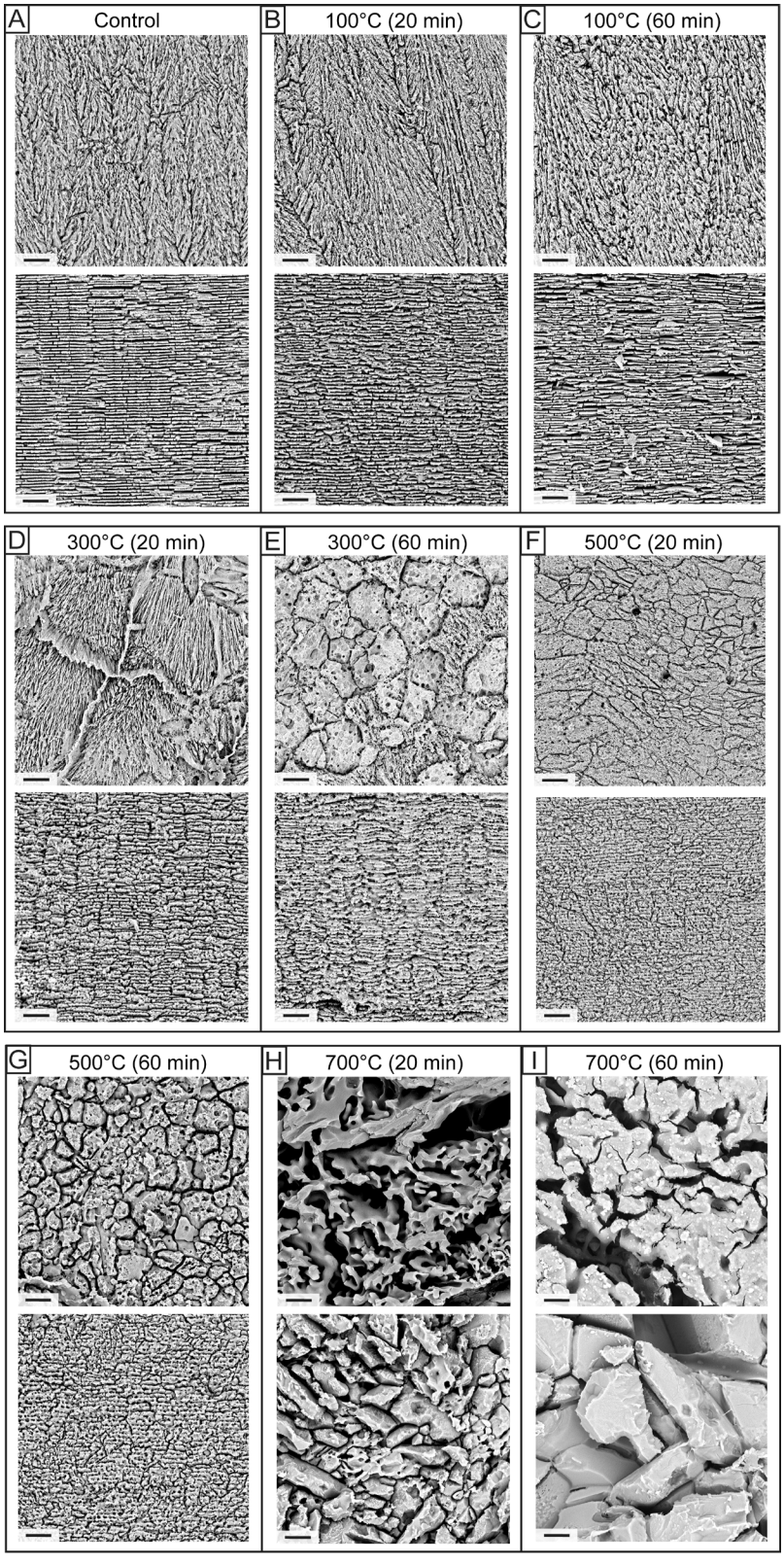

Fig. 3. SEM images of microstructure organization of uncooked (A) and cooked shells (B-I). In each figure, the upper SEM image refers to the OSL (outer shell layer) and the lower one refers to the nacre of the inner shell layer. Scale bars = 5 μm.

4.2 Mineralogy thermal behavior

Carbonate polymorphic transformations occur in association with increasing cooking temperatures. The aragonite spectra of both layers of untreated shells (Fig. 4A) are maintained after boiling for 20 and 60 min (Fig. 4B). In fact, Raman spectra show clearly visible aragonite diagnostic bands at 152 cm^{-1}, 180 cm^{-1}, 207 cm^{-1}, 707 cm^{-1} and 1086 cm^{-1}. Different behaviors are found in the two shell layers of roasted samples at 300 °C. The aragonite persists in the nacre but the outer layer shows an extra band at 281 cm^{-1} related to an aragonite-calcite transition phase (Fig. 4B). Both layers of shells roasted at 500 °C show spectra typical of biogenic calcite with two predominant bands at 153 cm^{-1}, 281 cm^{-1}, 713 cm^{-1} and 1087 cm^{-1} (Fig. 4C). Roasting at 700 °C causes alterations to the calcite spectra of the outer shell layer with the addition of one band at 641 cm^{-1}. However, the nacre phase remains calcitic (Fig. 4C). In general, no differences are detected between different time exposures within the same treatment.

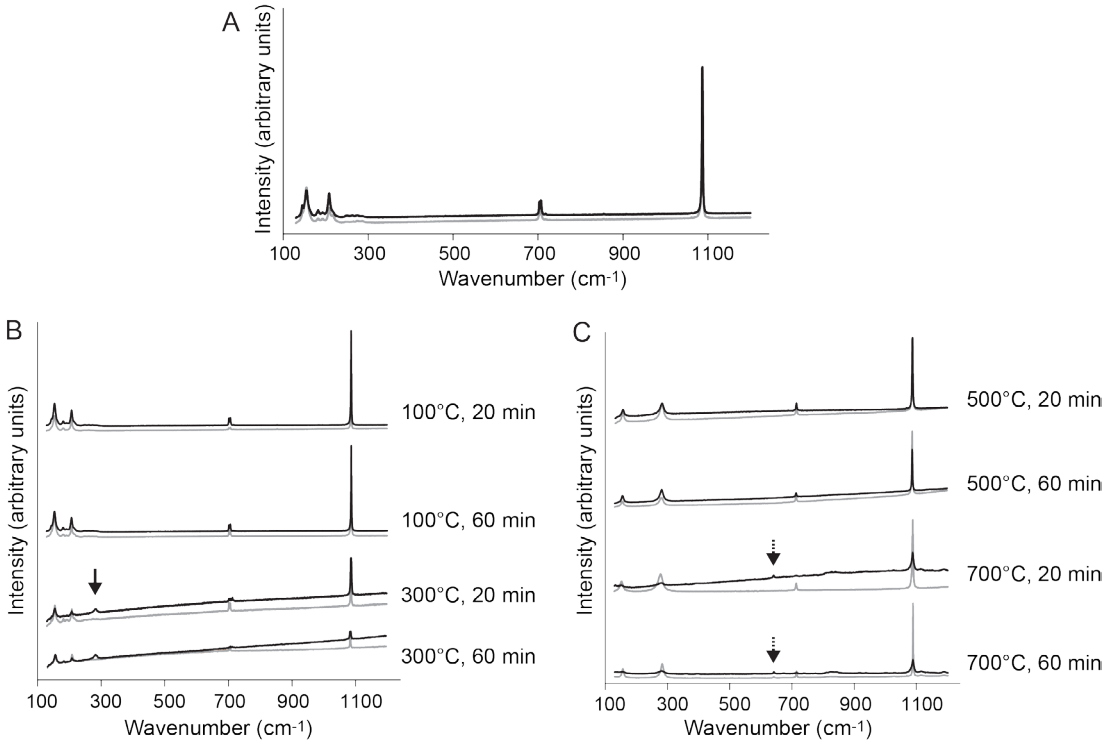

Fig. 4. Raman spectra of *Phorcus turbinatus* shells. (A) Spectrum of untreated shell, fully aragonitic. (B + C) Raman spectra of cooked shells at different exposure times and temperatures. Black arrow in (B) indicates the band at 281 cm^{-1} showing the transition phase aragonite to calcite. Dashed arrow in (C) indicates the extra band at 641 cm^{-1}. Black line refers to the outer shell layer; gray line refers to the inner shell layer.

4.3 Effects of cooking on shell isotopic composition

$\delta^{18}O_{shell}$ values of the uncooked samples range between -0.2 and +2.8 ‰ with an average of +1.0 ‰ (Tab. 2). Similar ranges are recorded by Prendergast et al., 2013 in Malta (min: -0.3 ‰, max: +2.1 ‰, arithmetic average: +1.0 ‰) and by Prendergast et al., 2015, in press at the same site as the present study (min: -0.3 ‰, max: +2.2 ‰, average: +1.0 ‰). In Italy, $\delta^{18}O_{shell}$ values between -0.1 and 2.8 ‰ were recorded by Mannino et al., 2008 and Colonese et al., 2009. The corresponding SSTs calculated using equation (1) range between 13.6 and 27.0 °C with an average of 21.4 °C. In line with previous studies on this species, reconstructed SSTs closely mirror the temperatures recorded by the satellites (Mannino et al., 2008; Prendergast et al., 2013; Prendergast et al., 2015 in press). The average difference between measured and calculated maximum temperature is 0.8 °C. A slightly larger underestimation (2.0 °C) occurs at the minimum SSTs, whereas the overall annual mean temperature reconstruction differs by only 0.4 °C from the satellite measurements. Similarly, previous works displayed this error to range from 0.5 to 3.0 °C (Mannino et al., 2008; Colonese et al., 2009; Prendergast et al., 2013; Prendergast et al., 2015, in press).

Tab. 2. Minimum, maximum and average $\delta^{18}O_{shell}$ measured for each treatment and corresponding SST calculated using equation 1. Values in bold indicate SST reconstructed by applying equation 2.

Treatment	$\delta^{18}O_{shell}$ (‰)	$\delta^{18}O_{shell}$ (‰)	$\delta^{18}O_{shell}$ (‰)	SST (°C)	SST (°C)	SST (°C)
	Minimum	Maximum	Average	Minimum	Maximum	Average
Control_1	-0.2	2.8	0.9	13.6	27.0	21.9
Control_2	0.3	2.5	1.2	14.9	24.7	20.9
20 min @ 100 °C	-0.2	2.6	0.8	14.8	26.9	22.6
20 min @ 100 °C	-0.3	3.1	1.1	12.5	27.1	21.0
60 min @ 100 °C	-0.4	2.5	0.9	14.9	27.5	21.8
60 min @ 100 °C	-0.1	2.0	0.7	17.3	26.2	22.7
20 min @ 300 °C	-0.9	1.7	0.7	18.6	29.7	22.7
60 min @ 300 °C	-0.7	2.1	0.3	16.8	29.1	24.8
20 min @ 500 °C	-0.9	1.8	0.4	17.9	29.9	24.2
20 min @ 500 °C	**-0.9**	**1.8**	**0.4**	**15.4**	**28.1**	**21.9**
60 min @ 500 °C	-1.8	1.7	-0.5	18.4	33.8	28.3
60 min @ 500 °C	**-1.8**	1.7	**-0.5**	**15.9**	**32.5**	**26.4**
20 min @ 700 °C	-1.2	1.4	-0.1	19.7	31.1	26.5
20 min @ 700 °C	**-1.2**	**1.4**	**-0.1**	**17.2**	**29.4**	**24.4**
60 min @ 700 °C	-3.3	1.4	-0.3	20.1	40.5	27.4
60 min @ 700 °C	**-3.3**	**1.4**	**-0.3**	**17.5**	**40.5**	**25.4**

The different cooking methods and temperatures induce important changes in the isotopic composition of the shells. Regarding the $\delta^{13}C_{shell}$ values, significant differences already occur between the two uncooked shells and between those and the rest of the cooked samples regardless of the cooking temperature used (Tab. 3). On the other hand, after boiling, $\delta^{18}O_{shell}$ values remain statistically similar to the untreated shells. $\delta^{18}O$ of shells cooked at temperatures of 300 °C and above result in significantly lowered $\delta^{18}O_{shell}$ by as much as 3.7 ‰ compared to the control shells (Tab. 2). As a result, reconstructed SSTs drastically change (Tab. 2). Applying equation 1 to all shells, the minimum temperature reaches 20.1 °C, the maximum reaches 40.5 °C and the average 28.3 °C. When using equation 2 for shells in which the aragonite of the nacreous layer has been transformed in calcite (500 and 700 °C), temperatures range between 12.5 and 40.5 °C, with an average of 23.1 °C. As shown in Figure 5, the offset between SSTs calculated from untreated and treated shells increases with increasing cooking temperature. At 100 °C, minimum, maximum and average SSTs differ from the control-calculated SSTs by 0.6, 1.1 and 0.6 °C, respectively (Fig. 5A). However, the difference is not statistically significant. From 300 °C to 700 °C, there is a significant overestimation that ranges between 2.6 and 5.8 °C for minimum SST, between 3.8 and 14.6 °C for maximum temperature and between 1.3 and 6.9 °C for average SST. This error is slightly lowered when the equation 2 is applied (Fig. 5B). In this case, it ranges between 1.1 and 4.3 °C for minimum SST, between 2.2 and 14.6 °C for maximum temperature and between 0.5 and 5.0 °C for average SST.

Tab. 3. p-values derived from Kruskal-Wallis test on $\delta^{18}O_{shell}$ and $\delta^{13}C_{shell}$. Each sample is compared against the two control shells (Control_1 and Control_2). Values in bold are significant ($p < 0.05$).

Treatment	$\delta^{18}O_{shell}$ (p value)		$\delta^{13}C_{shell}$ (p value)	
	Control_1	Control_2	Control_1	Control_2
20 min @ 100 °C	0.11	0.86	**0.02**	**0.00**
20 min @ 100 °C	0.86	0.22	**0.00**	**0.00**
60 min @ 100 °C	0.15	0.89	0.08	**0.00**
60 min @ 100 °C	0.08	0.73	**0.00**	**0.00**
20 min @ 300 °C	**0.02**	0.32	**0.00**	**0.03**
60 min @ 300 °C	**0.00**	**0.00**	**0.00**	**0.00**
20 min @ 500 °C	**0.00**	**0.03**	**0.00**	**0.00**
60 min @ 500 °C	**0.00**	**0.00**	**0.00**	**0.03**
20 min @ 700 °C	**0.00**	**0.00**	**0.00**	**0.00**
60 min @ 700 °C	**0.00**	**0.00**	**0.00**	**0.00**

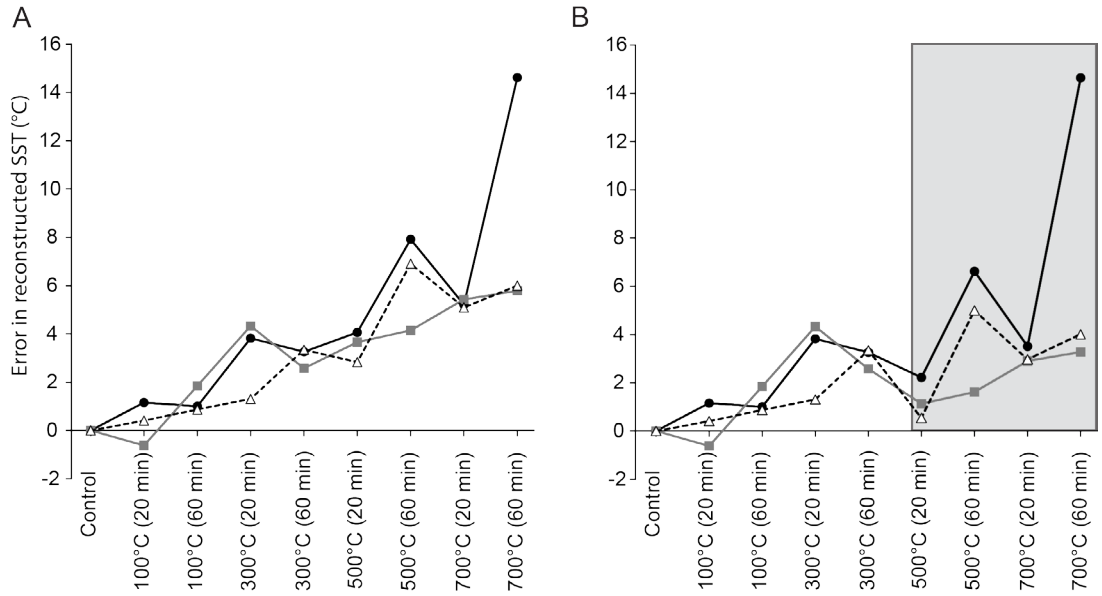

Fig. 5. Shell oxygen isotope-based temperature reconstructions of cooked samples. (A) Error in reconstructed sea surface temperature (SST) due to cooking calculated as difference between SST derived from cooked shells and control shells. SST was calculated by using equation 1 for all samples. (B) In the gray highlighted area, SST was calculated by using equation 2 given the calcitic mineralogy of the samples. Gray squares = minimum SST; open triangles = average SST; black circles = maximum SST.

5. Discussion

5.1 Impact of cooking on shell mineralogy and structure

Calcium carbonate exists in different polymorphic forms. Under ambient conditions, the orthorhombic aragonite is a metastable phase which transforms into the rhombohedral calcite when heated (Dasgupta, 1963; Boettcher and Wyllie, 1967; McTigue and Wenk, 1985). This heat-induced phase conversion is well-known in both geological and biogenic carbonate systems (Parker et al., 2010). The organic matter contained in biological-controlled aragonite is responsible for a reduction of the transition temperature from 450-500 °C down to 300-400 °C (Bourrat et al., 2007; Ren et al., 2009). The complete reversion of aragonitic mollusk shell material to calcite has been previously recorded around 500 °C (e.g., Lécuyer et al., 1996; Balmain et al., 1999; Maritan et al., 2007; Huang and Li, 2009). Likely, the results of the present study indicate that this transformation starts at 300 °C and it is finalized at 500 °C. The presence of the extra band in the Raman signature at 700 °C may be related to a further transformation from calcite to calcium oxide as previously observed by Balmain et al. (1999) and Huang and Li (2009). However, our results do not provide certainty in support to this assumption.

The thermally altered shells display dramatic changes in surface color, texture and microstructural organization starting at 300 °C. The external surface first darkens shifting to light brown and dark gray (300-500 °C) indicating a progressive combustion of organic matter and shell charring. At 700 °C, the shell becomes calcined, developing a characteristic cream coloration and an extremely brittle consistency. Similar observations have been previously made on bones (Brain, 1993; Stiner et al., 1995). Surface color change follows a gradient, which has previously been suggested to be a good indicator of cooking temperature (Bonucci and Graziani, 1975; Munro et al., 2007). Such alterations are also recorded in the nacre. The typical iridescent aspect is lost when temperature reaches 300 °C, changing to a patchy brown-white pattern and later to a gray color (500 °C). At 700 °C, the nacre presents a dark gray coloration and a very porous consistency. The uniformity of stacked platelets in the nacre is responsible for interference effects, which, in turn, contributes to its iridescence (Liu et al., 1999; Snow et al., 2004; Tan et al., 2004). When heated at a certain temperature, this regularity is altered resulting in loss of iridescent colors.

At the microstructural scale, a temperature of 100 °C for 60 min only slightly affects the shells causing a detachment of several single nacre platelets. Lattice relaxation of aragonitic shells in response to heat-induced organic degradation starts below 100 °C (Pokroy et al., 2006a). In particular, the release of CO_2 as a form of organic discharge starts at 70 °C reaching a maximum around 250 °C (Pokroy et al., 2006a). Generally, the organic matrix is a minor shell constituent accounting only for 1-5 % of the total weight (Kawaguchi and Watabe, 1993). In gastropods, the nacre contains circa 3.8 wt % organics (Zaremba et al., 1998). Although small in quantity, the role of organics in shell formation and organization is essential (Weiner and Addadi, 1997). The matrix is responsible for the template which determines microstructure size, shape and orientation (Nudelman et al., 2006). The organic phase is mainly present as intercrystalline envelope around single crystals (Harper, 2000) enhancing their functional properties (Merkel et al., 2007; Tushtev et al., 2008). The organic loss induced by heat causes the relaxation of the crystalline lattice and a subsequent thermal expansion (Pokroy et al., 2006b; Wardecki et al., 2008; Parker et al., 2010).

In accordance to these works, our results clearly show a progressive microstructure expansion with increasing cooking temperatures. As temperatures rise, single platelets and prismatic units fuse together to form much larger structures. The degree of alteration of the microstructures seems to be dependent not only on the cooking temperature but also on the type of microstructure within the same mineralogy. The SEM images show a different response of the different shell layers and associated microstructures. For instance, prismatic structures of the outer shell layer of *P. turbinatus* show drastic morphological changes at 300 °C whereas nacre integrity is better-conserved until 500 °C. Similarly, aragonite shells of the marine mollusk *Busycon carica* (conch shell) retained their crossed-lamellar microstructures until 500 °C (Li et al., 2015). The inconstancy of microstructural thermal behavior may potentially be related to the different organic matrix composition of the different structures (Samata, 1990; Kobayashi and Samata, 2006).

5.2 Impact of cooking on shell isotopic composition

When shells are heated, their isotopic composition can be altered (Epstein et al., 1953; Wierzbowsky, 2007). *P. turbinatus* $\delta^{18}O$ and $\delta^{13}C$ respond to cooking differently. Although they both decrease with the increasing cooking temperatures, $\delta^{13}C$ shows an extremely high natural variation between specimens within the same treatment or control conditions. Carbon content in the shells derives from different sources including the dissolved inorganic carbon in the water and the carbon assimilated through the diet and metabolism (McConnaughey and Gillikin, 2008). The metabolic portion could influence the thermal behavior of $\delta^{13}C$ in the shell when cooked on an inter-individual scale (Larsen, 2015). For these reasons, further discussion will focus only on the stable oxygen isotopes.

Along with the recrystallization process, shell oxygen isotopes are exchanged with the surrounding environment causing a significant ^{18}O alteration relative to the original composition (Andrus and Crowe, 2002; Larsen, 2015). In this case, low cooking temperatures (100 °C), at which no recrystallization occurs, do not significantly alter the $\delta^{18}O$ values. However, alteration of the mineral phase is not always related to changes in the oxygen isotope composition. In fact, nacre at 300 °C is still fully aragonitic but the isotopic composition significantly differs from the control shells. Other studies indicate that original isotopic values are preserved up to 400 °C in some mollusk shells (Larsen, 2015) and up to 250 °C in mammal bones (bioapatite; Munro et al., 2008). A higher resistance is found in otoliths, where isotopic properties are maintained up to 800 °C (Andrus and Crowe, 2002).

Heating has been used in the past as a form of pre-treatment in order to remove the organic matter believed to interfere with stable isotope analysis (Epstein et al., 1953; Mook, 1971). Gastropods, bivalves and corals were usually treated at 470 °C for 15 to 60 min (Wierzbowski, 2007). The alteration of $\delta^{18}O$ values due to heating is largely variable in the different genus and species considered. Table 4 shows the variation of $\delta^{18}O$ values found by previous researches in different organisms as gastropods, bivalves and corals. Our results, also included in Table 4, indicate that the difference of average $\delta^{18}O$ value between uncooked and roasted shells ranges between 0.5 to 1.3 ‰. This variation is statistically significant and leads to an overestimation by 2.3 ± 1.4 °C of the mean SST.

Tab. 4. Variations in $\delta^{18}O_{shell}$ of samples subjected to heat treatment relative to untreated samples.

Class	Species	Heating temperature (°C)	$\Delta\delta^{18}O_{shell}$ (‰)	Reference
Gastropoda	*Phorcus turbinatus*	300	0.5	Present study
	Phorcus turbinatus	500	1.1	Present study
	Phorcus turbinatus	700	1.3	Present study
	Haliotis rufescens	470	0.5	Epstein et al., 1953
	Helix sp.	400	0.4	Leone et al., 2000
	Limacina bulimoides	470	0.6	Grossman et al., 1986
	Strombus gigas	470	0.1	Epstein et al., 1953
Bivalvia	*Cerastoderma edule*	200	0.2	Wierzbowski, 2007
	Cerastoderma edule	340	0.2	Wierzbowski, 2007
	Cerastoderma edule	450	0.07	Wierzbowski, 2007
	Mytilus edulis	470	0.6	Mook, 1971
Anthozoa	scleractinian corals (species not given)	470	0.9	Land et al., 1975
	Porites lutea	340	0.6	Boiseau and Juillet-Leclerc, 1997

5.3 Prehistoric mollusk exploitation and firing events

This study aimed to mimic cooking techniques potentially used by prehistoric people. The important archeological site of Haua Fteah lies just few kilometers away from our modern collection locality in Sousa. The occupation sequence of this cave goes from at least Marine Isotope Stage (MIS) 5 (dated globally 130-74 ka) to the present day (McBurney, 1967; Farr et al., 2014) and it is one of the longest occupation sequences in North Africa (McBurney, 1967; Douka et al. 2014). Many mollusk shell remains (both marine and terrestrial) have been excavated from the Haua Fteah sequence (Barker et al., 2010; Hunt et al. 2011; Barker et al., 2012; Hill et al. 2015; Prendergast et al., 2015 in press). *P. turbinatus* and *Patella sp*. dominate the marine mollusk remains throughout the sequence (McBurney, 1967; Hunt et al., 2011; Barker et al., 2012). Evidence of mollusk exploitation has also been found in various other archeological sites in Western (Spain and Gibraltar; Stringer et al., 2008; Zilhão et al., 2010), Central (Italy and Lybia; Stiner, 1994; Mannino et al. 2007; Mannino et al., 2008; Colonese et al., 2009; Prendergast et al., 2013; Prendergast et al. in press) and Eastern Mediterranean (Turkey; Reese, 1991; Stiner et al., 2013; Bosch et al., in press). Since flesh extraction of *P. turbinatus* is challenging when raw, we hypothesize that shell remains represent food waste that

may have been subjected to some kind of cooking processing. In fact, cooking causes the shells to release their muscle attachment and shrink slightly thus making flesh extraction easier. Furthermore, the choice of cooking instead of eating mollusks raw could be related to a taste preference. In support of our assumption, several burnt shells have been found in different contexts of the Haua Fteah cave (Barker et al., 2010; Hunt et al., 2011; Douka et al., 2014; Hill et al. 2015) and in various Mediterranean sites in Gibraltar (Stringer et al., 2008), Israel (Stiner and Bar-Yosef, 2005), Morocco (Taylor et al., 2011) and Turkey (Stiner et al., 2013). In some cases, tools potentially used as picks for extracting the mollusks were found in association with the remains (Barker et al., 2012). Additional artifacts may have been used for food preparation, especially in the Neolithic period when the first pottery remains appear. In addition, evidence of tip removal from *P. turbinatus* shells were found in late glacial and Holocene parts of the sequence at Haua Fteah cave (Hill et al. 2015) and in Ksar Akil (Bosch et al., in press). This technique may have facilitated flesh extraction without cooking (Hill et al. 2015; Bosch et al., in press).

In this study, cooking temperatures have been selected in a range between 100 and 700 °C to simulate different food proximities to the flame and different cooking techniques such as boiling and roasting. Flame temperature of domestic woody fires generally ranges between 317 and 950 °C, with a median around 800 °C (Hanson and Cain, 2007; Wolf et al., 2013). Whereas, grass material burns at temperatures between 186 and 427 °C (Wolf et al., 2013).

At present, little is known about prehistoric seafood-processing techniques. However, traces of hearth structures related to burning features have been excavated throughout the Mediterranean region (Goldberg and Bar-Yosef, 1998). Fire was likely used, at least sometimes, for cooking and facilitating flesh extraction from the shells (Stringer et al., 2008). Generally, Middle and Upper Paleolithic burning events throughout the Mediterranean are characterized by unprepared surfaces located in natural or shallow dug hollows in the ground (Inglis, 2012). During this time frame, several evidences of hearths were found in Isreal (Goldberg and Bar-Yosef, 1998; Goldberg, 2003; Speth, 2006; Berna and Goldberg, 2008), Turkey (Goldberg and Bar-Yosef, 1998; Goldberg, 2003), Greece (Karkanas et al., 2004), Jordan (Henry et al., 2004), Spain (Vaquero et al., 2001; Vallverdú et al., 2010) and Gibraltar (Barton, 2000). At Haua Fteah, hearth structures were found in layers corresponding to the Neolithic (Barker et al., 2012) and the Middle Stone Age (MSA) (Inglis, 2012; Farr et al., 2014). The combustion fuel was most commonly a mixture primarily made of wood and secondarily made of grass (Inglis, 2012). These observations are in agreement with Albert et al. (2000); Lehndorff et al. (2015) on the predominance of wood fires during the Paleolithic in respect to grass fires during the Neolithic in Israel and Morocco.

5.4 Implications for paleoenvironmental and archeological studies

A cooking temperature of 100 °C does not cause any variation in the shell appearance. For this reason, archeological remains of shells cooked at low temperatures will be particularly challenging to discern from uncooked samples. Likewise, mineralogical and microstructural properties remain largely unaltered. However, from a paleoclimate reconstruction point of view, even when not recognized as cooked material, these shells will not lead to any erroneous temperature reconstruction as boiling does not result in any significant alteration of the oxygen isotope ratios. On the other hand, archeological preservation of whole mollusk shells cooked at very high temperatures (≥ 700 °C) is unlikely due to their extremely fragile and crumbly condition. However, ash and shell fragments may still be visible within the archeological sequence. Cooking techniques which involve temperatures between 300 and 500 °C will likely preserve the shell remains but, at the same time, they will drastically alter the mineralogy and isotopic composition of the shells. As a consequence, any paleotemperature reconstructions based on these altered shells will lead to an overestimation of the average SST between 1.3 and 6.9 °C (equation 1) or between 1.3 and 5.0 °C (equations 1 and 2), according to the equation used. It is therefore recommended that any shells with substantially altered appearance due to burning should be avoided for paleoenvironmental reconstructions. Based on the changes seen at both the macro and the micro scale, it should be easy to discard these samples for analysis so as to avoid erroneous paleoenvironmental reconstructions. Given the results of this study, the routine application of optical microscopy to shell sections in combination with examination of whole shell surface texture provides enough criteria to detect whether cooking temperatures have been too high for robust paleotemperature analyses. At present, one of the most common methods used by archaeologists and palaeoclimatologists to detect mineralogical diagenesis alteration is XRD (X-ray diffraction). However, shell structural information is lost due to the preparation requirement of powdered samples. SEM analysis, instead, provides additional information and therefore deeper insight in the subject increasing the accuracy of sample selection.

The transformations in shell external and internal appearance presented here can help with interpreting archeological findings. A comparison of archeological mollusk shell material with our results can help to identify between different cooking treatments and fire burning intensities. In this case, Raman and SEM analyses are advantageous techniques to use in order to carefully differentiate between different cooking processes and to investigate prehistoric human behavior and diet. Given the significant presence of *P. turbinatus* in various archeological sites along the Mediterranean coasts, our observations can be applied across a broad geographic and temporal scale. The multi-scale approach used in this study provides an effective toolkit for assessing alterations in shell mineralogy and structure. This has implications for sample selection for paleoenvironmental reconstructions from mollusk shells. It can also provide deeper insights into the cooking methods used by prehistoric groups, enabling a more detailed reconstruction of subsistence behaviors.

6. Conclusions

This study identifies shell thermal behavior on various scales. The results presented in this study have implications for the selection of archeological mollusk shells for paleoenvironmental reconstruction and for the interpretation of subsistence behaviours in relation to cooking methods from archeological sites. Cooking processes, at temperatures higher than 300 °C, significantly alter the structural, mineralogical and isotopic integrity of shells of the marine gastropod *P. turbinatus*. Shell surface coloration progressively and predictably shifts as temperatures are increased. Likewise, with higher temperatures, microstructures are reorganized in larger, blocky units. At temperatures above 300 °C, the stable carbon and oxygen isotopic composition is significantly altered and at temperatures between 300 °C and 500 °C aragonite is transformed into calcite. In turn, SST reconstruction from $\delta^{18}O_{shell}$ results in a critical overestimation compared to the untreated shells. Cooking shells by boiling at 100 °C does not result in any discernable changes in the appearance of whole shells and results in only very minor changes to shell microstructure but these changes do not affect the stable isotope ratios of the shells. Therefore, even if shells were boiled, they can still be reliably used for paleoenvironmental reconstruction.

7. Acknowledgements

The authors thank Dr. Tobias Häger for helping with Raman measurements. We gratefully acknowledge the help of Michael Maus during isotope analysis. We thank Dr Robin Inglis for discussions on Palaeolithic firing events in the Mediterranean. Funding for this study was kindly provided by the EU within the framework (FP7) of the Marie Curie International Training Network ARAMACC (604802) and by the Alexander von Humboldt post-doctoral fellowship to AP.

8. References

Albert, R.M., Weiner, S., Bar-Yosef, O., Meignen, L., 2000. Phytoliths in the Middle Palaeolithic deposits of Kebara Cave, Mt Carmel, Israel: Study of the plant materials used for fuel and other purposes. J. Archaeol. Sci. 27, 931-947. doi:10.1006/jasc.2000.0507

Andrus, C.F.T., Crowe, D.E., 2000. Geochemical analysis of *Crassostrea virginica* as a method to determine season of capture. J. Archaeol. Sci. 27, 33-42. doi: 10.1006/jasc.1999.0417

Andrus, C.F.T., Crowe, D.E., 2002. Alteration of otolith aragonite: Effects of prehistoric cooking methods on otolith chemistry. J. Archaeol. Sci. 29, 291-299. doi:10.1006/jasc.2001.0694

Aura, J., Jordá, J.F., Morales, J.V., Pérez, M., Villalba, M.P., Alcover, J.A., 2009. Economic transitions in finis terra: the western Mediterranean of Iberia, 15-7 ka BP. Before Farming 2. doi: 10.3828/bfarm.2009.2.4

Balmain, J., Hannoyer, B., Lopez, E., 1999. Fourier transform infrared spectroscopy (FTIR) and XRD analyses of mineral and organic matrix during heating of mother of pearl (nacre) from the shell of the mollusc *Pinctada maxima*. J. Biomed. Mater. Res. 48, 749-754. doi:10.1002/(SICI)1097-4636(1999)48

Bar-Yosef, O., 2007. The Upper Paleolithic revolution. Annu. Rev. Anthropol. 31, 363-393. doi:10.1177/0392192107076869

Barker, G., Antoniadou, A., Armitage, S., Brooks, I., Candy, I., Connell, K., Douka, K., Drake, N., Farr, L., Hill, E., Hunt, C., Inglis, R., Jones, S., Lane, C., Lucarini, G., Meneeley, J., Morales, J., Mutri, G., Prendergast, A., Rabett, R., Reade, H., Reynolds, T., Russell, N., Simpson, D., Smith, B., Stimpson, C., Twati, M., White, K., 2010. The Cyrenaican Prehistory Project 2010: the fourth season of investigations of the Haua Fteah cave and its landscape, and further results from the 2007-2009 fieldwork. Libyan Stud. 41, 63-88. doi:10.1017/S0263718900000273

Barker, G., Bennett, P., Farr, L., Hill, E., Hunt, C., Lucarini, G., Morales, J., Mutri, G., Prendergast, A., Pryor, A., Rabett, R., Reynolds, T., Spry-Marques, P., Twati, M., 2012. The Cyrenaican Prehistory Project 2012: the fifth season of investigations of the Haua Fteah cave. Libyan Stud. 43, 115-136. doi:10.1017/S026371890000008X

Barton, R.N.E., 2000. Mousterian hearths and shellfish: later Neanderthal activities on Gibraltar. In: C. B. Stringer, R. N. E. Barton, J. C. Finlayson, (Eds.). Neanderthals on the Edge. Oxford: Oxbow, 211-200.

Benedetti-Cecchi, L., Bertocci, I., Micheli, F., Maggi, E., Fosella, T., Vaselli, S., 2003. Implications of spatial heterogeneity for management of marine protected areas (MPAs): Examples from assemblages of rocky coasts in the northwest Mediterranean. Mar. Environ. Res. 55, 429-458. doi:10.1016/S0141-1136(02)00310-0

Berna, F. and Goldberg, P., 2008. Assessing Paleolithic pyrotechnology and associated hominin behavior in Israel. Isr. J. Earth Sci., 56, 107-121. doi:10.1560/IJES.56.2-4.107

Boettcher, A., Wyllie, P.J., 1967. Revision of the calcite-aragonite transition, with the location of a triple point between calcite I, calcite II and aragonite. Nature 213, 792-793. doi:10.1038/213792a0

Boiseau, M., Juillet-Leclerc, A., 1997. H_2O_2 treatment of recent coral aragonite: oxygen and carbon isotopic implications. Chem. Geol. 143, 171-180. doi:10.1016/S0009-2541(97)00112-5

Bonucci, E., Graziani, G., 1975. Comparative thermogravimetric, X- ray diffraction and electron microscope investigations of burnt bone from recent, ancient and prehistoric age. Atti Accademia Nazionale dei Lincei. Classe di Scienze, Fisiche, Matematiche e Naturali Rendiconti, pp. 517-532.

Bosch, M.D., Wesselingh, F.P., Mannino, M.A., 2015. The Ksâr 'Akil (Lebanon) mollusc assemblage: Zooarchaeological and taphonomic investigations. Quat. Int. In press, 1-17. doi:10.1016/j.quaint.2015.07.004

Bourrat, X., Francke, L., Lopez, E., Rousseau, M., Stempfle, P., Angellier, M., Alberic, P., 2007. Nacre biocrystal thermal behaviour. R. Soc. Chem. 9, 1205-1208. doi:10.1039/b709388h

Brain, C.K., 1993. The occurrence of burnt bones at Swartkrans and their implications for the control of fire by early hominids. In: Brain, C.K. (Ed.), Swartkrans: A Cave's Chronicle of Early Man. Transvaal Museum, Pretoria, pp. 229-242

Burchell, M., Cannon, A., Hallmann, N., Schwarcz, H.P., Schöne, B.R., 2013a. Refining estimates for the season of shellfish collection on the Pacific Northwest coast: Applying high-resolution stable oxygen isotope analysis and sclerochronology. Archaeometry 55, 258-276. doi:10.1111/j.1475-4754.2012.00684.x

Burchell, M., Cannon, A., Hallmann, N., Schwarcz, H., Schöne, B.R., 2013b. Refining estimates for the season of shellfish collection on the Pacific Northwest Coast: Applying high-resolution stable oxygen isotope analysis and sclerochronology. Archaeometry 55, 258-276. doi: 10.1111/j.1475-4754.2012.00684.x.

Carter, J. G., Harries, P. J., Malchus, N., Sartori, A. F., Anderson, L. C., Bieler, R., Bogan, A. E., Coan, E.V., Cope, J.C.W., Cragg, S.M., Garcia-March, J.R., Hylleberg, J., Kelley, P., Kleemann, K., Kriz, J., McRoberts, C., Mikkelsen, P.M., Pojeta, J. Jr., Temkin, I., Yancey, T., Zieritz, A. (2012). Illustrated glossary of the bivalvia. Treatise Online, 1(48). doi:10.17161/to.v0i0.4322

Caruso, T., Chemello, R., 2009. The size and shape of shells used by hermit crabs: A multivariate analysis of *Clibanarius erythropus*. Acta Oecol. 35, 349-354. doi:10.1016/j.actao.2009.03.002

Checa, A.G., Ramírez-Rico, J., González-Segura, A., Sánchez-Navas, A., 2009. Nacre and false nacre (foliated aragonite) in extant monoplacophorans (=Tryblidiida: Mollusca). Naturwissenschaften 96, 111-122. doi:10.1007/s00114-008-0461-1

Clark II, G.R., 1975. Periodic growth and biological rhythms in experimentally grown bivalves. In: Rosenberg, G.D., Runcorn, S.K. (Eds.): Growth Rhythms and the History of the Earth's Rotation. J. Wiley and Sons, New York, pp. 103-117.

Colonese, A.C., Troelstra, S., Ziveri, P., Martini, F., Lo Vetro, D., Tommasini, S., 2009. Mesolithic shellfish exploitation in SW Italy: seasonal evidence from the oxygen isotopic composition of *Osilinus turbinatus* shells. J. Archaeol. Sci. 36, 1935-1944. doi:10.1016/j.jas.2009.04.021

Colonese, A.C., Mannino, M.A., Bar-Yosef Mayer, D.E., Fa, D.A., Finlayson, J.C., Lubell, D., Stiner, M.C., 2011. Marine mollusc exploitation in Mediterranean prehistory: An overview. Quat. Int. 239, 86-103. doi:10.1016/j.quaint.2010.09.001

Colonese, A.C., Vetro, D. Lo, Martini, F., 2014. Holocene coastal change and intertidal mollusc exploitation in the central Mediterranean: variations in shell size and morphology at Grotta d'Oriente (Sicily). Archeofauna 23, 181-192.

Craig, O.E., Biazzo, M., Colonese, A.C., Di Giuseppe, Z., Martinez-Labarga, C., Lo Vetro, D., Lelli, R., Martini, F., Rickards, O., 2010. Stable isotope analysis of late Upper Palaeolithic human and faunal remains from Grotta del Romito (Cosenza), Italy. J. Archaeol. Sci. 37, 2504-2512. doi:10.1016/j.jas.2010.05.010

Crothers, J.H., 2001. Common topshells : An introduction to the biology of *Osilinus lineatus* with notes on other species in the genus. F. Stud. 10, 115-160.

Dasgupta, D.R., 1963. The oriented transformation of aragonite into calcite. Miner. Mag. 33, 924-928. doi:10.1180/minmag.1964.033.265.09

Dauphin, Y., Cuif, J.P., Massard, P., 2006. Persistent organic components in heated coral aragonitic skeletons-Implications for palaeoenvironmental reconstructions. Chem. Geol. 231, 26-37. doi:10.1016/j.chemgeo.2005.12.010

Dettman, D.L., Reische, A.K., Lohmann, K.C., 1999. Controls on the stable isotope composition of seasonal growth bands in aragonitic fresh-water bivalves (unionidae). Geochim. Cosmochim. Acta 63, 1049-1057. doi: 10.1016/S0016-7037(99)00020-4

Donald, K.M., Preston, J., Williams, S.T., Reid, D.G., Winter, D., Alvarez, R., Buge, B., Hawkins, S.J., Templado, J., Spencer, H.G., 2012. Phylogenetic relationships elucidate colonization patterns in the intertidal grazers *Osilinus* Philippi, 1847 and *Phorcus* Risso, 1826 (Gastropoda: Trochidae) in the northeastern Atlantic Ocean and Mediterranean Sea. Mol. Phylogenet. Evol. 62, 35-45. doi:10.1016/j.ympev.2011.09.002

Douka, K., Jacobs, Z., Lane, C., Grün, R., Farr, L., Hunt, C., Inglis, R.H., Reynolds, T., Albert, P., Aubert, M., Cullen, V., Hill, E., Kinsley, L., Roberts, R.G., Tomlinson, E.L., Wulf, S., Barker, G., 2014. The chronostratigraphy of the Haua Fteah cave (Cyrenaica, northeast Libya). J. Hum. Evol. 66, 39-63. doi:10.1016/j.jhevol.2013.10.001

Epstein, S., Buchsbaum, R., Lowenstam, H., Urey, H.C., 1951. Carbonate-water isotopic temperature scale. Geol. Soc. Am. Bull. 62, 417-426. doi:10.1130/0016-7606(1951)62[417:CITS]2.0.CO;2

Epstein, S., Buchsbaum, R., Lowenstam, H.M., Urey, H.C., 1953. Revised carbonate-water isotopic temperature scale. Bull. Geol. Soc. Am. 64, 1315-1326.

Erlandson, J.M., 2001. The Archaeology of aquatic adaptations: Paradigm for a new millennium. J. Archaeol. Res. 9, 287-350. doi:10.1023/A:1013062712695

Farr, L., Lane, R., Abdulazeez, F., Bennett, P., Holman, J., Marasi, A., Prendergast, A., Al-Zweyi, M., Barker, G., 2014. The Cyrenaican Prehistory Project 2013: the seventh season of excavations in the Haua Fteah cave. Libyan Stud. 45, 163-173. doi:10.1017/lis.2014.2

Ferguson, J.E., Henderson, G.M., Fa, D.A., Finlayson, J.C., Charnley, N.R., 2011. Increased seasonality in the Western Mediterranean during the last glacial from limpet shell geochemistry. Earth Planet. Sci. Lett. 308, 325-333. doi:10.1016/j.epsl.2011.05.054

Garcia Guixe, E., Richards, M.P., Eulalia Subira, M., 2006. Paleodiets of human and fauna at the Spanish mesolithic site of El Collado. Curr. Anthropol. 47, 549-556.

Gillikin, D.P., Lorrain, A., Meng, L., Dehairs, F., 2007. A large metabolic contribution to the $\delta^{13}C$ record in marine aragonitic bivalve shells. Geochim. Cosmochim. Acta 71, 2936-2946. doi:10.1016/j.gca.2007.04.003

Goldberg, P., 2003. Some observations on Middle and Upper Paleolithic ashy cave and rochshelter deposits in the Near East. In: A. N. Goring-Morris, A. Belfer-Cohen (Eds.). More than meets the eye: studies on Upper Paleolithic diversity in the Near East, pp. 19-32. Oxford: Oxbow.

Goldberg, P. and Bar-Yosef, O., 1998. Site formation processes in Kebara and Hayonim caves and their significance in Levantine prehistoric caves. In: T. Akazawa, K. Aoki, O. Bar-Yosef (Eds.). Neanderthals and Modern Humans in Western Asia, pp. 107-126. New York: Plenum Press. doi:10.1007/0-306-47153-1

Grossman, E.L., Betzer, P.R., Dudley, W.C., Dunbar, R.B., 1986. Stable isotopic variation in pteropods and atlantids from North Pacific sediment traps. Mar. Micropaleontol. 10, 9-22. doi:10.1016/0377-8398(86)90022-8

Grossman, E.L., Ku, T., 1986. Oxygen and carbon isotope fractionation in biogenic aragonite: Temperature effects. Chem. Geol. 59, 59-74. doi:10.1016/0168-9622(86)90057-6

Hanson, M., Cain, C.R., 2007. Examining histology to identify burned bone. J. Archaeol. Sci. 34, 1902-1913. doi:10.1016/j.jas.2007.01.009

Harper, E.M., 2000. Are calcitic layers an effective adaptation against shell dissolution in the Bivalvia? J. Zool. 251, 179-186. doi:10.1017/S095283690000604X

Henry, D. O., Hietala, H. J., Rosen, A. M., Demidenko, Y. E., Usik, V. I., Armagan, T. L., 2004. Human behavioral organization in the Middle Paleolithic: Were Neanderthals different? Am. Anthr. 106, 17-31. doi:10.1525/aa.2004.106.1.17

Hill, E.A., Hunt, C.O., Lucarini, G., Mutri, G., Farr, L., Barker, G., 2015. Land gastropod piercing during the Late Pleistocene and Early Holocene in the Haua Fteah, Libya. J. Archaeol. Sci. Rep., 4, 320-325. doi:10.1016/j.jasrep.2015.09.003

Huang, Z., Li, X., 2009. Nanoscale structural and mechanical characterization of heat treated nacre. Mater. Sci. Eng. C 29, 1803-1807. doi:10.1016/j.msec.2009.02.007

Hunt, C.O., Reynolds, T.G., El-Rishi, H.A., Buzaian, A., Hill, E., Barker, G.W., 2011. Resource pressure and environmental change on the North African littoral: Epipalaeolithic to Roman gastropods from Cyrenaica, Libya. Quat. Int. 244, 15-26. doi:10.1016/j.quaint.2011.04.045

Inglis, R.H., 2012. Human occupation and changing environments during the Middle to Later Stone Ages: soil micromorphology at the Haua Fteah, Libya. Doctoral dissertation, University of Cambridge.

Jones, D.S., 1980. Annual cycle of shell growth increment formation in two continental shelf bivalves and its paleoecologic significance. Paleobiol. 6, 331-340. doi:10.1017/S0094837300006837

Karkanas, P., Koumouzelis, M., Kozlowski, J. K., Sitlivy, V., Sobczyk, K., Berna, F., Weiner, S., 2004. The earliest evidence for clay hearths : Aurignacian features in Klisoura Cave 1, southern Greece. Antiq. 78, 513-525.

Katsanevakis, S., Lefkaditou, E., Galinou-Mitsoudi, S., Koutsoubas, D., Zenetos, A., 2008. Molluscan species of minor commercial interest in Hellenic seas: Distribution, exploitation and conservation status. Mediterr. Mar. Sci. 9, 77-118. doi:10.12681/mms.145

Kawaguchi T., Watabe N., 1993. The organic matrices of the shell of the American oyster *Crassostrea virginica.* J. Exp. Mar. Biol. Ecol. 170, 11-28. doi:10.1016/0022-0981(93)90126-9

Kim, S.-T., Mucci, A., Taylor, B.W., 2007. Phosphoric acid fractionation factors for calcite and aragonite between 25 and 75 °C: Revisited. Chem. Geol. 246, 135-146. doi:10.1016/j.chemgeo.2007.08.005

Klein, R.T., Lohmann, K.C., Thayer, C.W., 1996. Sr/Ca and $^{13}C/^{12}C$ ratios in skeletal calcite of *Mytilus trossulus*: covariation with metabolic rate, salinity, and carbon isotopic composition of seawater. Geochim. Cosmochim. Acta 60, 4207-4221. doi:10.1016/S0016-7037(96)00232-3

Kobayashi, I., Samata, T., 2006. Bivalve shell structure and organic matrix. Mater. Sci. Eng. C 26, 692-698. doi:10.1016/j.msec.2005.09.101

Land, L.S., Lang, J.C., Barnes, D.J., 1975. Extension rate: A primary control on the isotopic composition of West Indian (Jamaica) scleractinian reef coral skeletons. Mar. Biol. 33, 221-233. doi:10.1007/BF00390926

Larsen, S.C., 2015. Recrystallization of biogenic aragonite shells from archaeological contexts and implications for paleoenvironmental reconstruction. Master's thesis, Western Washington University.

Lécuyer, C., 1996. Effects of heating on the geochemistry of biogenic carbonates. Chem. Geol. 129, 173-183. doi:10.1016/0009-2541(96)00005-8

Lécuyer, C., Reynard, B., Martineau, F., 2004. Stable isotope fractionation between mollusc shells and marine waters from Martinique Island. Chem. Geol. 213, 293-305. doi:10.1016/j.chemgeo.2004.02.001

Lehndorff, E., Linstadter, J., Kehl, M., Weniger, G., 2015. Fire history reconstruction from black carbon analysis in Holocene cave sediments at Ifri Oudadane, Northeastern Morocco. The Holocene 25, 398-402. doi:10.1177/0959683614558651

Leone, G., Bonadonna, F., Zanchetta, G., 2000. Stable isotope record in mollusca and pedogenic carbonate from Late Pliocene soils of Central Italy. Palaeogeogr. Palaeoclimatol. Palaeoecol. 163, 115-131. doi:10.1016/S0031-0182(00)00148-6

Li, H., Jin, D., Li, R., Li, X., 2015. Structural and mechanical characterization of thermally treated conch shells. J. Miner. Met. Mater. Soc. 67, 720-725. doi:10.1007/s11837-015-1330-y

Liu, Y., Shigley, J., Hurwit, K., 1999. Iridescent color of a shell of the mollusk *Pinctada margaritifera* caused by diffraction. Opt. Express 4, 177-182. doi:10.1364/OE.4.000177

Lubell, D., Jackes, M., Schwarcz, H., Knyf, M., Meiklejohn, C., 1994. The Mesolithic-Neolithic transition in Portugal: Isotopic and dental evidence of diet. J. Archaeol. Sci. doi:10.1006/jasc.1994.1022

Mannino, M.A., Thomas, K.D., 2002. Depletion of a resource? The impact of prehistoric human foraging on intertidal mollusc communities and its significance for human settlement, mobility and dispersal. World Archaeol. 33, 452-474. doi:10.1080/00438240120107477

Mannino, M.A., Spiro, B.F., Thomas, K.D., 2003. Sampling shells for seasonality: oxygen isotope analysis on shell carbonates of the inter-tidal gastropod *Monodonta lineata* (da Costa) from populations across its modern range and from a Mesolithic site in southern Britain. J. Archaeol. Sci. 30, 667-679. doi:10.1016/S0305-4403(02)00238-8

Mannino, M.A., Thomas, K.D., Leng, M.J., Piperno, M., Tusa, S., Tagliacozzo, A., 2007. Marine resources in the Mesolithic and Neolithic at the Grotta dell'Uzzo (Sicily): Evidence from isotope analyses of marine shells. Archaeometry 49, 117-133. doi:10.1111/j.1475-4754.2007.00291.x

Mannino, M.A., Thomas, K.D., Leng, M.J., Sloane, H.J., 2008. Shell growth and oxygen isotopes in the topshell *Osilinus turbinatus*: resolving past inshore sea surface temperatures. Geo-Marine Lett. 28, 309-325. doi:10.1007/s00367-008-0107-5

Mannino, M.A., Thomas, K.D., Leng, M.J., Di Salvo, R., Richards, M.P., 2011. Stuck to the shore? Investigating prehistoric hunter-gatherer subsistence, mobility and territoriality in a Mediterranean coastal landscape through isotope analyses on marine mollusc shell carbonates and human bone collagen. Quat. Int. 244, 88-104. doi:10.1016/j.quaint.2011.05.044

Maritan, L., Mazzoli, C., Freestone, I., 2007. Modelling changes in mollusc shell internal microstructure during firing: Implications for temperature estimation in shell-bearing pottery. Archaeometry 49, 529-541. doi:10.1111/j.1475-4754.2007.00318.x

McBurney, C., 1967. The Haua Fteah (Cyrenaica) and the Stone Age in the South-East Mediterranean. Cambridge University Press, Cambridge. doi:10.1002/ajpa.1330290330

McConnaughey, T.A., Gillikin, D.P., 2008. Carbon isotopes in mollusk shell carbonates. Geo-Marine Lett. 28, 287-299. doi:10.1007/s00367-008-0116-4

McTigue, Jr., J.W., Wenk, H., 1985. Microstructures and orientation relationship in the dry-state aragonite-calcite and calcite-lime phase transformations. Am. Mineral. 70, 1253-1261.

Menzies, R., Cohen, Y., Lavie, B., Nevo, E., 1992. Niche adaptation in two marine gastropods, *Monodonta turbiformis* and *M. turbinata.* Bolletino di Zool. 59, 297-302. doi:10.1080/11250009209386685

Merkel, C., Griesshaber, E., Kelm, K., Neuser, R., Jordan, G., Logan, A., Mader, W., Schmahl, W.W., 2007. Micromechanical properties and structural characterization of modern inarticulated brachiopod shells. J. Geophys. Res. 112. doi:10.1029/2006JG000253

Metref, S., Rousseau, D. D., Bentaleb, I., Labonne, M., Vianey-Liaud, M., 2003. Study of the diet effect on $\delta^{13}C$ of shell carbonate of the land snail *Helix aspersa* in experimental conditions. Earth Planet. Sc. Lett. 211, 381-393. doi:10.1016/S0012-821X(03)00224-3

Milner, N., 2001. At the cutting edge: Using thin sectioning to determine season of death of the European oyster, *Ostrea edulis*. J. Archaeol. Sci. 28, 861-873. doi:10.1006/jasc.2000.0618

Minnett, P.J., Evans, R.H., Kearns, E.J., Brown, O.B., 2002. Sea-surface temperature measured by the Moderate Resolution Imaging Spectroradiometer (MODIS), in: Geoscience and Remote Sensing Symposium, 2002. pp. 1177-1179. doi:10.1109/IGARSS.2002.1025872

Mook, W., 1971. Paleotemperatures and chlorinities from stable carbon and oxygen isotopes in shell carbonate. Palaeogeogr. Palaeoclimatol. Palaeoecol. 9, 245-263. doi:10.1016/0031-0182(71)90002-2

Munro, L.E., Longstaffe, F.J., White, C.D., 2007. Burning and boiling of modern deer bone: Effects on crystallinity and oxygen isotope composition of bioapatite phosphate. Palaeogeogr. Palaeoclimatol. Palaeoecol. 249, 90-102. doi:10.1016/j.palaeo.2007.01.011

Munro, L.E., Longstaffe, F.J., White, C.D., 2008. Effects of heating on the carbon and oxygen-isotope compositions of structural carbonate in bioapatite from modern deer bone. Palaeogeogr. Palaeoclimatol. Palaeoecol. 266, 142-150. doi:10.1016/j.palaeo.2008.03.026

Nakahara, H., 1991. Nacre formation in bivalve and gastropod molluscs. In: S. Suga, H. Nakahara (Eds.). Mechanisms and phylogeny of mineralization in biological systems, pp. 343-350. Berlin, Germany: Springer. doi:10.1007/978-4-431-68132-8_55

Nudelman, F., Gotliv, B.A., Addadi, L., Weiner, S., 2006. Mollusk shell formation: Mapping the distribution of organic matrix components underlying a single aragonitic tablet in nacre. J. Struct. Biol. 153, 176-187. doi:10.1016/j.jsb.2005.09.009

O'Neil, J.R., 1969. Oxygen isotope fractionation in divalent metal carbonates. J. Chem. Phys. 51, 5547-5558. doi:10.1063/1.1671982

Parker, J.E., Thompson, S.P., Lennie, A.R., Potter, J., Tang, C.C., 2010. A study of the aragonite-calcite transformation using Raman spectroscopy, synchrotron powder diffraction and scanning electron microscopy. R. Soc. Chem. 12, 1590-1599. doi:10.1039/b921487a

Pierre, C., 1999. The oxygen and carbon isotope distribution in the Mediterranean water masses. Mar. Geol. 153, 41-55. doi:10.1016/S0025-3227(98)00090-5

Pokroy, B., Fitch, A.N., Lee, P.L., Quintana, J.P., Caspi, E.N., Zolotoyabko, E., 2006a. Anisotropic lattice distortions in the mollusk-made aragonite: A widespread phenomenon. J. Struct. Biol. 153, 145-150. doi:10.1016/j.jsb.2005.10.009

Pokroy, B., Fitch, A.N., Marin, F., Kapon, M., Adir, N., Zolotoyabko, E., 2006b. Anisotropic lattice distortions in biogenic calcite induced by intra-crystalline organic molecules. J. Struct. Biol. 155, 96-103. doi:10.1016/j.jsb.2006.03.008

Poppe, G.T., Goto, Y., 1991. European Seashells. Volume 1 (Polyplacophora, Caudofoveata, Solenogastra, Gastropoda). Verlag Christa Hemmen, Germany.

Prendergast, A.L., Azzopardi, M., O'Connell, T.C., Hunt, C., Barker, G., Stevens, R.E., 2013. Oxygen isotopes from *Phorcus (Osilinus) turbinatus* shells as a proxy for sea surface temperature in the central Mediterranean: A case study from Malta. Chem. Geol. 345, 77-86. doi:10.1016/j.chemgeo.2013.02.026

Prendergast, A.L., Stevens, R.E., O'Connell, T.C., Fadlalak, A., Touati, M., Al-Mzeine, A., Schöne, B.R., Hunt, C.O., Barker, G., 2015. Changing patterns of eastern Mediterranean shellfish exploitation in the Late Glacial and Early Holocene: Oxygen isotope evidence from gastropod in Epipaleolithic to Neolithic human occupation layers at the Haua Fteah cave, Libya. Quat. Int. In press. doi:10.1016/j.quaint.2015.09.035

Prendergast, A.L., Stevens, R.E., Hill, E. Hunt, C., Barker, G., O'Connell, T. C. (in press b) Carbon isotope signatures from land snail shells: implications for palaeovegetation reconstruction in the eastern Mediterranean. Quaternary International. doi: 10.1016/j.quaint.2014.12.053

Reese, D. 1991. Marine shells in the Levant: Upper Palaeolithic, Epipalaeolithic and Neolithic. In: Bar-Yosef and Valla (Eds.). The Natufian Culture in the Levant. Archaeological series 1, pp. 613-627. Ann Arbor: International Monographs in Prehistory.

Regis, M.B., 1972. Étude comparée de la croissance des Monodontes (Gastéropodes Prosobranches) en Manche et le long des côtes atlantiques et méditerranéennes françaises. In: Battaglia, B. (Ed.), Proceedings of the 5th European Marine Biology Symposium. Piccin, Padova, pp. 259-267.

Ren, F., Wan, X., Ma, Z., Su, J., 2009. Study on microstructure and thermodynamics of nacre in mussel shell. Mater. Chem. Phys. 114, 367-370. doi:10.1016/j.matchemphys.2008.09.036

Richards, M.P., Hedges, R.E.M., 1999. Stable isotope evidence for similarities in the types of marine foods used by Late Mesolithic humans at sites along the Atlantic coast of Europe. J. Archaeol. Sci. 26, 717-722. doi:10.1006/jasc.1998.0387

Samata, T., 1990. Ca-binding glycoproteins in molluscan shell with different types of ultrastructure. Veliger 33, 190-201.

Schifano, G., 1983. Allometric growth as influenced by environmental temperature in *Monodonta turbinata* shells. Palaeogeogr. Palaeoclimatol. Palaeoecol. 44, 215-222. doi:http://dx.doi.org/10.1016/0031-0182(83)90104-9

Schifano, G., Censi, P., 1983. Oxygen isotope composition and rate of growth of *Patella coerulea, Monodonta turbinata* and *M. articulata* shells from the western coast of Sicily. Palaeogeogr. Palaeoclimatol. Palaeoecol. 42, 305-311. doi:10.1016/0031-0182(83)90028-7

Schöne, B.R., Tanabe, K., Dettman, D.L., Sato, S., 2003. Environmental controls on shell growth rates and $\delta^{18}O$ of the shallow marine bivalve mollusk *Phacosoma japonicum* in Japan. Mar. Biol. 142, 473-485. doi:10.1007/s00227-002-0970-y

Schöne, B.R., Freyre Castro, A.D., Fiebig, J., Houk, S.D., Oschmann, W., Kröncke, I., 2004. Sea surface water temperatures over the period 1884-1983 reconstructed from oxygen isotope ratios of a bivalve mollusk shell (*Arctica islandica*, southern North Sea). Palaeogeogr. Palaeoclimatol. Palaeoecol. 212, 215-232. doi:10.1016/j.palaeo.2004.05.024

Schöne, B.R., Rodland, D.L., Wehrmann, A., Heidel, B., Oschmann, W., Zhang, Z., Fiebig, J., Beck, L., 2007. Combined sclerochronologic and oxygen isotope analysis of gastropod shells (*Gibbula cineraria*, North Sea): life-history traits and utility as a high-resolution environmental archive for kelp forests. Mar. Biol. 150, 1237-1252. 10.1007/s00227-006-0435-9

Schöne, B.R., Wanamaker, A.D. Jr., Fiebig, J., Thébault, J., Kreutz, K.J., 2011. Annually resolved $\delta^{13}C_{shell}$ chronologies of long-lived bivalve mollusks (*Arctica islandica*) reveal oceanic carbon dynamics in the temperate North Atlantic during recent centuries. Palaeogeogr. Palaeoclimatol. Palaeoecol. 302, 31-42, doi:10.1016/j.palaeo.2010.02.002

Shackleton, N.J., 1973. Oxygen isotope analysis as a means of determining season of occupation of prehistoric midden sites. Archaeometry 15, 133-141. doi:10.1111/j.1475-4754.1973.tb00082.x

Shackleton, N.J., 1974. Attainment of isotopic equilibrium between ocean water and the benthonic foraminifera genus Uvigerina: Isotopic changes in the ocean during the last glacial. Colloq. Int. Cent. Natl. la Rech. Sci. 219, 203-210.

Snow, M.R., Pring, A., Self, P., Losic, D., Shapter, J., 2004. The origin of the color of pearls in iridescence from nano-composite structures of the nacre. Am. Mineral. 89, 1353-1358. doi:10.2138/am-2004-1001

Speth, J. D., 2006. Housekeeping, Neandertal- Style. In: Transitions before the transition (pp. 171-188). Springer US. doi:10.1007/0-387-24661-4

Stiner, M.C., 1994. Honor among thieves: A zooarchaeological study of Neandertal ecology. NJ. Priceton University Press, Princeton. doi:10.1002/ajpa.1330990204

Stiner, M.C., Kuhn, S., Weiner, S., Bar-Yosef, O., 1995. Differential burning, recrystallization, and fragmentation of archaeological bone. J. Archaeol. Sci. 22, 223-237. doi:10.1006/jasc.1995.0024

Stiner, M.C., Bar-Yosef, O., 2005. The faunas of Hayonim Cave, Israel: A 200,000-year record of Paleolithic diet, demography, and society. No. 48. Harvard University Press.

Stiner, M.C., Kuhn, S.L., Güleç, E., 2013. Early Upper Paleolithic shell beads at Üçagızlı Cave I (Turkey): Technology and the socioeconomic context of ornament life-histories. J. Hum. Evol. 64, 380-398. doi:10.1016/j.jhevol.2013.01.008

Stott, L.D., 2002. The influence of diet on the $\delta^{13}C$ of shell carbon in the pulmonate snail *Helix aspersa*. Earth Planet. Sc. Lett. 195, 249-259. doi:10.1016/S0012-821X(01)00585-4

Stringer, C.B., Finlayson, J.C., Barton, R.N.E., Fernández-Jalvo, Y., Cáceres, I., Sabin, R.C., Rhodes, E.J., Currant, A.P., Rodríguez-Vidal, J., Giles-Pacheco, F., Riquelme-Cantal, J.A., 2008. Neanderthal exploitation of marine mammals in Gibraltar. Proc. Natl. Acad. Sci. U.S.A. 105, 14319-24. doi:10.1073/pnas.0805474105

Surge, D., Barrett, J.H., 2012. Marine climatic seasonality during medieval times (10^{th} to 12^{th} centuries) based on isotopic records in Viking Age shells from Orkney, Scotland. Palaeogeogr. Palaeoclimatol. Palaeoecol. 350-352, 236-246. doi:10.1016/j.palaeo.2012.07.003

Tan, T., Wong, D., Lee, P., 2004. Iridescence of a shell of mollusk *Haliotis glabra*. Opt. Express 12, 4847-4854. doi:10.1364/OPEX.12.004847

Taylor, V.K., Barton, R.N.E., Bell, M., Bouzouggar, A., Collcutt, S., Black, S., Hogue, J.T., 2011. The Epipalaeolithic (Iberomaurusian) at Grotte des Pigeons (Taforalt), Morocco: A preliminary study of the land Mollusca. Quat. Int. 244, 5-14. doi:10.1016/j.quaint.2011.04.041

Tushtev, K., Murck, M., Grathwohl, G., 2008. On the nature of the stiffness of nacre. Mater. Sci. Eng. C 28, 1164-1172. doi:10.1016/j.msec.2007.10.039

Vallverdú, J., Vaquero, M., Cáceres, I., Allué, E., Rosell, J., Saladié, P., Chacon, G., Olle, A., Canals, A., Sala, R., Courty, M., Carbonell, E., 2010. Sleeping activity area within the site structure of archaic human groups. Curr. Anthropol. 51, 137-145. doi:10.1086/649499

Vaquero, M., Vallverdú, J., Rosell, J., Pastó, I., Allué, E., 2001. Neandertal behavior at the middle Palaeolithic site of Abric Romani, Capellades, Spain. J. Field Archaeol. 28, 93-114. doi:10.2307/3181461

Wardecki, D., Przeniosło, R., Brunelli, M., 2008. Internal pressure in annealed biogenic aragonite. R. Soc. Chem. 10, 1450-1453. doi:10.1039/b805508d

Wefer, G., Berger, W.H., 1991. Isotope paleontology: Growth and composition of extant calcareous species. Mar. Geol. 100, 207-248. doi:10.1016/0025-3227(91)90234-U

Weiner, S., Addadi, L., 1997. Design strategies in mineralized biological materials. J. Mater. Chem. 7, 689-702. doi:10.1039/a604512j

Wierzbowski, H., 2007. Effects of pre-treatments and organic matter on oxygen and carbon isotope analyses of skeletal and inorganic calcium carbonate. Int. J. Mass Spectrom. 268, 16-29. doi:10.1016/j.ijms.2007.08.002

Wolf, M., Lehndorff, E., Wiesenberg, G.L.B., Stockhausen, M., Schwark, L., Amelung, W., 2013. Towards reconstruction of past fire regimes from geochemical analysis of charcoal. Org. Geochem. 55, 11-21. doi:10.1016/j.orggeochem.2012.11.002

Zaremba, C.M., Morse, D.E., Mann, S., Hansma, P.K., Stucky, G.D., 1998. Aragonite-hydroxyapatite conversion in gastropod (Abalone) nacre. Chem. Mater. 10, 3813-3824. doi:10.1021/cm970785g

Zilhão, J., Angelucci, D.E., Badal-Garcia, E., d'Errico, F., Daniel, F., Dayet, L., Douka, K., Higham, T.F.G., Martinez-Sanchez, M.J., Montes-Bernardez, R., Murcia-Mascaros, S., Perez-Sirvent, C., Roldan-Garcia, C., Vanhaeren, M., Villaverde, V., Wood, R., Zapata, J., 2010. Symbolic use of marine shells and mineral pigments by Iberian Neandertals. Proc. Natl. Acad. Sci. 107, 1023-1028. doi:10.1073/pnas.0914088107

Žmak, I., Jakovljević, S., Bernat, M., 2015. Comparison of microstructure of the Adriatic Monodonta and the Mediterranean limpet, in: MATRIB 2015. pp. 407-417.

Manuscript IV

The effects of environment on *Arctica islandica* shell formation and architecture

Submitted to Biogeosciences

Stefania Milano[1], Gernot Nehrke[2], Alan D. Wanamaker Jr. [3], Irene Ballesta- Artero[4,5], Thomas Brey[2], Bernd R. Schöne[1]

[1] Institute of Geosciences, University of Mainz, Joh.-J.-Becherweg 21, 55128 Mainz, Germany

[2] Alfred Wegener Institute for Polar and Marine Research, Am Handelshafen 12, 27570 Bremerhaven, Germany

[3] Department of Geological and Atmospheric Sciences, Iowa State University, Ames, Iowa, 50011-3212, USA

[4] Royal Netherlands Institute for Sea Research and Utrecht University, PO Box 59, 1790 AB Den Burg, Texel, The Netherlands

[5] Department of Animal Ecology, VU University Amsterdam, The Netherlands

Author contribution

Concept: SM, GN, ADW, IBA, TB, BRS
Execution: SM, GN, IBA
Analysis: SM, GN
Data interpretation: SM, GN, BRS
Writing: SM, GN, ADW, IBA, TB, BRS

Abstract

Mollusks record valuable information on the ambient environment in their hard parts. For this reason, the shells serve as excellent archives that can be used to reconstruct past climate variability. However, complex animal biology and poorly understood biomineralization processed can make the decoding of environmental signals a challenging task. Many of the routinely used proxies are sensitive to multiple different environmental and physiological variables. Therefore, the identification and interpretation of individual environmental signals (e.g. water temperature) may result particularly difficult. Novel proxies independent of other variables and physiology would be a great value in the field of paleoclimatology. The aim of this study is to investigate the potential use of structural properties of *Arctica islandica* shells as environmental proxy. A total of eleven specimens were analyzed to study if changes of the microstructural organization of this species are related to changes of the environment. In order to limit the interference of multiple parameters, the samples were cultured under controlled conditions. Three shells were grown at two different water temperatures (10 °C and 15 °C), and eight specimens were reared at three different dietary regimes. Shell material was analyzed with two techniques: (1) Confocal Raman microscopy (CRM) was used to quantify changes of the orientation of microstructural units and pigment distribution and (2) Scanning electron microscopy (SEM) was used to detect changes in microstructural organization. Our results indicate that A. islandica microstructure is not sensitive to changes of the food source. Likely, shell pigments are not altered by diet. However, at 15 °C the orientation of the biomineral units is significantly different from units formed at 10 °C. According to the results of this study the crystallographic orientation of biomineral units of A. islandica may serve as an alternative proxy for temperature.

Keywords: Confocal Raman microscopy; Scanning electron microscopy; Shell microstructure; Water temperature; Diet; Bivalve shell

1. Introduction

Biomineralization is a process through which living organisms produce a protective, hard tissue. The considerable diversity of biomineralizing species contributes to high variability in terms of shape, organization and mineralogy of the structures produced (Lowenstam and Weiner, 1989; Carter et al., 2012). Different architectures at the micrometer and nanometer scale and different biochemical compositions determine material properties that serve specific functions (Weiner and Addadi, 1997; Currey, 1999; Merkel et al., 2007). Besides these differences, all mineralized tissues are hybrid materials consisting in hierarchical arrangements of biomineral units surrounded by organic matrix, also known as "microstructures" (Bøggild, 1930; Carter and Clark, 1985; Rodriguez-Navarro et al., 2006) or "ultrastructures" (Blackwell et al., 1977; Olson et al., 2012) or overall "fabrics" (Schöne, 2013; Schöne et al., 2013). The carbonate and organic phases represent the fundamental level of the organization of biomaterials (Aizenberg et al., 2005; Meyers et al., 2006). The mechanisms of microstructure formation and shaping, especially in mollusks, has attracted increasing attention during the last decades. At present, it is commonly accepted that the organic compounds play an important role in the formation of the inorganic phases of biominerals (Weiner and Addadi, 1991; Berman et al., 1993; Dauphin et al., 2003; Nudelman et al., 2006). However, the identification of the forces driving the process is still an open research question. Previous studies conducted on mollusks show that environmental parameters can influence microstructure formation (Lutz, 1984; Tan Tiu and Prezant, 1987; Tan Tiu, 1988; Nishida et al., 2012). These results set the stage for a research interest toward the use of shell microstructures as proxy for reconstructing environmental conditions (Tan Tiu, 1988; Tan Tiu and Prezant, 1989; Olson et al., 2012; Milano et al., 2015).

Mollusks are already being successfully employed as climate proxy archives because they can record a large amount of environmental information in their shells (Richardson, 2001; Schöne and Gillikin, 2013). Whereas structures at nanometric level are still underexplored as environmental recorders, shell patterns at lower magnification, such as growth increments, are commonly used for this purpose (Jones, 1983; Schöne et al., 2005; Marali and Schöne, 2015). Mollusks deposit skeletal material on a periodic basis and at different rates (Thompson et al., 1980; Deith, 1985). During periods of fast growth, growth increments are formed whereas during periods of slower growth, growth lines are formed (Schöne, 2008; Schöne and Gillikin, 2013). The periodicity of such structures ranges from tidal to annual (Gordon and Carriker, 1978; Schöne and Surge, 2012). By cross-dating time-series with similar growth patterns it is possible to construct century and millennia-long master chronologies (Marchitto et al., 2000; Black et al. 2008; Butler et al., 2013). This basic approach, in combination with geochemical methods, has great potential in reconstructing past climatic conditions (Wanamaker et al., 2011). At present, the most frequently used and well-accepted geochemical proxy is $\delta^{18}O_{shell}$ (Epstein, 1953; Grossman and Ku, 1986; Schöne et al., 2004) which serves as a paleothermometer and paleosalinometer (Mook, 1971; Andrus, 2011). However, $\delta^{18}O_{shell}$-based temperature reconstructions are particularly challenging in habitats

with fluctuating salinity and hence $\delta^{18}O_{water}$ signature such as brackish areas (Gillikin et al., 2005). There is hence a growing interest in identifying alternative proxies for environmental variables in mollusk shells.

This study investigates the possibility of shell microstructure to serve as a new environmental proxy. For this purpose, the effects of changing water temperature and food supply on the microstructural units of *Arctica islandica* cultured under controlled conditions were analyzed and quantified. *A. islandica* was chosen as model species because of its great importance in paleoclimatology. Its extreme longevity of up to more than 500 years makes this species a highly suitable archive for long-term paleoclimate reconstructions (Schöne et al., 2005; Wanamaker et al., 2008; Butler et al., 2013).

2. Materials and Methods

The analyses were conducted on eleven *A. islandica* shells. Three *A. islandica*, aged four and five years old, were collected alive in March 2011 at Damariscotta River estaury, Maine and grown at two different temperature regimes for 16 weeks at the Darling Marine Center, Walpole, Maine (Table 1). Eight one-year old juveniles were collected in July 2014 from Kiel Bay, Baltic Sea (54° 32′ N, 10° 42′ E; Fig. 1) and kept alive in tanks at 7 °C for six months at the Alfred Wegener Institute for Polar and Marine Research (AWI), Bremerhaven, Germany. During this time interval, the animals were fed with an algal mix of *Nannochloropsis* sp., *Isochrysis galbana* and *Pavlova lutheri*. Then, they were transferred to the Royal Netherlands Institute for Sea Research (NIOZ), Texel, The Netherlands, and cultured in tanks at three different dietary conditions for 11 weeks (Table 1).

2.1 Temperature experiment

The temperature experiment started on 27 March 2011 and ended on 21 July 2011. Prior to the start of the experiment the animals were marked with calcein. The staining leaves a clear fluorescent marker in the shells that can be used to identify which shell material has formed prior to and during the experiment. Initially, the animals were kept at 10.3 ± 0.2 °C for 48 days. Then, they were briefly removed from the tanks and marked again. Subsequently, the clams were cultured for 69 more days at 15.0 ± 0.3 °C. Ambient seawater was pumped from the adjacent Damariscotta River estuary and adjusted to desired temperature. The salinity was measured with a Hydrolab® MiniSonde. It ranged between 30.2 ± 0.7 and 30.7 ± 0.7, in the two experimental phases, respectively. At the end of the experiment the soft tissues were removed.

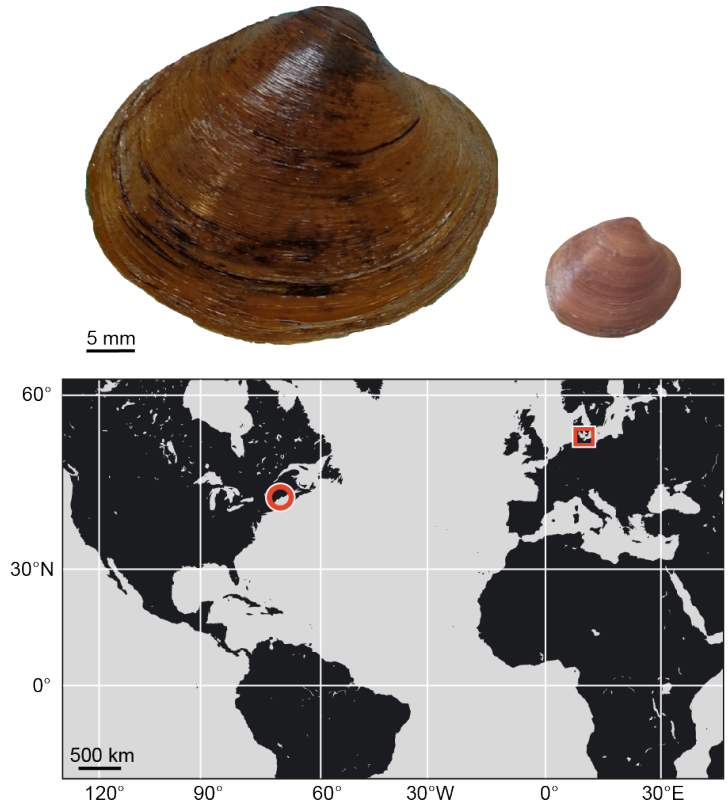

Fig. 1. Shell of adult *Arctica islandica* used in the temperature experiment (left) and juvenile from the Baltic Sea used in the food experiment (right). The map indicates the localities where the two sets of shells where collected: Damariscotta River estaury, Maine (circle) and Kiel Bay (square).

Table 1. List of the studied speciemen of *Arctica islandica* and experimental conditions.

Sample ID	Locality	Age	Experiment	Treatment
A2	Maine	5	Temperature	10 °C + 15 °C
A4	Maine	4	Temperature	10 °C + 15 °C
A5	Maine	4	Temperature	10 °C + 15 °C
S12	Kiel Bay	1	Diet	Food 1
S14	Kiel Bay	1	Diet	Food 1
S15	Kiel Bay	1	Diet	Food 1
G11	Kiel Bay	1	Diet	Food 2
G12	Kiel Bay	1	Diet	Food 2
G15	Kiel Bay	1	Diet	Food 2
N13	Kiel Bay	1	Diet	No additional food
N15	Kiel Bay	1	Diet	No additional food

2.2 Food experiment

The food experiment was carried out from 9 February 2015 to 29 April 2015. The animals were placed in aquaria inside a climate room at 9 °C. Water temperature in the tanks ranged between 8 and 10 °C. Water salinity was measured by using an ENDECO 102 refractometer and ranged between 29.6 and 29.9 ± 0.1 in each aquarium. The 15-liter tanks were constantly supplied with aerated water from the Wadden Sea. The clams were acclimated for three weeks before the start of the experiment. Three dietary regimes were chosen. One treatment consisted of feeding the animals with Microalgae Mix (food type 1), a ready-made solution of four marine microalgae (25 % *Isochrysis*, 25 % *Tetraselmis*, 25 % *Thalassiosira*, 25 % *Nannochloropsis*) with a particle size range of 2 - 30 µm. A second treatment was based on PhytoMaxx (food type 2), a solution of living *Nannochloropsis* algae with 2 - 5 µm size range. A third treatment served as control, i.e., the animals were not fed with any additional food. In treatments with food type 1 and 2, microalgae were provided at the constant optimum concentration of 20×10^6 cells/liter (Winter, 1969). A dispenser equipped with a timer was used to distribute the food five times per day. At the end of the experiment the soft tissues were removed. A distinct dark line in the shells indicated the transposition to the NIOZ aquaria and the associated stress. This line marks the beginning of the tank experiment.

2.3 Sample preparation

The right valve of each specimen was cut into two 1.5 millimeter-thick sections along the axis of maximum growth. For this purpose, a low speed precision saw (Buehler Isomet 1000) was used. Given the small size and fragility of the juvenile shells used in the food experiment, the valves were fully embedded in a block of Struers EpoFix (epoxy) and air-dried overnight prior the sectioning. Sections of the clams used in the temperature experiment were embedded in epoxy after the cutting. All samples were ground using a Buehler Metaserv 2000 machine equipped with Buehler silicon carbide papers of different grit sizes (P320, P600, P1200, P2500). In addition, the samples were manually ground with Buehler P4000 grit paper and polished with a Buehler diamond polycrystalline suspension (3 µm). Sample surfaces were rinsed in demineralized water and air-dried. In the samples of the temperature experiment, the calcein marks were located under a fluorescence light microscope (Zeiss Axio Imager.A1m microscope equipped with a Zeiss HBO100 mercury lamp and filter set 38: excitation wavelength, ca. 450 - 500 nm; emission wavelength, ca. 500 - 550 nm).

2.4 *A. islandica* shell organization

The shell of *A. islandica* consists or pure aragonite and it is divided in two major layers, an outer (OSL) and the inner shell layer (ISL). The OSL is further subdivided in outer (oOSL) and inner portion (iOSL) (Schöne, 2013). These layers are characterized by specific microstructures (Ropes et al., 1984). The oOSL largely consists of homogenous

microstructure with a bulky and granular aspect (Schöne et al., 2013). The iOSL and ISL are largely composed of crossed-lamellar to cross-acicular microstructures (Dunca et al., 2009). The present study focuses on ventral margin of the shells. Analyses were carried out exclusively in the OSL.

Similar to other mollusks, the shell of *A. islandica* contains pigment polyenes which are very well visible when using CRM (Hedegaard et al., 2006). Polyenes are organic compounds containing single (C-C) and double (C=C) carbon-carbon bonds forming a polyenic chain. Their distribution across the shell is not homogenous. The pigments are abundant in the oOSL whereas they become scarce in the iOSL (Stemmer and Nehrke, 2014).

2.5 Confocal Raman microscopy and image processing

Shells were mapped with a WITec alpha 300 R (WITec GmbH, Germany) confocal Raman microscope. Scans of 50 × 50 µm, 100 × 50 µm and 150 × 50 µm were performed using a piezoelectric scanner table. All Raman measurements were carried out using a 488 nm diode laser. A spectrometer (UHTS 300, WITec, Germany) was used with a 600 mm^{-1} grating, a 500 nm blaze and an integration time of 0.03 s. On each sample two to six scans were made, depending of the thickness of the shell. For instance, in juvenile shells (food experiment), two scans of each sample were made. On larger shells used in the temperature experiment, six maps were completed, i.e., two maps in the oOSL, two in the middle of the iOSL and two in the inner portion of the iOSL. Each scan contained between 40,000 and 120,000 data points, depending on the map size. The spatial resolution equaled 250 nm. Half of the maps were performed on the shell portion formed before the experiments. The other half were made on the shell portion formed under experimental conditions. In order to avoid areas affected by transplantation or marking stress, the scans were located far off the calcein and stress lines. Raman maps on food experiment shells were performed 300 µm away from the stress line. In the shells from the temperature experiment, the scans were made 1 mm away from the calcein mark.

Polarized Raman microscopy is known to provide comprehensive information about the crystallographic properties of the materials (Hopkins and Farrow, 1985). The aragonite spectrum is characterized by two lattice modes (translation mode Ta, 152 cm^{-1} and librational mode La, 206 cm^{-1}) and the two internal modes (in-plane band ν_4, 705 cm^{-1} and symmetric stretch ν_1, 1085 cm^{-1}). The ratio ($R_{\nu1/Ta}$) between peak intensities belonging to ν_1 and T_a is caused by different crystallographic orientations of the aragonitic units (Hopkins and Farrow, 1985; Nehrke and Nouet, 2011). Within each scan, $R_{\nu1/Ta}$ was calculated for each data point. New spectral images were generated using WITecProject software (version 4.1, WITec GmbH, Germany). These images were then binarized by replacing all values above 2.5 with 1 and the others with 0. The orientation was quantified by calculating the area formed by pixels of value 1 over the total scan area. The imaging software Gwyddion (http://gwyddion.net/last checked: June 2016) was used for this purpose.

The results were expressed in percentage.

The Raman scans of the food experiment shells were analyzed to investigate the pigment composition. Polyene peaks have definite positions in the spectrum according to the number of the C-C and C=C bonds of the chain, which are specific for certain types of pigments. The two major polyene peaks at ~ 1130 (R_1) and 1520 cm^{-1} (R_4) were identified by using the "multipeak fitting 2" routine of IGOR Pro (version 7.00, WaveMetrics, USA). Their exact position was determined adopting a Gaussian fitting function (Fig. 2). The number of single (N_1) and double carbon bonds (N_4) was calculated by applying the equations by Schaffer et al. (1991):

(1) $N_1 = 476 (R_1 - 1{,}082)$

(2) $N_4 = 830 (R_4 - 1{,}438)$

Spectral images of the R_4 band were used to locate the polyenes in the shell and measure the thickness of the pigmented layer. This analysis was conducted only on the shells of the food experiment. Given the larger size of the shells used in the temperature experiment, the spectral maps were not sufficient for a correct localization of the pigmented layer boundaries and estimation of its thickness.

To quantify changes of the orientation of individual biomineral units of the juvenile shells (food experiment), the spectral maps were subdivided into two portions. The outermost shell portion (oOSL) was enriched in pigments whereas the iOSL showed a decrease in polyene content.

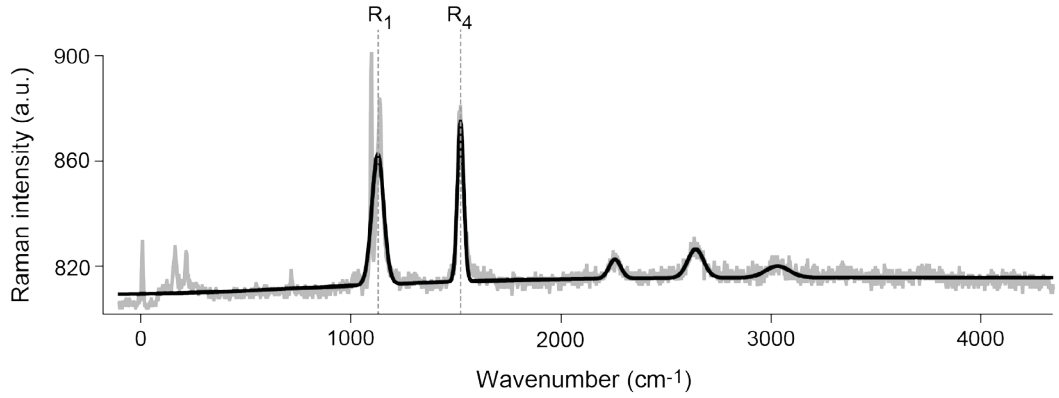

Fig. 2. Raman spectrum of *Arctica islandica* showing the typical aragonite peaks (grey line). The exact position of the polyene peaks R_1 and R_4 was determined by using a peak fitting routine based on a Gaussian function (black line).

2.6 Scanning electron microscopy

After being used for Raman measurements, the samples were prepared for SEM analysis. Each shell slab was ground with a Buehler Metaserv 2000 machine and Buehler silicon F2500 grit carbide paper. To reduce the impact of grinding on the sample surface of juvenile shells, extra grinding was done by hand. Then, the slabs were polished with a Buehler diamond polycrystalline suspension (3 µm). Afterward,

shell surfaces were etched in 0.12 N HCl solution for 10 (food experiment samples) to 90 s (temperature experiment samples) and subsequently placed in 6 vol % NaClO solution for 30 min. After being rinsed in demineralized water, air-dried samples were sputter-coated with a 2 nm-thick platinum film by using a Low Vacuum Coater Leica EM ACE200.

A scanning electron microscope (LOT Quantum Design 2nd generation Phenom Pro desktop SEM) with backscattered electron detector and 10 kV accelerating voltage was used to analyze the shells. Images were taken at the same distances from the calcein and stress lines as in the case of the Raman measurements to assure comparability of the data.

In addition, stitched SEM images of the ventral margins were used to accurately determine the shell growth advance during the culturing experiments. Growth increment widths were measured with the software Panopea (© Schöne and Peinl). Given the difference in duration of the two phases of the temperature experiment, the measurements were expressed as total growth and instantaneous growth rate (Fig. 3a + b). The latter was calculated using the following equation (Brey et al., 1990; Witbaard et al., 1997):

(3) Instantaneous growth rate = $(\ln (y_t / y_0) / a)$

where y_0 represents the initial shell height, y_t is the final shell height and a is the duration of the experiment. In the case of the food experiment, only the total growth was calculated (Fig. 3c).

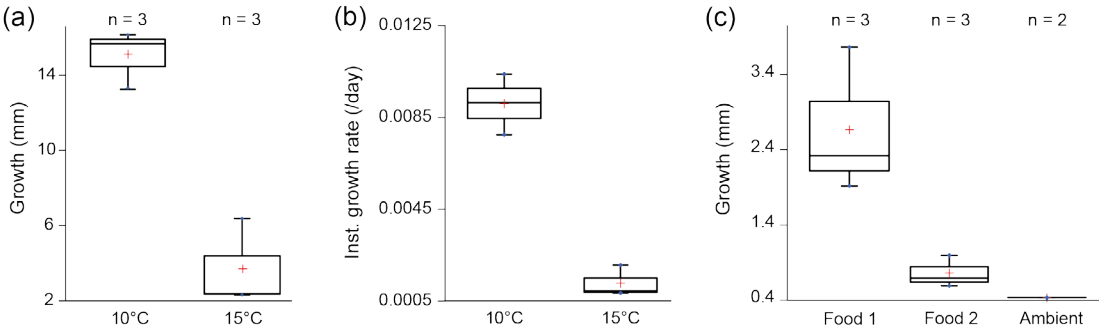

Fig. 3. *Arctica islandica* shell growth under controlled conditions. (a) Total growth and (b) instantaneous growth rate during the temperature experiment. (c) Total growth during the food experiment.

3. Results

3.1 Effect of temperature and diet on *A. islandica* shell growth

When exposed to a water temperature of 10 °C, the shells grew between 11.67 and 14.17 mm during a period of 48 days. During a period of 69 days at 15 °C, the growth ranged between 2.32 and 5.77 mm (Fig. 3a). Instantaneous growth rate showed a decrease between the two experimental phases. At 10 and 15 °C, the average instantaneous growth per day was 0.0091 and 0.0013, respectively (Fig. 3b). The decrease in total growth and growth rate between the two temperatures was statistically significant (t-test, $p < 0.01$).
During the food experiment, shells grew between 0.37 and 3.71 mm with large differences due to the different food types. Growth of specimens exposed to food type 1 ranged between 1.87 to 3.71 mm, whereas those cultured with food type 2 grew between 0.55 to 0.96 mm. Both control specimens added 0.37 mm of shell during the experimental phase (Fig. 3c). ANOVA and Tukey´s HSD post hoc tests showed significant differences between specimens cultured with food type 1 and 2 ($p < 0.05$) and between food type 1 and control shells ($p < 0.05$).

3.2 Effect of temperature on *A. islandica* microstructure

At a water temperature of 10 °C, the area occupied by microstructural units oriented with $R_{v1/Ta}$ higher than 2.5 a.u. (= arbitrary units) ranged between 31.3 and 50.6 % in the oOSL and between 21.3 and 33.5 % in the iOSL. When exposed to 15 °C, values ranged between 25.6 and 48.7 % and between 45.7 and 55.9 % in the oOSL and iOSL, respectively (Fig. 4). Whereas the slight difference of area with Rv1/Ta > 2.5 in the oOSL was not significant between the two water temperatures (t-test, $p = 0.62$), the area with $R_{v1/Ta} > 2.5$ in the iOSL significantly increased at 15 °C (t-test, $p = 0.02$). Under the SEM, no difference was visible between units formed at 10 °C and 15 °C (Fig. 5).

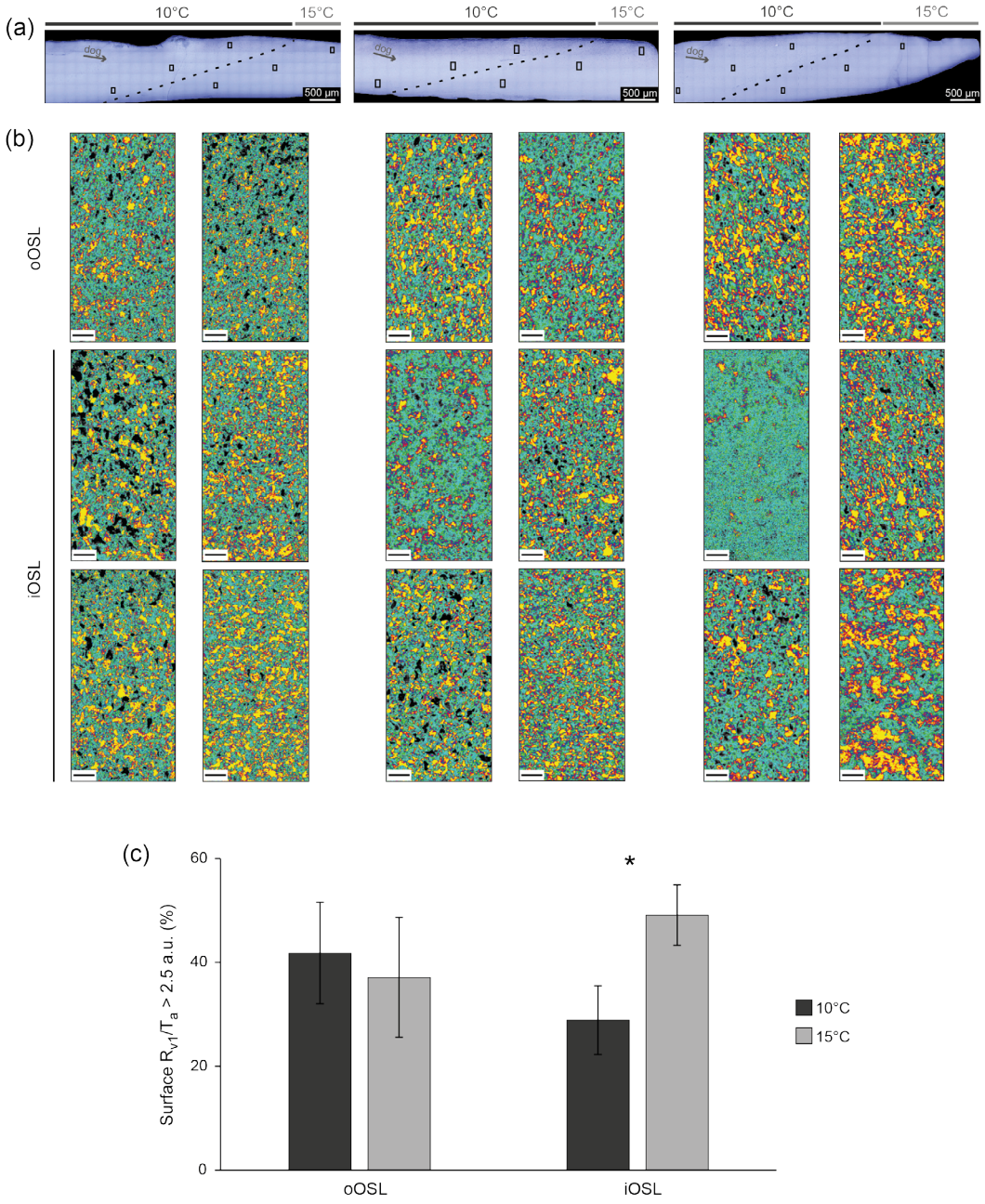

Fig. 4. Effect of temperature increase on biomineral orientation. (a) Position of the Raman maps of the three specimens reared at 10 °C and 15 °C. Dotted lines indicate the location of the calcein marks. dog = direction of growth. (b) Raman spectral maps of $R_{v1/Ta}$. Left images of each column represents shell portion formed at 10 °C, right images represent shell portions formed at 15 °C. First row of pairs refers to oOSL, the other two represent the iOSL. Scale bars = 10 µm. (c) Proportions of biominerals with $R_{v1/Ta}$ > 2.5 a.u. with respect to the total map area. Asterisks indicate significant difference between the orientation of iOSL microstructures formed at 10 and 15°C ($p < 0.05$).

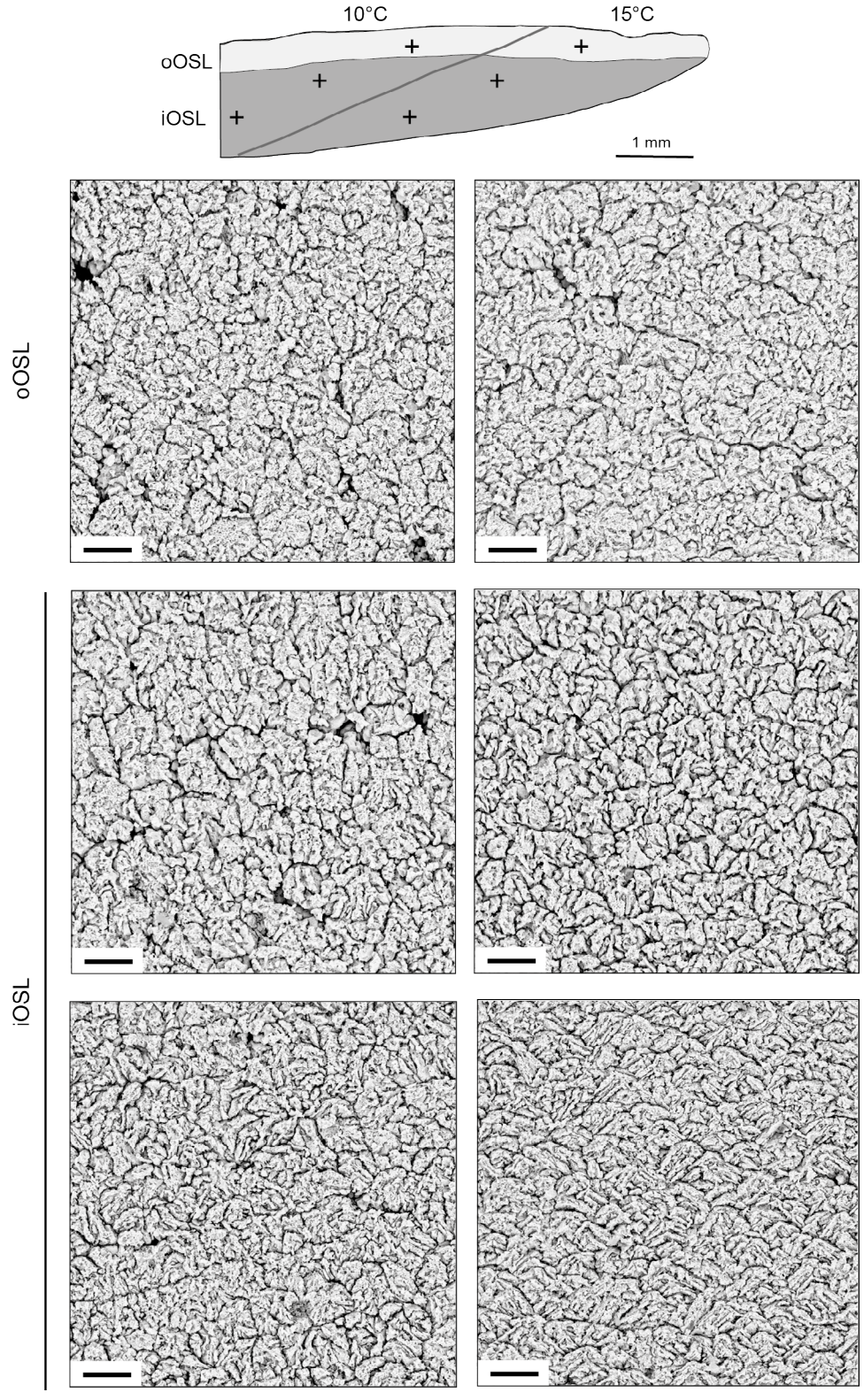

Fig. 5. SEM images of *Arctica islandica* shell microstructures formed at 10 °C (left column) and at 15 °C (right column). The sketch indicates the position of the images 1 mm away from the calcein mark (grey line). The first row of images refers to the oOSL, the other two row refers to the iOSL. Scale bars if not otherwise indicated = 5 µm.

3.3 Effect of food on *A. islandica* microstructure and pigments

In the shells cultured with food type 1, the area occupied by biomineral units oriented with $R_{v1/Ta}$ higher than 2.5 a.u. during the experiment ranged between 24.8 % (oOSL) and 43.0 % (iOSL). In the shell portion deposited before the experiment, the ratio varied between 19.4 % (oOSL) and 36.2 % (iOSL). Although a trend was recognized, these variations were not statistically different (t-tests. OSL: p = 0.43; ISL: p = 0.57; Fig. 6a). On the contrary, in the clams exposed to food type 2, the area occupied by units oriented with $R_{v1/Ta}$ > 2.5 ranged between 11.7 % (oOSL) and 20.4 % (iOSL). Before the experiment, the proportions were higher, i.e., 18.1% (oOSL) and 26.3% (iOSL) (Fig. 6b). As for the other treatment, the difference was not significant (t-tests. oOSL: p = 0.34; iOSL: p = 0.28). In the control shells grown with no extra food supply, the area with $R_{v1/Ta}$ > 2.5 ranged between 24.6 % (oOSL) and 44.8 % (iOSL) during the experiment and 21.2 % (oOSL) and 44.5 % (iOSL) before the experiment (Fig. 6c). Hence, no trend was visible and the two portions did not show significant differences (t-tests. oOSL: p = 0.59; iOSL: p = 0.99). As for the temperature experiment, under the SEM, the microstructure of the shells from the food experiment did not show any change (Fig. 7).

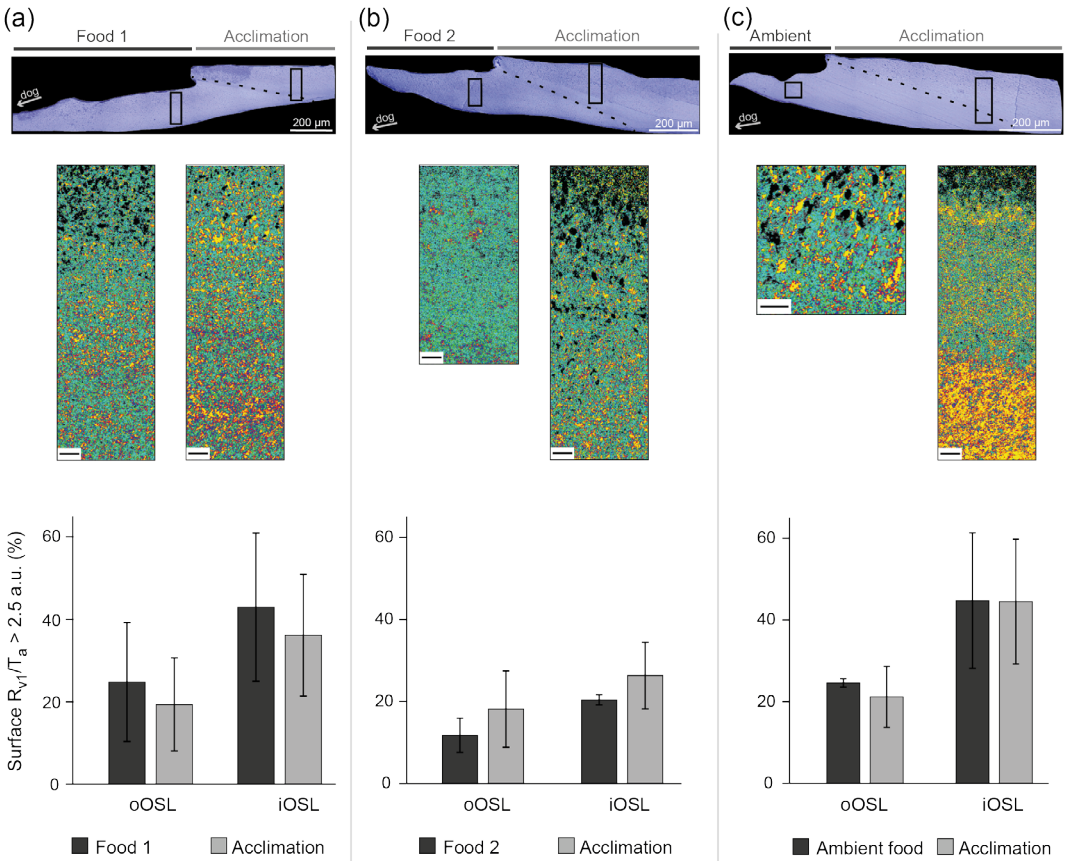

Fig. 6. Effect of different diets based on (a) food type 1, (b) food type 2 and (c) ambient food on biomineral orientation. The optical microscope images indicate the position of the Raman scans. Dotted line marks the start of the experiment. The portion of shell prior the line was formed during the acclimation phase. dog = direction of growth. The Raman spectral maps indicate the ratio $R_{v1/Ta}$ for each data point of the scan. (caption continued on next page)

(caption continued from previous page) For each shell, maps on the left represent shell portions during the experiment, maps on the right represent shell portions formed during the acclimation phase. In the acclimation portion of the sample reared with ambient food, a significant change in the microstructure orientation is visible. The respective area of the Raman map was not considered in further calculations because it was influenced by the emersion and transportation stress at the start of the experiment. Scale bars = 10 µm. The graphs show the proportions of biominerals of oOSL and iOSL with $R_{v1/Ta} > 2.5$ a.u. with respect to the total map area.

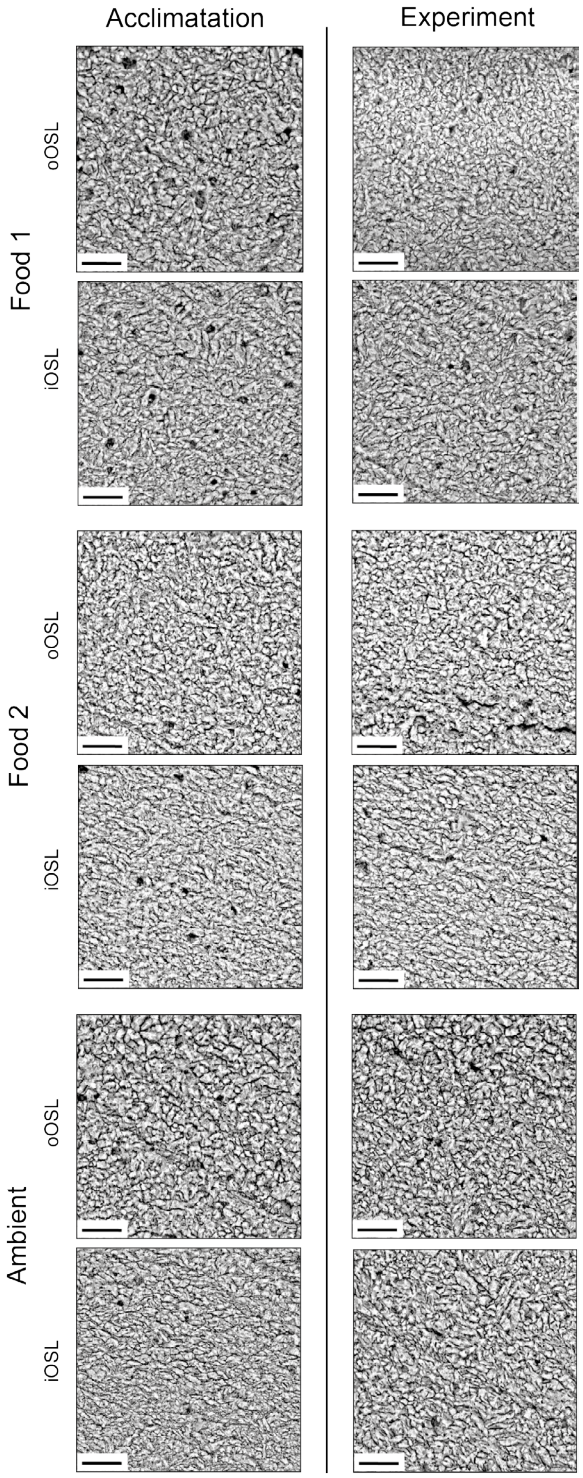

Fig. 7. SEM images of *Arctica islandica* shell microstructures formed during the acclimation phase at AWI (left column) and during the food experiment (right column). Scale bars = 4 µm.

All treatments showed a slightly thicker pigmented layer formed during the experiment than during the acclimation phase (Fig. 8a). During the experiment, clams cultured with food type 1 showed, on average, a thickening by 6.4 %. In the food type 2 specimens, the layer thickness increased by 9.9 %. Control shells showed an increase of 10.4 % (Fig. 8b). However, none of these differences was statistically significant (t-test. Food type 1: $p = 0.43$; Food type 2: $p = 0.39$; Control: $p = 0.10$). According to the position of the polyene peaks, the number of single carbon bonds in the pigment chain did not change between the acclimation and experimental phase ($N_1 = 10.1 \pm 1.3$ and $N_1 = 10.0 \pm 0.9$, respectively). Likely, no significant variation was observed in the number of double carbon bonds ($N_4 = 10.5 \pm 0.2$ and $N_4 = 10.4 \pm 0.3$, respectively; Table 2).

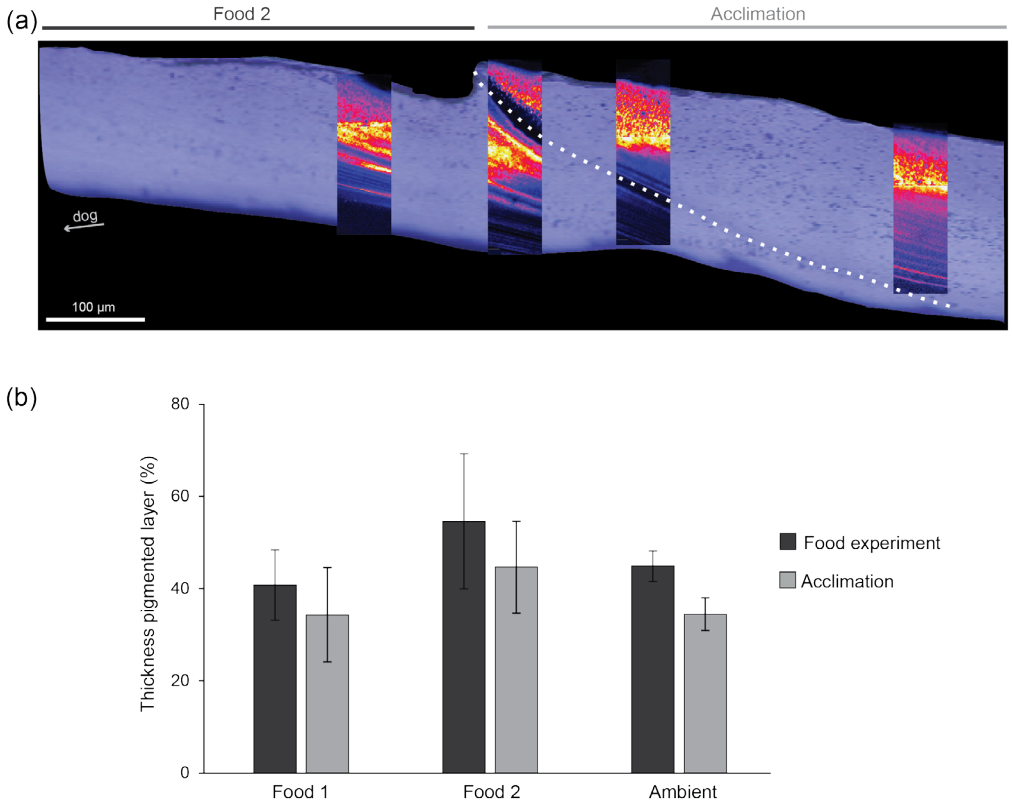

Fig. 8. Effects of diet on shell pigment distribution. (a) Raman spectral maps of the 1524 cm^{-1} band representing the distribution of the polyenes in the shell cultured with food type 2. Dotted line marks the start of the experiment. dog = direction of growth. (b) The graph shows the thickness of the pigmented layer over the whole shell thickness before and during the food experiments.

Table 2. Details of the pigment composition of the *Arctica islandica* shells used in the food experiment. The position of the major polyene peaks R_1 and R_4 in the Raman spectrum is indicated together with the number of single and double carbon bonds of the pigment molecular chain (N_1 and N_4). Each shell was analyzed in the portions formed before and during the experimental phase.

Sample ID	Shell portion	R_1 (cm^{-1})	R_4 (cm^{-1})	N_1	N_4
S12	Acclimation	1130.9	1515.2	9.7	10.8
	Food 1	1121.4	1515.3	12.1	10.7
S14	Acclimation	1133.2	1519.4	9.3	10.2
	Food 1	1132.2	1518.6	9.5	10.3
S15	Acclimation	1129.5	1516.5	10.0	10.6
	Food 1	1132.1	1519.8	9.5	10.1
G11	Acclimation	1132.6	1518.4	9.4	10.3
	Food 2	1129.5	1517.0	10.0	10.5
G12	Acclimation	1131.7	1518.7	9.6	10.3
	Food 2	1132.1	1518.2	9.5	10.4
G15	Acclimation	1132.4	1519.5	9.4	10.2
	Food 2	1128.0	1520.9	10.3	10.0
N13	Acclimation	1130.2	1515.6	9.9	10.7
	Ambient food	1131.4	1514.1	9.6	10.9
N15	Acclimation	1117.9	1516.0	13.3	10.6
	Ambient food	1130.7	1517.0	9.8	10.5
Average		1129.7 ± 4.2	1517.5 ± 2.0	10.1 ± 1.1	10.4 ± 0.3

4. Discussion

According to the results, variations of both food type and water temperature can influence the shell production rate of *A. islandica*. However, the shell microstructure and pigmentationreact differently to these two environmental variables. Whereas changes of the dietary conditions do not affect the shell architecture and pigment composition, the crystallographic orientation of the biomineral units responds to temperature fluctuations.

4.1 Environmental influence on shell microstructure

The environmental conditions experienced by mollusks during the process of biomineralization appear to influence shell organization (Carter, 1980). Among the different environmental variables, water temperature is the most studied driving force of structural changes of the shell. For instance, shell mineralogy can vary depending on water temperature (Carter, 1980). According to the thermal potentiation hypothesis, nucleation and growth of calcitic structural

units is favored at low temperatures by kinetic factors (Carter et al., 1998). As a consequence, bivalve species living in cold water environments exhibit additional or thicker calcitic layers compared to the corresponding species from warm waters (Lowenstam, 1954; Taylor and Kennedy, 1969). Changes in the calcium carbonate polymorph also affect the type of microstructures (Milano et al., 2016). However, architectural variations often occur without mineralogical impact (Carter, 1980).

The present results indicate that temperature induces a change in the crystallographic orientation of the biomineral units of *A. islandica*. Although water temperature was previously shown to have an impact on microstructure formation, the attention has been mainly addressed to the effects on the morphometric characteristics (e.g. size and shape) or on the type of microstructure. Size and elongation of prismatic structural units of *Cerastoderma edule* were observed to be positively correlated with the growing season temperatures (Milano et al., 2015). Likely, low temperatures induced the formation of small nacre tablets in *Geukensia demissa* (Lutz, 1984). Seasonal changes of the microstructural type were reported in the freshwater bivalve *Corbicula fluminea* (Prezant and Tan Tiu, 1986; Tan Tiu and Prezant, 1989). During the warm months, crossed acicular structure was produced, whereas simple crossed-lamellae were formed during the winter period. So far, variations of the crystallographic properties of bivalve biominerals have been exclusively investigated as a response to hypercapnic (acidified) conditions. *Mytilus galloprovincialis* and *Mytilus edulis* showed a significant change in the orientation of the prisms forming shell calcitic layer when subjected to hypercapnia (Hahn et al., 2012; Fitzer et al., 2014). Altered crystallographic organization may derive from the animal exposure to suboptimal conditions. These findings together with the present results suggest that thermal- and hypercapnic-induced stress are likely to affect the ability of the bivalves to preserve the orientation of their microstructural units (Fitzer et al., 2015).

Different food sources do not significantly influence the orientation of the biomineral units or the composition and distribution of pigments in shells of *A. islandica*. In previous studies, the relationship between microstructure and diet was virtually overlooked resulting in a lack of data in the literature. As suggested by Hedegaard et al., (2006), however, the type of polyenes is influenced by food. The ingestion of pigment-enriched microalgae potentially leads to an accumulation of pigments in mollusk tissues and the shell (Soldatov et al., 2013). On the other hand, it has been argued that polyenes do not generate from food sources like other pigments (i.e., carotenoids), but they are locally synthesized (Karampelas et al., 2009). In accordance to Stemmer and Nehrke (2014), the results presented here support the view that the specific diets on which the animals rely on do not influence shell pigment composition. The chemical characteristics of the polyenes are likely to be specie-specific and independent from the habitats.

4.2 Confocal Raman microscopy as tool for microstructural analysis

From a methodological perspective, the present study represents an innovative approach in the investigation of shell microstructural organization. Electron backscatter diffraction (EBSD) has been previously used to determine the crystallographic orientation of gastropod (Fryda et al., 2009; Pérez-Huerta et al., 2011) and bivalve microstructural units (Checa et al., 2006; Frenzel et al., 2012; Karney et al., 2012). Whereas, CRM on mollusk shells is generally applied within studies on taphonomic mineralogical alteration and pigment identification (Stemmer and Nehrke, 2014; Beierlein et al., 2015). Both techniques provide considerably high spatially resolved analysis up to 250 nm, allowing the identification of individual structural units at µm- and nm-scale (Cusack et al., 2008; Karney et al., 2012). CRM offers important advantages supporting a broader application of this methodology in the biomineralization research field. For instance, samples do not require any pre-treatment. Unlike EBSD, there is no need of preparing thin-sections (~ 150 µm thick) or etching the shell surface (Griesshaber et al., 2010; Hahn et al., 2012). Therefore, further structural and geochemical analyses can be easily performed on the same sections (Nehrke et al., 2012). In addition, the size of CRM scans can be remarkably large (~ 7-8 mm^2) without compromising the achievable resolution. By overlapping adjacent scans, it is possible to produce stitched scans allowing to further increase the region of interest on the shell surface.

SEM has previously been demonstrated to provide a convenient approach for the identification of individual structural units and the quantification of potential changes occurring within them (Milano et al., 2015, 2016b). However, SEM exclusively provides information about the morphometric characteristics of the microstructural units. As highlighted by the present study, to achieve an exhaustive examination, it is suggested to combine SEM with techniques assessing crystallographic properties of the biomaterials. For instance, our results show that the effect of water temperature is detectable in crystallographic orientation but not in morphometric features of the biomineral units.

4.3 Environmental influence on shell growth

Numerous previous studies demonstrated that growth rate of *A. islandica* - and many other bivalves - is linked to environmental variables (e.g., Witbaard et al., 1997, 1999; Schöne et al., 2004; Butler et al., 2010). However, the relative importance of the main factors, temperature and food supply/quality driving shell formation are still not well understood. Positive correlations between shell growth and water temperature have been identified (i.e., Schöne et al., 2005; Wanamaker et al., 2008; Marali et al., 2015), but the relationship between shell growth and environment is more complex (Marchitto et al., 2010; Stott et al., 2010; Schöne et al., 2013) and likely dependent on the synergic effect of food availability and water temperature (Butler et al., 2013; Lohmann and Schöne, 2013). Tank experiments

were run in order to precisely identify the role of these two parameters of shell growth of *A. islandica* (Witbaard et al., 1997; Hiebenthal et al., 2012). A tenfold increase in instantaneous growth rate was observed between 1 and 12 °C, with the greatest variation occurring below 6 °C (Witbaard et al., 1997). On the contrary, a temperature increase between 4 and 16 °C was shown to produce a slowdown of shell production (Hiebenthal et al., 2012). Our results are in agreement with the latter study and show a decrease in the instantaneous growth rate between 10 and 15 °C. High temperatures are often associated with an increase of free radical production (Abele et al., 2002). A large amount of energy then has to be allocated to limit oxidative cellular damage (Abele and Puntarulo, 2004). This translates into a higher accumulation of lipofuscin and slower shell production rate (Hiebenthal et al., 2013). The contrasting results of previous studies may be explained by individual differences in the tolerance toward temperature change (Marchitto et al., 2000).

Along with water temperature, food availability was also shown to influence *A. islandica* shell growth (Witbaard et al., 1997). At high algal cell densities, the siphon activity increased. This, in turn, was positively correlated to shell growth. Previous experiments used different combinations of algae such as *Isochrysis galbana* and *Dunaliella marina* (Witbaard et al., 1997), or *Nannochloropsis oculata*, *Phaeodactylum tricornutum* and *Chlorella* sp. (Hiebenthal et al., 2012) to grow the clams. However, there are still uncertainties about the composition of the primary food source for this species (Butler et al., 2010). Even though it is challenging to determine the preferred algal species, our results show that the use of a mixture of different algal species results in significantly faster shell growth than the used of just one algal species. In the natural environment, suspension feeders such as *A. islandica* preferentially ingest certain particle sizes (Rubenstein and Koehl, 1977; Jorgensen, 1996; Baker et al., 1998). The exposure to a limited algal size range, as in the case of food type 2, may affect shell growth. Furthermore, multispecific solutions contain a higher variability of biochemical components that better meet the nutritional requirements of the animal (Widdows, 1991). Our results are in good agreement with previous findings. For instance, it has been shown by Strömgren and Cary (1984) that *Mytilus edulis* shell growth increased as a result of a diet based on three different algal species. Furthermore, Epifanio (1979) tested the differences on the growth of *Crasssostrea virginica* and *Mercenaria mercenaria* of a mixed diet composed by *Isochrysis galbana* and *Thalassiosira pseudonana* and diets consisting of the single species. Faster growth was measured in the mixed diet treatment, indicating a synergic effect of the relative food composition (Epifanio, 1979). Likely, *Mytilus edulis* grew faster when reared with different types of mixed diets as opposed to monospecific diets (Galley et al., 2010).

5. Conclusions

Arctica islandica shell growth and biomineral orientation vary with changes in water temperature. However, exposure to different food sources affect shell deposition rate but do not the organization of the biomineral units. Given the exclusive sensitivity to one environmental variable, the orientation of biomineral units may represent a promising new temperature proxy for paleoenvironmental reconstructions. However, additional studies are needed to further explore the subject. In particular, intra-individual variability influence on the results needs to be assessed. In the present study, a variation in the orientation between individuals was well visible and the risks associated have to be taken in account when considering further application of the possible proxy. Furthermore, the effect of other environmental variables such as salinity needs to be tested.

The innovative application of CRM for microstructural orientation and proxy development proved that the technique has large potential in this research direction. More studies are needed to validate its suitability in paleoclimatology experimental works.

6. Acknowledgements

The authors acknowledge the research staff at the Darling Marine Center in Walpole, Maine, for conducting the temperature experiment. Funding for this study was kindly provided by the EU within the framework of the Marie Curie International Training Network ARAMACC (604802).

7. References

Abele, D., Heise, K., Pörtner, H. O. and Puntarulo, S.: Temperature-dependence of mitochondrial function and production of reactive oxygen species in the intertidal mud clam *Mya arenaria*, J. Exp. Biol., 205, 1831-1841, doi:10.1016/j.ecolind.2011.04.007, 2002.

Abele, D. and Puntarulo, S.: Formation of reactive species and induction of antioxidant defence systems in polar and temperate marine invertebrates and fish, Comp. Biochem. Physiol. Part A, 138(4), 405-415, doi:10.1016/j.cbpb.2004.05.013, 2004.

Aizenberg, J., Weaver, J. C., Thanawala, M. S., Sundar, V. C., Morse, D. E. and Fratzl, P.: Skeleton of *Euplectella* sp.: structural hierarchy from the nanoscale to the macroscale, Science, 309(5732), 275-278, doi:10.1126/science.1112255, 2005.

Andrus, C. F. T.: Shell midden sclerochronology, Quat. Sci. Rev., 30(21-22), 2892-2905, doi:10.1016/j.quascirev.2011.07.016, 2011.

Baker, S. M., Levinton, J. S., Kurdziel, J. P. and Shumway, S. E.: Selective feeding and biodeposition by zebra mussels and their relation to changes in phytoplankton composition and seston load, J. Shellfish Res., 17, 1207-1213, 1998.

Beierlein, L., Nehkre, G. and Brey, T.: Confocal Raman microscopy in sclerochronology: A powerful tool to visualize environmental information in recent and fossil biogenic archives, Geochemistry Geophys. Geosystems, 16, 325-335, doi:10.1002/2014GC005684.Key, 2015.

Berman, A., Hanson, J., Leiserowitz, L., Koetzle, T. F., Weiner, S. and Addadi, L.: Biological control of crystal texture: a widespread strategy for adapting crystal properties to function, Science, 259(5096), 776-779, doi:10.1126/science.259.5096.776, 1993.

Black, B. A., Gillespie, D. C., MacLellan, S. E. and Hand, C. M.: Establishing highly accurate production-age data using the tree-ring technique of crossdating: a case study for Pacific geoduck (*Panopea abrupta*), Can. J. Fish. Aquat. Sci., 65, 2572-2578, doi:10.1139/F08-158, 2008.

Bøggild, O. B.: The shell structure of the mollusks, in Det Kongelige Danske Videnskabernes Selskabs Skrifter, Natruvidenskabelig og Mathematisk, pp. 231-326, Afdeling., 1930.

Brey, T., Arntz, W. E., Pauly, D. and Rumohr, H.: *Arctica* (*Cyprina*) *islandica* in Kiel Bay (Western Baltic): growth, production and ecological significance, J. Exp. Mar. Bio. Ecol., 136(3), 217-235, doi:10.1016/0022-0981(90)90162-6, 1990.

Butler, P. G., Richardson, C. A., Scourse, J. D., Wanamaker, A. D. Jr, Shammon, T. M. and Bennell, J. D.: Marine climate in the Irish Sea: analysis of a 489-year marine master chronology derived from growth increments in the shell of the clam *Arctica islandica*, Quat. Sci. Rev., 29(13-14), 1614-1632, doi:10.1016/j.quascirev.2009.07.010, 2010.

Butler, P. G., Wanamaker, A. D. Jr, Scourse, J. D., Richardson, C. A. and Reynolds, D. J.: Variability of marine climate on the North Icelandic Shelf in a 1357-year proxy archive based on growth increments in the bivalve *Arctica islandica*, Palaeogeogr. Palaeoclimatol. Palaeoecol., 373, 141-151, doi:10.1016/j.palaeo.2012.01.016, 2013.

Carter, J. G.: Environmental and biological controls of bivalve shell mineralogy and microstructure, in Skeletal Growth of Aquatic Organisms: Biological Records of Environmental Change (Topics in Geobiology), edited by D. C. Rhoads and R. A. Lutz, pp. 69-113, Plenum, N. Y, 1980.

Carter, J. G. and Clark, G. R. I.: Classification and phylogenetic significance of molluscan shell microstructure, in Mollusks, Notes for a Short Course, edited by T. W. Broadhead, pp. 50-71., 1985.

Carter, J. G., Barrera, E. and Tevesz, M. T. S.: Thermal potentiation and mineralogical evolution in the Bivalvia (Mollusca), J. Paleontol., 72(6), 991-1010, 1998.

Carter, J. G., Harries, P. J., Malchus, N., Sartori, A. F., Anderson, L. C., Bieler, R., Bogan, A. E., Coan, E. V., Cope, J. C. W., Cragg, S. M., Garcia-March, J. R., Hylleberg, J., Kelley, P., Kleemann, K., Kriz, J., McRoberts, C., Mikkelsen, P. M., Pojeta, J. J., Temkin, I., Yancey, T. and Zieritz, A.: Illustrated glossary of the bivalvia, Treatise Online, 1(48), 2012.

Checa, A. G., Okamoto, T. and Ramírez, J.: Organization pattern of nacre in Pteriidae (Bivalvia: Mollusca) explained by crystal competition., Proc. Biol. Sci., 273(1592), 1329-37, doi:10.1098/rspb.2005.3460, 2006.

Currey, J. D.: The design of mineralised hard tissues for their mechanical functions, J. Exp. Biol., 202, 3285-3294, 1999.

Cusack, M., Parkinson, D., Freer, A., Pérez-Huerta, A., Fallick, A. E. and Curry, G. B.: Oxygen isotope composition in *Modiolus modiolus* aragonite in the context of biological and crystallographic control, Mineral. Mag., 72(2), 569-577, doi:10.1180/minmag.2008.072.2.569, 2008.

Dauphin, Y., Cuif, J. P., Doucet, J., Salomé, M., Susini, J. and Willams, C. T.: In situ chemical speciation of sulfur in calcitic biominerals and the simple prism concept, J. Struct. Biol., 142(2), 272-280, doi:10.1016/S1047-8477(03)00054-6, 2003.

Deith, M. R.: The composition of tidally deposited growth lines in the shell of the edible cockle, *Cerastoderma edule*, J. Mar. Biol. Assoc. United Kingdom, 65(3), 573-581, 1985.

Dunca, E., Mutvei, H., Göransson, P., Mörth, C.-M., Schöne, B. R., Whitehouse, M. J., Elfman, M. and Baden, S. P.: Using ocean quahog (*Arctica islandica*) shells to reconstruct palaeoenvironment in Öresund, Kattegat and Skagerrak, Sweden, Int. J. Earth Sci., 98(1), 3-17, doi:10.1007/s00531-008-0348-6, 2009.

Epifanio, C. E.: Growth in bivalve molluscs: nutritional effects of two or more species of algae in diets fed to the American oyster *Crassostrea virginica* (Gmelin) and the hard clam *Mercenaria mercenaria* (L.), Aquaculture, 18, 1-12, 1979.

Epstein, S., Buchbaum, R., Lowenstam, H. A. and Urey, H. C.: Revised carbonate-water isotopic temperature scale. Bull. Geol. Soc. Am., 64, 1315-1326, 1953.

Fitzer, S. C., Cusack, M., Phoenix, V. R. and Kamenos, N. A.: Ocean acidification reduces the crystallographic control in juvenile mussel shells, J. Struct. Biol., 188, 39-45, doi:10.1016/j.jsb.2014.08.007, 2014.

Fitzer, S. C., Zhu, W., Tanner, K. E., Phoenix, V. R., Nicholas, A. K. and Cusack, M.: Ocean acidification alters the material properties of *Mytilus edulis* shells, J. R. Soc. Interface, 12(103), doi:10.1098/rsif.2014.1227Published, 2015.

Frenzel, M., Harrison, R. J. and Harper, E. M.: Nanostructure and crystallography of aberrant columnar vaterite in *Corbicula fluminea* (Mollusca), J. Struct. Biol., 178(1), 8-18, doi:10.1016/j.jsb.2012.02.005, 2012.

Fryda, J., Bandel, K. and Frydova, B.: Crystallographic texture of Late Triassic gastropod nacre: Evidence of long-term stability of the mechanism controlling its formation, Bull. Geosci., 84(4), 745-754, doi:10.3140/bull.geosci.1169, 2009.

Galley, T. H., Batista, F. M., Braithwaite, R., King, J. and Beaumont, A. R.: Optimisation of larval culture of the mussel *Mytilus edulis* (L.), Aquac. Int., 18(3), 315-325, doi:10.1007/s10499-009-9245-7, 2010.

Gillikin, D. P., De Ridder, F., Ulens, H., Elskens, M., Keppens, E., Baeyens, W. and Dehairs, F.: Assessing the reproducibility and reliability of estuarine bivalve shells (*Saxidomus giganteus*) for sea surface temperature reconstruction: Implications for paleoclimate studies, Palaeogeogr. Palaeoclimatol. Palaeoecol., 228(1-2), 70-85, doi:10.1016/j.palaeo.2005.03.047, 2005.

Gordon, J. and Carriker, M. R.: Growth lines in a bivalve mollusk: subdaily patterns and dissolution of the shell, Science, 202, 519-521, doi:10.1126/science.202.4367.519, 1978.

Griesshaber, E., Neuser, R. D. and Schmahl, W. W.: The application of EBSD analysis to biomaterials : microstructural and crystallographic texture variations in marine carbonate shells, Semin Soc Esp Miner., 7, 22-34, 2010.

Grossman, E. L. and Ku, T.: Oxygen and carbon isotope fractionation in biogenic aragonite: Temperature effects, Chem. Geol., 59, 59-74, 1986.

Hahn, S., Rodolfo-Metalpa, R., Griesshaber, E., Schmahl, W. W., Buhl, D., Hall-Spencer, J. M., Baggini, C., Fehr, K. T. and Immenhauser, A.: Marine bivalve shell geochemistry and ultrastructure from modern low pH environments: environmental effect versus experimental bias, Biogeosciences, 9, 1897-1914, doi:10.5194/bg-9-1897-2012, 2012.

Hedegaard, C., Bardeau, J. F. and Chateigner, D.: Molluscan shell pigments: An in situ resonance Raman study, J. Molluscan Stud., 72(2), 157-162, doi:10.1093/mollus/eyi062, 2006.

Hiebenthal, C., Philipp, E., Eisenhauer, A. and Wahl, M.: Interactive effects of temperature and salinity on shell formation and general condition in Baltic Sea *Mytilus edulis* and *Arctica islandica*, Aquat. Biol., 14(3), 289-298, doi:10.3354/ab00405, 2012.

Hiebenthal, C., Philipp, E. E. R., Eisenhauer, A. and Wahl, M.: Effects of seawater pCO_2 and temperature on shell growth, shell stability, condition and cellular stress of Western Baltic Sea *Mytilus edulis* (L.) and *Arctica islandica* (L.), Mar. Biol., 160, 2073-2087, doi:10.1007/s00227-012-2080-9, 2013.

Hopkins, J. B. and Farrow, L. A.: Raman microprobe determination of local crystal orientation, J. Appl. Phys., 59(4), 1103-1110, doi:10.1063/1.336547, 1985.

Jones, D. S.: Sclerochronology: Shell record of the molluscan shell, Am. Sci., 71(4), 384-391, 1983.

Jorgensen, C. B.: Bivalve filter feeding revisited, Mar. Ecol. Prog. Ser., 142(1-3), 287-302, doi:10.3354/meps142287, 1996.

Karampelas, S., Fritsch, E., Mevellec, J. Y., Sklavounos, S. and Soldatos, T.: Role of polyenes in the coloration of cultured freshwater pearls, Eur. J. Mineral., 21(1), 85-97, doi:10.1127/0935-1221/2009/0021-1897, 2009.

Karney, G. B., Butler, P. G., Speller, S., Scourse, J. D., Richardson, C. A., Schröder, M., Hughes, G. M., Czernuszka, J. T. and Grovenor, C. R. M.: Characterizing the microstructure of *Arctica islandica* shells using NanoSIMS and EBSD, Geochemistry, Geophys. Geosystems, 13(4), doi:10.1029/2011GC003961, 2012.

Lohmann, G. and Schöne, B. R.: Climate signatures on decadal to interdecadal time scales as obtained from mollusk shells (*Arctica islandica*) from Iceland, Palaeogeogr. Palaeoclimatol. Palaeoecol., 373, 152-162, doi:10.1016/j.palaeo.2012.08.006, 2013.

Lowenstam, H. A.: Factors affecting the aragonite: calcite ratios in carbonate-secreting marine organisms, J. Geol., 62(3), 284-322, 1954.

Lowenstam, H. A. and Weiner, S.: On biomineralization, Oxford University Press, New York., 1989, pp.324.

Lutz, R. A.: Paleoecological implications of environmentally-controlled variation in molluscan shell microstructure, Geobios, 17, 93-99, doi:10.1016/S0016-6995(84)80161-8, 1984.

Marali, S. and Schöne, B. R.: Oceanographic control on shell growth of *Arctica islandica* (Bivalvia) in surface waters of Northeast Iceland - Implications for paleoclimate reconstructions, Palaeogeogr. Palaeoclimatol. Palaeoecol., 420, 138-149, doi:10.1016/j.palaeo.2014.12.016, 2015.

Marchitto, T. M., Jones, G. A., Goodfriend, G. A. and Weidman, C. R.: Precise temporal correlation of Holocene mollusk shells using sclerochronology, Quat. Res., 53, 236-246, doi:10.1006/qres.1999.2107, 2000.

Merkel, C., Griesshaber, E., Kelm, K., Neuser, R., Jordan, G., Logan, A., Mader, W. and Schmahl, W. W.: Micromechanical properties and structural characterization of modern inarticulated brachiopod shells, J. Geophys. Res., 112(G02008), doi:10.1029/2006JG000253, 2007.

Milano, S., Schöne, B. R. and Witbaard, R.: Changes of shell microstructural characteristics of *Cerastoderma edule* (Bivalvia) - A novel proxy for water temperature, Palaeogeogr. Palaeoclimatol. Palaeoecol., doi:10.1016/j.palaeo.2015.09.051, 2015.

Milano, S., Prendergast, A. L. and Schöne, B. R.: Effects of cooking on mollusk shell structure and chemistry: Implications for archeology and paleoenvironmental reconstruction, J. Archaeol. Sci. Reports, 7, 14-26, doi: 10.1016/j.jasrep.2016.03.045, 2016.

Milano, S., Schöne, B. R., Wang, S. and Müller, W. E.: Impact of high pCO2 on shell structure of the bivalve *Cerastoderma edule*, Mar. Environ. Res., 119, 144-155, doi:10.1016/j.marenvres.2016.06.002, 2016b.

Mook, W.: Paleotemperatures and chlorinities from stable carbon and oxygen isotopes in shell carbonate, Palaeogeogr. Palaeoclimatol. Palaeoecol., 9(4), 245-263, doi:10.1016/0031-0182(71)90002-2, 1971.

Nehrke, G. and Nouet, J.: Confocal Raman microscope mapping as a tool to describe different mineral and organic phases at high spatial resolution within marine biogenic carbonates: case study on *Nerita undata* (Gastropoda, Neritopsina), Biogeosciences, 8, 3761-3769, doi:10.5194/bg-8-3761-2011, 2011.

Nishida, K., Ishimura, T., Suzuki, A. and Sasaki, T.: Seasonal changes in the shell microstructure of the bloody clam, *Scapharca broughtonii* (Mollusca: Bivalvia: Arcidae), Palaeogeogr. Palaeoclimatol. Palaeoecol., 363-364, 99-108, doi:10.1016/j.palaeo.2012.08.017, 2012.

Nudelman, F., Gotliv, B. A., Addadi, L. and Weiner, S.: Mollusk shell formation: mapping the distribution of organic matrix components underlying a single aragonitic tablet in nacre, J. Struct. Biol., 153, 176-187, doi:10.1016/j.jsb.2005.09.009, 2006.

Pérez-Huerta, A., Dauphin, Y., Cuif, J. P. and Cusack, M.: High resolution electron backscatter diffraction (EBSD) data from calcite biominerals in recent gastropod shells, Micron, 42(3), 246-51, doi:10.1016/j.micron.2010.11.003, 2011.

Pérez-Huerta, A., Etayo-Cadavid, M. F., Andrus, C. F. T., Jeffries, T. E., Watkins, C., Street, S. C. and Sandweiss, D. H.: El Niño impact on mollusk biomineralization-implications for trace element proxy reconstructions and the paleo-archeological record. PLoS One, 8(2), e54274, doi:10.1371/journal.pone.0054274, 2013.

Prezant, R. S. and Tan Tiu, A.: Spiral crossed-lamellar shell growth in *Corbicula* (Mollusca: Bivalvia), Trans. Am. Microsc. Soc., 105(4), 338-347, 1986.

Richardson, C. A.: Molluscs as archives of environmental change, Oceanogr. Mar. Biol. an Annu. Rev., 39, 103-164, 2001.

Rodríguez-Navarro, A. B., CabraldeMelo, C., Batista, N., Morimoto, N., Alvarez-Lloret, P., Ortega-Huertas, M., Fuenzalida, V. M., Arias, J. I., Wiff, J. P. and Arias, J. L.: Microstructure and crystallographic-texture of giant barnacle (*Austromegabalanus psittacus*) shell, J. Struct. Biol., 156, 355-362, doi:10.1016/j.jsb.2006.04.009, 2006.

Ropes, J. W., Jones, D. S., Murawski, S. A., Serchuk, F. M. and Jearld, A.: Documentation of annual growth lines in ocean quahogs, Artica islandica Linne, Fish. Bull., 82(1), 1-19, 1984.

Rubenstein, D. I. and Koehl, M. A. R.: The mechanisms of filter feeding: some theoretical considerations, Am. Nat., 111, 981-994, 1977.

Schaffer, H. E., Chance, R. R., Silbey, R. J., Knoll, K. and Schrock, R. R.: Conjugation length dependence of Raman scattering in a series of linear polyenes: Implications for polyacetylene, J. Chem. Phys., 94(6), 4161, doi:10.1063/1.460649, 1991.

Schöne, B. R.: The curse of physiology—challenges and opportunities in the interpretation of geochemical data from mollusk shells, Geo-Marine Lett., 28, 269-285, doi:10.1007/s00367-008-0114-6, 2008.

Schöne, B. R.: *Arctica islandica* (Bivalvia): a unique paleoenvironmental archive of the northern North Atlantic Ocean, Glob. Planet. Change, 111, 199-225, doi:10.1016/j.gloplacha.2013.09.013, 2013.

Schöne, B. R. and Surge, D. M.: Part N , revised , volume 1 , chapter 14 : bivalve sclerochronology and geochemistry, Treatise Online, 1(46), 1-24, 2012.

Schöne, B. R. and Gillikin, D. P.: Unraveling environmental histories from skeletal diaries — Advances in sclerochronology, Palaeogeogr. Palaeoclimatol. Palaeoecol., 373, 1-5, doi:10.1016/j.palaeo.2012.11.026, 2013.

Schöne, B. R., Freyre Castro, A. D., Fiebig, J., Houk, S. D., Oschmann, W. and Kröncke, I.: Sea surface water temperatures over the period 1884-1983 reconstructed from oxygen isotope ratios of a bivalve mollusk shell (*Arctica islandica*, southern North Sea), Palaeogeogr. Palaeoclimatol. Palaeoecol., 212, 215-232, doi:10.1016/j.palaeo.2004.05.024, 2004.

Schöne, B. R., Fiebig, J., Pfeiffer, M., Gleß, R., Hickson, J., Johnson, A. L. A., Dreyer, W. and Oschmann, W.: Climate records from a bivalved Methuselah (*Arctica islandica*, Mollusca; Iceland), Palaeogeogr. Palaeoclimatol. Palaeoecol., 228(1-2), 130-148, doi:10.1016/j.palaeo.2005.03.049, 2005.

Schöne, B. R., Radermacher, P., Zhang, Z. and Jacob, D. E.: Crystal fabrics and element impurities (Sr/Ca, Mg/Ca, and Ba/Ca) in shells of *Arctica islandica*—Implications for paleoclimate reconstructions, Palaeogeogr. Palaeoclimatol. Palaeoecol., 373, 50-59, doi:10.1016/j.palaeo.2011.05.013, 2013.

Soldatov, A. A., Gostyukhina, O. L., Borodina, A. V. and Golovina, I. V.: Qualitative composition of carotenoids, catalase and superoxide dismutase activities in tissues of bivalve mollusc *Anadara inaequivalvis* (Bruguiere, 1789), J. Evol. Biochem. Physiol., 49(4), 3889-398, doi:10.1134/S0022093013040026, 2013.

Stemmer, K. and Nehrke, G.: The distribution of polyenes in the shell of *Arctica islandica* from North Atlantic localities: a confocal Raman microscopy study, J. Molluscan Stud., 80, 365-370, doi:10.1093/mollus/eyu033, 2014.

Stott, K. J., Austin, W. E. N., Sayer, M. D. J., Weidman, C. R., Cage, A. G. and Wilson, R. J. S.: The potential of *Arctica islandica* growth records to reconstruct coastal climate in north west Scotland, UK, Quat. Sci. Rev., 29(13-14), 1602-1613, doi:10.1016/j.quascirev.2009.06.016, 2010.

Strömgren, T. and Cary, C.: Growth in length of *Mytilus edulis* L. fed on different algal diets, J. Exp. Mar. Bio. Ecol., 76(1), 23-34, doi:10.1016/0022-0981(84)90014-5, 1984.

Tan Tiu, A.: Temporal and spatial variation of shell microstructure of *Polymesoda caroliniana* (Bivalvia: Heterodonta), Am. Malacol. Bull., 6(2), 199-206, 1988.

Tan Tiu, A. and Prezant, R. S.: Temporal variation in microstructure of the inner shell surface of *Corbicula fluminea* (Bivalvia: Heterodonta), Am. Malacol. Bull., 7(1), 65-71, 1989.

Tan Tiu, A. and Prezant, R. S.: Shell microstructural responses of *Geukensia demissa granosissima* (Mollusca: Bivalvia) to continual submergence, Am. Malacol. Bull., 5(2), 173-176, 1987.

Taylor, J.D. and Kennedy, W.J.: The shell structure and mineralogy of *Chama pellucida* inst electron microscope, Veliger 11: 391-398, 1969.

Thompson, I., Jones, D. S. and Dreibelbis, D.: Annual internal growth banding and life history of the ocean quahog *Artica islandica* (Mollusca: Bivalvia), Mar. Biol., 57, 25-34, 1980.

Wanamaker, A. D. Jr, Kreutz, K. J., Schöne, B. R. and Introne, D. S.: Gulf of Maine shells reveal changes in seawater temperature seasonality during the Medieval Climate Anomaly and the Little Ice Age, Palaeogeogr. Palaeoclimatol. Palaeoecol., 302(1), 43-51, doi:10.1016/j.palaeo.2010.06.005, 2011.

Wanamaker, A. D. Jr, Heinemeier, J., Scourse, J. D., Richardson, C. A., Butler, P. G., Eiríksson, J. and Knudsen, K. L.: Very long-lived mollusks confirm 17th century ad tephra-based radiocarbon reservoir ages for North Icelandic shelf waters, Radiocarbon, 50(3), 399-412, 2008.

Weiner, S. and Addadi, L.: Acidic macromolecules of mineralized tissues: the controllers of crystal formation, Trends Biochem. Sci., 16, 252-256, 1991.

Weiner, S. and Addadi, L.: Design strategies in mineralized biological materials, J. Mater. Chem., 7, 689-702, doi:10.1039/a604512j, 1997.

Widdows, J.: Physiological ecology of mussel larvae, Aquaculture, 94(2-3), 147-163, doi:10.1016/0044-8486(91)90115-N, 1991.

Winter, J. E.: Über den Einfluß der Nahrungskonzentration und anderer Faktoren auf Filtrierleistung und Nahrungsausnutzung der Muscheln *Arctica islandica* und *Modiolus modiolus*, Mar. Biol., 4(2), 87-135, doi:10.1007/BF00347037, 1969.

Witbaard, R., Franken, R. and Visser, B.: Growth of juvenile *Arctica islandica* under experimental conditions, Helgolaender Meeresuntersuchungen, 51, 417-431, doi:10.1007/BF02908724, 1997.

Witbaard, R., Duineveld, G. C. A. and de Wilde, P. A. W. J.: Geographical differences in growth rates of *Arctica islandica* (Mollusc: Bivalvia) from the North Sea and adjacent waters, J. Mar. Biol. Assoc. United Kingdom, 79, 907-915, 1999.

Chapter 3 - Summary

The results of this thesis provide new insights into a better understanding of the microstructural organization of mollusk shells and its relationship with the environment. Manuscripts I and IV highlight the potential of using microstructures to reconstruct water temperature. Manuscripts II and IV suggest that the influence of other environmental parameters may be very limited. According to findings reported in manuscript III, changes of microstructures may provide a tool for paleodiet reconstructions.

In manuscript I, a change in the prismatic microstructure of *C. edule* (outermost shell layer) during the growing season was observed. Size and elongation of the prisms increased during summer months (June to August). In order to determine which environmental variables were driving these changes, microstructural data were compared to instrumental records. Salinity, water turbidity and chlorophyll a concentration were found not to be correlated with the variation of prism size and shape. Likely, the relationship with growth rate was negligible. However, microstructural changes were well explained by water temperature fluctuations. Models were developed based on this correlation. The model using both properties, prism size and elongation, successfully reconstructed water temperature with an error of ± 1.7 °C. The sensitivity of the microstructures to water temperature may be explained by the fact that very warm conditions, beyond the species optimum, may induce a decrease in the production of organic matrices. In addition, the precipitation of $CaCO_3$ is promoted at high temperatures by a kinetic effect. This results in the formation of larger units with lower amounts of organic during summer months. The findings indicated that the microstructure of *C. edule* is sensitive to water temperature and may serve as a proxy for temperature.

Manuscript 2 demonstrated that hypercapnia does not have an effect on the formation and organization of prismatic microstructures in *C. edule*. However, acidification has negatively affected shell growth and integrity. In fact, the amount of shell produced and the number of days of growth decreased with increasing CO_2 content. Furthermore, the outermost shell layer of ontogenetically young portions was clearly damaged by dissolution. Although these deteriorations may disrupt shell protective capacity on the long term, the newly formed material displayed a great stability. Prism size and shape did not vary significantly. Likely, shell hardness was not altered. This indicates that prisms of *C. edule* cannot be used as a proxy for water acidification. However, a relevant correlation between microstructure and mechanical properties was found. Large prisms were characterized by low hardness. In fact, organic content decreases with prism size and makes the material more brittle and prone to crack propagation. In conclusion, shell hardness likely serves as a paleotemperature proxy.

The results of manuscript III show that shell material is affected by cooking treatments. Although boiling at 100 °C did not affect *P. turbinatus* shells, cooking temperatures between 300 °C and 700 °C had a significant impact on the material. The overall color shifted to shadings of brown, then grey and finally white. The nacre gradually lost its iridescence, and the outer shell layer became brittle and fell off. Prisms of the outer layer drastically changed their appearance at 300 °C

forming new irregular shaped blocky microstructures. Likely, nacre tablets lost their individual definition to fuse into larger structures. At 300 °C, the outer layer went to recrystallization into calcite and at 500 °C the mineralogy of the whole shell was transformed. Above 300 °C, the oxygen isotopic composition became more negative so that reconstructions overestimated actual temperatures by up to 6.9 °C. These results offered the opportunity for a more accurate selection of the samples used in paleoenvironmental studies. Shells cooked over 300 °C should be avoided. Furthermore, the thermal responses of the material provide a toolkit for reconstructing prehistoric food processing methods.

Manuscript IV showed that water temperature and diet influenced *A. islandica* shell production. Higher water temperatures, monospecific diet and ambient food were related to a significant reduction in shell growth. However, organization at microstructural level did not seem to be affected by the different food sources. Likely, diet did not influence the composition and distribution of the pigments in the shell. On the other hand, the increase in water temperature caused a change of the crystallographic orientation of the homogenous microstructure. These findings suggest that *A. islandica* microstructures can potentially record temperature changes and may serve as novel paleothermometer.

3.1 Future research perspectives

The accuracy and resolution that can be achieved with mollusk shells makes them a powerful tool to infer past environmental conditions. In order to fully exploit their potential, a universally applicable and independent proxies are needed. Future studies should focus on the exploration of shell properties that satisfy the following criteria: (i) sensitivity to environmental fluctuations, (ii) exclusive response to one variable, (iii) independence from physiological processes and ontogeny, (iv) prospect for quantification, (v) identification by using accessible analytical techniques, (vi) broader application to multiple species, fossils and large number of samples.

From a methodological perspective, the effect of the environment on shell production and organization has to be assessed carefully. Tank experiments under controlled conditions represent an excellent opportunity to define the influence of single environmental variable on the shell. To verify the results achieved herein, field studies should be conducted.

Advancing the knowledge on the process of biomineralization is certainly a critical precondition for developing new environmental proxies and better understand those which are challenging to interpret, i.e., affected by vital effects. Given the biomineral complexity, more studies are needed to better understand the organo-mineral relationships and their responses to the environment (Crenshaw, 1972; Samata et al., 1999; Levi-Kalisman et al., 2001). For this reason, it will be important to (i) assess the specific distribution and composition of the organic compounds in the different microstructures and within the same structures and to

(ii) investigate gene regulation, potentially sensitive to changes in the external conditions.

Another critical research question to target in future studies is the relationship between trace elements and microstructures. It has been observed that the mineralogy partly determines the concentration of minor elements incorporated in the crystals (Dauphin et al., 2005; 2007). However, the incorporation of chemical elements into the carbonate crystals and its relationship with the surrounding environment is still not completely understood (Schöne, 2008; Schöne et al., 2013; Zhao et al., 2015). In particular, attention should be addressed to (i) examine active and passive transportation of minor elements (i.e., Sr^{2+} and Mg^{2+}) into the shell, (ii) investigate the role of crystallography on their incorporation into the crystal lattice, (iii) explore and quantify potential changes occurring simultaneously in trace element concentrations and microstructural organization.

Since most of the previous studies on microstructure formation focused on nacre (Checa and Rodriguez-Navarro, 2001; Nudelman et al., 2006; Cartwright and Checa, 2007), there is the need to broaden the research to other types of microstructures. For instance, prismatic and crossed-lamellar are among the most common structures found in bivalves and gastropods, but the mechanisms of their formation are mostly unexplored. Furthermore, due to the use of extremely long-lived species in paleoclimatic reconstructions, particular attention should be paid to unveil to which extent physiology affects microstructure organization.

3.2 References

Cartwright, J.H.E., Checa, A.G., 2007. The dynamics of nacre self-assembly. J. R. Soc. Interface 4, 491-504.

Checa, A.G., Rodríguez-Navarro, A., 2001. Geometrical and crystallographic constraints determine the self-organization of shell microstructures in Unionidae (Bivalvia: Mollusca). Proc. R. Soc. B Biol. Sci. 268, 771-778.

Crenshaw, M.A., 1972. The soluble matrix from *Mercenaria mercenaria* shell. Biomineralization, 6, pp.6-11.

Dauphin, Y., Cuif, J.P., Salomé, M., Susini, J., 2005. Speciation and distribution of sulfur in a mollusk shell as revealed by in situ maps using X-ray absorption near-edge structure (XANES) spectroscopy at the S K-edge. Am. Mineral. 90, 1748-1758.

Dauphin, Y., Williams, C.T., Salomé, M., Susini, J. and Cuif, J.P., 2007. Microstructures and compositions of multilayered shells of *Haliotis* (Mollusca, Gastropoda). Biomineralization: from paleontology to materials science. In: Proceedings of the 9th international Symp. Biomineralization, pp. 265-272.

Levi-Kalisman, Y., Falini, G., Addadi, L., Weiner, S., 2001. Structure of the nacreous organic matrix of a bivalve mollusk shell examined in the hydrated state using cryo-TEM. J. Struct. Biol. 135, 8-17.

Nudelman, F., Gotliv, B.A., Addadi, L., Weiner, S., 2006. Mollusk shell formation: mapping the distribution of organic matrix components underlying a single aragonitic tablet in nacre. J. Struct. Biol. 153, 176-187.

Samata, T., Hayashi, N., Kono, M., Hasegawa, K., Horita, C., Akera, S., 1999. A new matrix protein family related to the nacreous layer formation of *Pinctada fucata*. FEBS Lett. 462, 225-229.

Schöne, B.R., 2008. The curse of physiology—challenges and opportunities in the interpretation of geochemical data from mollusk shells. Geo-Marine Lett. 28, 269-285.

Schöne, B.R., Radermacher, P., Zhang, Z., Jacob, D.E., 2013. Crystal fabrics and element impurities (Sr/Ca, Mg/Ca, and Ba/Ca) in shells of *Arctica islandica*—Implications for paleoclimate reconstructions. Palaeogeogr. Palaeoclimatol. Palaeoecol. 373, 50-59.

Zhao, L., Schöne, B.R., Mertz-Kraus, R., 2015. Controls on strontium and barium incorporation into freshwater bivalve shells (*Corbicula fluminea*). Palaeogeogr. Palaeoclimatol. Palaeoecol. 53, 160.

Appendix

Curriculum Vitae

Not displayed for reasons of data protection.